Microwave Curing of Carbon-Epoxy Composites: Process Development and Material Evaluation

A thesis submitted to

Imperial College London

for the degree of

Doctor of Philosophy



Imperial College London

Department of Aeronautics

Museok Kwak

2016

Abstract

Conventional heating methods offer limited opportunities in cycle time reduction due to the low thermal conductivity of polymer matrices. Microwaves can offer advantages in this sense, however past limitations in hardware, software and lack of suitable operating procedures led to inconsistent results and conclusions.

In the present study 2.4 mm, 4.8 mm and 60 mm thick out-of-autoclave unidirectional carbon-epoxy composites were cured using a homogeneous microwave system at 2.45 GHz. A methodology to measure the microwave penetration depth, and to cure carbon fibre reinforced polymer composites without arcing (thus producing reliable and consistent results) were proposed.

The results of the curing methodology adopted was demonstrated by measuring the degree of cross-link, axial and transverse tension, axial compression, in-plane shear, indentation, mode I interlaminar fracture and fibre push-out testing.

With a suitable microwave cure cycle, the axial tensile performance was similar to those cured using a conventional process. The transverse tensile and in-plane shear strength of microwave-cured samples were lower than those produced using conventional means. In axial compression tests, the microwave-cured samples exhibited a significant increase in strength. In interlaminar fracture testing, conventional oven-cured samples showed lower fracture toughness values with little variation with crack propagation, whereas the microwave-cured samples showed an increasing trend with crack propagation, and a greater average toughness value. The fibre-matrix interfacial shear strength was also greater in the microwave-cured samples. The increase in fibre-matrix interfacial shear strength was proportional to the increase in the interlaminar fracture toughness.

The changes in properties were due to a change at the microscopic level of the matrix, where the preferential microwave heating of the carbon fibres produced a microstructure where the epoxy closest to the fibres reached a higher degree of cure compared with the rest of the matrix, as well as an increased fibre-matrix interfacial bond. Away from the fibre the matrix was more rubbery, thus producing a multi-phase brittle-ductile region.

The contribution to knowledge in the thesis was the conclusion of pragmatic studies, which now permits the manufacture of unidirectional composites cured using microwaves without the damage and inconsistencies that occurred using previous methodologies.

Declaration of Originality

I (Museok Kwak) hereby confirm that the work presented in this thesis is the author's own, unless referenced in the text. The work contains work carried out at TWI Ltd. (the Sponsor of the project) and Imperial College London unless stated otherwise. No part of this thesis has been submitted elsewhere for any other degree or qualification.

Copyright Declaration

The copyright of this thesis rests with the author and is made available under a Creative Commons Attribution Non-Commercial No Derivatives licence. Researchers are free to copy, distribute or transmit the thesis on the condition that they attribute it, that they do not use it for commercial purposes and that they do not alter, transform or build upon it. For any reuse or redistribution, researchers must make clear to others the licence terms of this work.

Acknowledgements

The author would like to take this opportunity to gratefully acknowledge the many individuals who have contributed to the development of this work, whether directly or indirectly.

First of all, thanks to TWI Ltd for the opportunity to join the company, and TWI's Member Companies for funding the present work through the Core Research Programme (CRP), thus making this research possible, especially Rafael Avila (Airbus Operations Spain) for agreeing to participate as the industrial mentor.

The author would also like to gratefully acknowledge his PhD supervisors Prof. Paul Robinson (Imperial College London), Prof. Alexander Bismarck (Imperial College London) and Dr. Roger Wise (TWI).

TWI colleagues Sylvain Lannes, Kevin Kong, Jose Vecino, Steve Willis, Damaso De Bono and Mihalis Kazilas (just to name a few, in no particular order) for all the hours spent having insightful (and sometimes not so insightful) discussions throughout the years.

The author would also like to thank his line manager, and TWI's CRP Manager Dr. Marcus Warwick for the trust and support provided, and being a great role model for many of us in the team.

The author would like to specially thank Yasuhiro Akita and Andrew Willett for the trust placed in the author and the technology, and the encouragement provided to continuously improve through the numerous projects that were jointly carried out.

Finally, special thanks to my family for all their continued support despite the long distance.

It is thanks to all of you that the current work has been possible – thank you.

Contents

Abstract	i
Declaration of Originality	iii
Copyright Declaration	iv
Acknowledgements	v
Contents	vi
List of Figures	xii
List of Tables	xvii
Abbreviations	xviii
Nomenclature	xxi
List of Publications	xxiv
Chapter 1. Introduction	1
Chapter 2. Literature Review	8
2.1 Alternative Heating Methods	8
2.1.1 Quickstep	8
2.1.2 Laser	10
2.1.3 Electron Beam (EB)	13

2.1.4 Induction 15

2.1.5 Microwave (MW) 16

2.2. Microwaves and Microwave Heating 18

2.2.1 Fundamentals of Microwaves 18

2.2.2 Fundamentals of Microwave Heating 20

2.2.3 Arcing/Electric Discharge 28

2.2.4 Penetration/Skin Depth 28

2.3 Influence of IFSS on Mechanical Properties of Composite Materials 29

2.4 Microwave Processing of Polymer Matrix Composites – Past Work 30

2.5 Summary 34

Chapter 3. Experimental Procedure 38

3.1 Materials, Consumables and Equipment 38

3.1.1 Carbon-Epoxy Composite Material and Lay-up Sequence 38

3.1.2 Consumables 39

3.1.3 Vötsch Hephaistos Microwave (VHM) System 40

3.2 MW Heating of Water 43

3.3 Curing Methods and Procedures 44

3.3.1 MW Curing of Carbon-Epoxy SPARPREG 44

3.3.2 Conventional Oven Curing of Carbon-Epoxy SPARPREG 50

3.4 Degree of Cure 53

3.5 Determination of the Fibre Volume (V_f) and Void Volume (V_v) Content 54

3.6 Microwave Penetration Depth (D_p) 56

3.7 Mechanical Testing 58

3.7.1 Tensile Testing 58

3.7.2 Compression Testing 59

3.7.3 In-Plane Shear (IPS) Testing 59

3.7.4 Mode I Interlaminar Fracture Toughness (G_{1C}) Testing 60

3.7.5 Fibre Push-Out Testing 62

3.7.5.1 Sample Preparation 62

3.7.5.2 Testing Methodology 63

3.7.6 Failure Mode Assessment of Tested Samples 64

3.7.7 Matrix Indentation Testing 64

Chapter 4. Results 66

4.1 Microwave Field Distribution 66

4.2 Microwave and Oven Heating Profiles 68

4.2.1 Microwave Heating Profiles of 2.4 mm and 4.8 mm Thick Laminates 68

4.2.2 Oven Heating Profiles of 2.4 mm and 4.8 mm Thick Laminates 73

4.2.3 Microwave Heating Profile of 60 mm Thick Laminate 74

4.2.4 Oven Heating Profile of 60 mm Thick Laminate 76

4.2.5 Heating Profile MW vs Oven – 2.4 mm and 4.8 mm Thick Laminates 78

4.2.6 Heating Profile MW vs Oven – 60 mm Thick Laminates 79

4.3 Degree of Cure 80

4.4 Fibre Volume (V_f) and Void Volume (V_v) Content 81

4.5 Microwave Penetration Depth 83

4.6 Mechanical Testing 85

4.6.1 Tensile Testing 85

4.6.2 Compression Testing 87

4.6.3 In-Plane Shear (IPS) Testing 88

4.6.4 Mode I Interlaminar Fracture Toughness (G_{1C}) Testing 89

4.6.5 Fibre Push-Out Testing 94

4.6.6 Failure Mode Assessment of Tested Samples 96

4.6.7 Matrix Indentation Testing 100

4.7 Results – Summary 101

Chapter 5. Discussions 106

5.1 The MW Penetration Depth of SPARPREG Composites	106
5.2 Microwave Field and Cure Homogeneity	107
5.2.1 Water Heating	108
5.2.2 Temperature Profiles During Curing of 2.4 mm and 4.8 mm Thick Laminates	109
5.2.3 Temperature Profiles During Curing of 60 mm Thick Laminates	112
5.2.4 Homogeneity in Degree of Cure	115
5.2.5 Laminate Quality and Consistency	116
5.2.5.1 Differences in V_f and V_v of Microwave-Cured and Oven-Cured Laminates	116
5.2.5.2 Matrix Indentation Modulus of Microwave-Cured and Oven-Cured Laminates	117
5.2.5.3 Tensile Test Performance of Microwave-Cured and Oven-Cured Laminates	118
5.2.5.4 Differences in Interfacial Shear Strength Between Microwave-Cured and Oven-Cured Composites	119
5.3 Failure Mode of Microwave-Cured and Oven-Cured SPARPREG Composites	123
5.4 Discussions – Summary	125
Chapter 6. Conclusions	129
Chapter 7. Future Work	134

References 137

List of Figures

Figure 2.1	Schematic of the Quickstep process [29].
Figure 2.2	The electromagnetic spectrum [57].
Figure 2.3	A schematic of an electromagnetic wave (λ = wavelength) [57].
Figure 2.4	Relation between dielectric constant, dielectric loss, frequency and temperature of water [66].
Figure 2.5	Theoretical (lines) and experimental (points) dielectric constant of epoxy as a function of temperature and degree of cure [67].
Figure 2.6	Theoretical (lines) and experimental (points) dielectric loss of epoxy as a function of temperature and degree of cure [67].
Figure 2.7	Dielectric properties of Nylon 66 at 3GHz [68].
Figure 2.8	Dielectric constant and dielectric loss of water as a function of MW frequency [69].
Figure 2.9	Theoretical (line) and experimental (points) dielectric constant (ε') and dielectric loss (ε'') of uncured epoxy as a function of frequency at a constant temperature 70°C [70].
Figure 3.1	VHM 100/100 system located in TWI North-East (Middlesbrough).
Figure 3.2	Schematic drawing of waveguides used in VHM 100/100.
Figure 3.3	MW field distribution simulation [110]. Left: hexagonal chamber, right: circular chamber
Figure 3.4	Schematic of vacuum bagging setup used [111].

Figure 3.5	A burnt CFRP laminate when heated in the VHM 100/100 with no shielding at the edges of the laminate.
Figure 3.6	Position of the five fibre optic probes that were used to record temperature in the VHM.
Figure 3.7	Schematic of the layup used for curing thick laminates (For test S25_MW90, T4 was labelled T_{MW}, and T5 was T4).
Figure 3.8	Location of the four thermocouples that were used to record temperature in the conventional oven to cure the 2.4 mm thick laminates S19 to S22_O45.
Figure 3.9	PP beakers containing water in six different configurations to assess the MW distribution.
Figure 3.10	DSC result of a typical semi-cured sample.
Figure 3.11	DSC result of a typical MW-cured sample (Sample S15_MW45, 45 mins dwell at 120°C)
Figure 3.12	Representative micrographs of; top: oven-cured (S26-2_O90), and, bottom: MW-cured (S25-2_MW90) which were used for V_f and V_v measurements.
Figure 3.13	Schematic for testing the MW penetration depth of CFRPs.
Figure 3.14	Schematic of a mode I DCB interlaminar fracture toughness test coupon.
Figure 3.15	Representative graph of sample S25-2_MW90 of $C^{1/3}$ against 'a' as described by the modified beam theory (MBT).
Figure 3.16	Schematic of; (a) basic principle of fibre push-out testing, (b) test setup/methodology [117].
Figure 4.1	MW heating of water – Temperature vs Time as a function of location.

Figure 4.2	2.4 mm thick, MW-cured UD laminates with 30-minute dwell at 120°C.
Figure 4.3	2.4 mm thick, MW-cured UD laminates with 35-minute dwell at 120°C.
Figure 4.4	2.4 mm thick, MW-cured UD laminates with 40-minute dwell at 120°C.
Figure 4.5	2.4 mm thick, MW-cured UD laminates with 45-minute dwell at 120°C.
Figure 4.6	2.4 mm thick MW-cured (±45°)2S laminates with 40-min dwell at 120°C.
Figure 4.7	Differences in MW power used to cure laminates S7_MW40 and S28_MW40.
Figure 4.8	Cure cycle of MW-cured 4.8 mm thick laminate with 40-minute dwell at 120°C.
Figure 4.9	2.4 mm thick, oven-cured laminates (UD and $(\pm 45°)_{2S}$) with 45-minute dwell at 120°C.
Figure 4.10	Cure cycle of 4.8 mm thick laminates at 120°C dwell; left: MW-cured with 40-minute dwell, right: oven-cured with 45-minute dwell.
Figure 4.11	MW cure cycle of 60 mm thick laminate. a) Full cycle, b) ramp-up phase, c) dwell phase.
Figure 4.12	Conventional oven cure cycle of 60 mm thick laminate. a) Full cycle, b) ramp-up phase, c) dwell phase.
Figure 4.13	Change in water temperature as a function of carbon-epoxy laminate thickness after ten mins, 1kW MW heating.
Figure 4.14	Longitudinal tensile strength and modulus, and degree of cure.
Figure 4.15	Transverse tensile strength and modulus, and degree of cure.
Figure 4.16	Transverse tensile strength (columns) and modulus (circles) as a function of coupon location across laminate.

Figure 4.17	Longitudinal compressive strength and modulus, and degree of cure.
Figure 4.18	In-plane shear strength and shear chord modulus of elasticity.
Figure 4.19	R-curves – Oven-cured laminate S24_O45 (Average G_{1C} = 179.9J/m^2).
Figure 4.20	R-curves – MW-cured laminate S23_MW40 (Average G_{1C} = 233.1J/m^2).
Figure 4.21	R-curves – Sub-laminates of oven-cured laminate S26_O90.
Figure 4.22	R-curves – Sub-laminates of MW-cured laminate S25_MW90.
Figure 4.23	Average interlaminar fracture toughness values obtained for laminates S25_MW90 and S26_O90, where '-2' is the sub-laminate closest to the mould, and '-13' is farthest.
Figure 4.24	Average mode I interlaminar fracture initiation values of 60 mm thick oven-cured (S26_O90) and MW-cured (S25_MW90) laminates.
Figure 4.25	IFSS values obtained using fibre push-out testing from laminates S23_MW40 and S24_O45.
Figure 4.26	Fracture toughness (G_{1C}) and IFSS of samples S23_MW40 and S24_O45 ($\Delta G_{1C} \approx 23\%$, $\Delta IFSS \approx 28\%$).
Figure 4.27	Fracture surface SEM of 90° tensile test. Sample S22-5_O45, 45min at 120°C (Oven-cured).
Figure 4.28	Fracture surface SEM of 90° tensile test. Sample S16-5_MW45-5, 45min at 120°C (MW-cured).
Figure 4.29	Fracture surface SEM of 90° tensile test. Sample S6-5_MW40, 40min at 120°C (MW-cured).

Figure 4.30	Oven-cured sample S24_O45 fracture surface after G_{1C} testing.
Figure 4.31	MW-cured sample S23_MW40 fracture surface after G_{1C} testing.
Figure 4.32	Calculated elastic modulus based on indentation modulus as a function of sub-laminate location.
Figure 5.1	Schematic of composite laminate.
Figure 5.2	Schematic showing the differences in crack propagation in MW-cured and oven-cured CFRP composites, where the former will have a tendency to propagate along the matrix, and the latter propagates along the fibre-matrix interface.

List of Tables

Table 2.1	Physical and mechanical properties of conventionally-cured and EB-cured composites [38,43].
Table 2.2	The dielectric constants of some common materials [64,65].
Table 3.1	SPARPREG cure cycles recommended by Gurit* [107], and MW cure cycles used in the present study.
Table 3.2	MW-cured laminates showing curing dwell time, laminate size, lay-up sequence, test method and laminate number.
Table 3.3	Oven-cured laminates showing curing dwell time, laminate size, lay-up sequence, test method and laminate number.
Table 4.1	Degree of cure of laminates. S25_MW90 and S26_O90 shown as a function of sub-laminate through-thickness (TT) location.
Table 4.2	V_f and V_v for all laminates.
Table 4.3	Change in temperature as a function of laminate thickness.

Abbreviations

AFP	Automated Fibre Placement
ASTM	American Society for Testing and Materials
ATL	Automated Tape Lay
ATP	Automated Tow Placement
CFRP	Carbon Fibre Reinforced Polymer
CPT	Cured Ply Thickness
CTE	Coefficient of Thermal Expansion
DC	Direct Current
DCB	Double Cantilever Beam
DSC	Differential Scanning Calorimetry/Calorimeter
EB	Electron Beam
EM	Electromagnetic
ETFE	Ethylene-tetra-fluoro-ethylene
FBG	Fibre Bragg Grating
FEA	Finite Element Analysis
GFRP	Glass Fibre Reinforced Polymer

HTF	Heat Transfer Fluid
IFSS	Interfacial Shear Strength
ILSS	Interlaminar Shear Strength
IPA	Isopropyl Alcohol
IPS	In-Plane Shear
IPSS	In-Plane Shear Strength
IR	Infra-Red
ISM	Industrial, Scientific and Medical
ISO	International Organization for Standardization
MBT	Modified Beam Theory
MD	Multi-Directional
MRCC	Manufacturer's Recommended Cure Cycle
MW	Microwave
OoA	Out of Autoclave
PA	Polyamide
PAN	Poly-acrylonitrile
PE	Polyethylene
PMC	Polymer Matrix Composite

PMMA	Poly-methyl-methacrylate
PP	Polypropylene
PTFE	Poly-tetra-fluoro-ethylene
SBS	Short Beam Shear
SEM	Scanning Electron Microscopy/Microscope
TRL	Technology Readiness Level
TT	Through-Thickness
UCS	Ultimate Compressive Strength
UD	Uni-directional
UKAS	United Kingdom Accreditation Service
UTS	Ultimate Tensile Strength
UV	Ultra-Violet
VFM	Variable Frequency Microwave
VHM	Vötsch Hehaphaistos Microwave

Nomenclature

a	Crack length
A	Cross-sectional Area
b	Coupon Width
d_f	Fibre Diameter
D_p	Microwave Penetration Depth
δ	Displacement
E_c	Compressive Modulus of Elasticity
E_{in}	Indenter Modulus
E_r	Reduced (or Indentation) Modulus
E_t	Tensile Modulus of Elasticity
ε_c	Compressive Strain
ε_t	Tensile Strain
ε^*	Complex Permittivity/Complex dielectric constant
ε'	Permittivity/Dielectric Constant
ε''	Dielectric Loss
f	Microwave Frequency

F_{max}	Maximum Fibre Push-out Force
γ_{12}	Shear Strain
G_{1C}	Mode I Interlaminar Fracture Toughness
G_{12}^{Chord}	Chord Shear Modulus of Elasticity
H	Enthalpy
l_{emb}	Embedded Fibre Length
λ	Wavelength
μ^*	Complex Permeability
μ'	Magnetic Permeability
μ''	Magnetic Loss
ν	Poisson's Ratio
ν_{in}	Indenter Poisson's Ratio
$P_{c,max}$	Maximum Compressive Load
$P_{t,max}$	Maximum Tensile Load
σ_{ec}	Electrical Conductivity
$\sigma_{c,max}$	Maximum Compressive Strength
$\sigma_{t,max}$	Maximum Tensile Strength
$\tan\delta_{dielectric}$	Dielectric Loss Tangent

t_c	Curing or Dwelling Time
T_c	Curing Temperature
T_g	Glass Transition Temperature
τ_{IFSS}	Fibre-Matrix Interfacial Shear Strength
τ_{12}	In-Plane Shear Strength
V_f	Fibre Volume Fraction
V_m	Matrix Volume Fraction
V_v	Void Volume Fraction

List of Publications

- Kwak M, Robinson P, Bismarck A, Wise R, Wienrich M, Kalinka G, 2015, Microwave curing of carbon-epoxy composites: Fracture toughness as a function of fibre-matrix interfacial shear strength. *(Manuscript submitted to Composites Part A: Applied Science and Manufacturing).*
- Kwak M, Robinson P, Bismarck A, Wise R, 2015, Microwave curing of carbon-epoxy composites: Penetration depth and material characterisation, Composites Part A: Applied Science and Manufacturing, Vol: 75, Pages: 18-27, ISSN: 1359-835X.
- Kwak M, Robinson P, Bismarck A and Wise R. Curing of composite materials using the recently developed HEPHAISTOS microwave. In: Proc Int Conf Compos Mater-19, Jeju island, Korea, 2011. p.T11-2-IF1073.

The author would also like to mention that the present work acted as the basis of two patent applications, namely;

- "Method and device for curing a thermosetting polymer", Patent Publication Number: WO 2012149973 A1.
- "Tool for implementing a composite material", Patent Publication Number: EP 2777908 A1.

Chapter 1

Introduction

This thesis reports the study of the microwave (MW) curing of out-of-autoclave (OoA) carbon-epoxy composites. In this work the benefits and drawbacks of MW curing as a rapid composite manufacturing method were assessed through testing and analysis of the cured materials.

Composite materials, particularly those with a polymeric matrix, are becoming more popular in industry mainly due to their high specific properties. However, there are two major drawbacks with composite materials: the high cost of raw materials (the cost of carbon fibres is currently estimated to be 570 times that of steel by weight [1]) and the energy intensive and lengthy processing – typically over 100°C for several hours – usually associated with these materials. Since the first factor is very highly dependent on market supply-demand (and there are only a handful of companies capable of producing large enough volumes to make a difference in the market), it is very difficult to make a significant difference (i.e. cost reduction) in this sense. Therefore it is not surprising that the application of composites, particularly those with continuous carbon fibre reinforcement, have generally been restricted to high value products. However, the increasing demand for new composite intensive aircrafts such as the Boeing 787, Airbus A350XWB and Bombardier C-series meant that increased productivity of cured composite components is a key future requirement. In other applications such as automotive, increasing emissions regulations have pushed vehicle manufacturers to further extend the use of materials with high specific properties such as composite materials. In a production environment where parts are typically made in 'a few minutes', increased productivity and manufacturing cost reduction is key.

Broadly speaking, there are two methods to increase productivity, namely; i) increased automation (e.g. automated tape lay (ATL), automated tow placement (ATP) and automated fibre placement

(AFP)), and, ii) use of alternative heating methods (existing heating methods have inherent limitations in terms of heating rate and efficiency).

Current manufacturing of composite components relies on energy intensive and time-consuming conduction heating methods. The heat is typically generated by electric heaters, and the heat travels to the surface of the composite part via the gas medium (usually air or nitrogen, which is a relatively good insulator with a thermal conductivity of 0.024 W/m.K or 0.026 W/m.K respectively) in an oven chamber, and through the mould (which usually can weigh several tons when manufacturing an average sized aircraft component). Since the transverse thermal conductivity of polymer matrix composites (PMCs) is typically very low (typically <10W/m.K, compared to >200W/m.K for aluminium), it takes a relatively long time for the material to reach thermal equilibrium. Therefore, it is no surprise that there is a risk that the degree of cure will not be homogenous throughout a composite part when using well-established techniques such as thermal ovens and autoclaves [2-4]. This is especially the case when curing thick composites [5-7] and often long cure cycles (in excess of 24 hours in some cases) are required to achieve a reasonably uniform degree of cure.

In this regard, the key potential advantages of MW for curing of composite components are [8-26];

i. *Rapid and efficient heating.* Only the part is heated and thus the need to heat unnecessary thermal mass (i.e. air and mould) is reduced. Therefore, the time and energy required to cure a part is generally significantly lower with MWs than with conventional methods. This is particularly the case when curing thick composite laminates where typical heating rates in a conventional oven is less than 1.0 °C/min.

ii. *Volumetric heating.* Materials can be classified as predominantly reflective, absorptive or transparent in terms of their interaction with MWs although generally, all materials exhibit all three behaviours to a greater or lesser degree. Reflective or transparent materials do not heat (or the heating level is negligible), whereas absorptive materials will heat by dielectric heating and/or other mechanisms. In such cases, MWs will heat volumetrically through the material to a penetration depth (called skin depth for metals) – explained in Section 2.2.4 – which is related to the material's dielectric constant, dielectric loss, magnetic permeability

and electrical conductivity properties. If the thickness of the part is similar to the penetration depth value, it is generally assumed the part will heat evenly through the thickness assuming there is negligible heat loss to the surrounding environment.

iii. *Selective heating.* The properties that influence the heating ability of a material in a MW environment were listed in (ii) above. For a given material and depending on the processing conditions (i.e. temperature, moisture, frequency and material composition), one property will usually dominate over the others, thus heating certain sections preferentially. One example is polyamide (PA), which is typically known to have high moisture absorption, and depending on the quality of the manufactured part, the areas with moisture concentration will tend to heat more than the rest. In the case of carbon-epoxy composites, both the carbon fibres and the epoxy matrix have the necessary properties to absorb MWs and so produce heat, however with an equal volume of carbon and epoxy, typically the carbon will produce greater levels of heat, making carbon the dominant constituent in this case. Therefore, the volumetric heating ability and heating pattern of the carbon-epoxy composite will be highly influenced by the fibre volume fraction (V_f), fibre diameter and fibre orientation. The ability to heat selectively means that in theory one could add MW susceptors in certain regions to encourage more heating on one area than another, such as in a composite welding process where substantially greater heating is required at the joint interface as opposed to the rest of the part. Conversely, one could shield certain parts of the structure to avoid heating by using a MW reflector on the surface, thus providing a variety of processing possibilities.

iv. *Self-limiting.* Certain materials, such as epoxies, exhibit a reduction in dielectric loss properties with increasing degree of cure, thus providing a self-limiting mechanism whereby the heat generated by the epoxy, or the epoxy's ability to generate heat, when irradiated with MWs reduces with increasing degree of cure. This is beneficial because it can reduce the likelihood of thermal runaway due to the resin's exothermic reaction during curing. This could be particularly beneficial when curing thick composites, where very slow heating rates (i.e. <1.0°C) are necessary to avoid such undesirable effect.

v. *Continuous production.* MW systems with continuous throughput have been used in the past in the food industry for example, which could be adopted to produce composite parts. This increase in automation could lead to savings in time, and can improve overall process efficiency.

vi. *Reduction in non-conforming parts*. It is common practice for producers of composite parts to cure multiple parts in a single run in order to optimise the use of the oven or autoclave. In the aerospace industry for example, there are standards which require thermocouples to control the curing cycle. The aim is that all parts should reach a minimum cure temperature (T_c) and maintain this for a minimum time (t_c), but not exceeding a maximum time (typically t_c + 60 minutes). When a part exceeds the maximum time at T_c, then the part has to be recorded and traced by a "non-conformity" procedure, which creates a lot of additional bureaucracy and associated financial costs. These "out-of-standard" parts are as a result of the uneven heating within the oven or autoclave due to the uncontrolled flow of hot air, and the differences in the geometry and thermal masses of the parts and the moulds. MW curing, if designed appropriately, could reduce the number of non-conforming parts by heating only the material irrespective of the mould thus producing a lower scatter in the temperature distribution of the different parts.

To date the application of MWs for curing composite structural parts has been considered to be at a medium technology readiness level (TRL) at best [27,28], and some major challenges remain, including:

- *Even energy distribution and consistency*. This is one of the prime obstacles to the industrialisation of MW curing of composites. In other applications where MWs are used for heating, e.g. food industry and wood drying, it is not imperative that the entire part is heated evenly. On the other hand, because composite materials are generally used for structural parts, it is absolutely critical that the entire part is heated and cured evenly throughout. Additionally, because MWs have a fixed wavelength as a function of its frequency, it can be very difficult to obtain a MW field which will produce such highly homogeneous heating and curing. This

is the reason why it has been so challenging to up-scale the technology in a good, consistent manner.

- *Arcing*. A phenomenon typically observed when sharp electrically conducting medium is introduced into a MW environment, *arcing* has been, together with *even energy distribution and consistency*, two of the biggest challenges to date that have limited the progress of MW heating of carbon fibre reinforced polymer (CFRP) composites. The former however poses a more serious issue as arcing at the tips of the carbon fibres will most likely lead to combustion, damaging the material and causing a serious health and safety issue.
- *Tooling design*. In today's composites industry, tooling materials are typically made of metallic or carbon fibre reinforced composite materials – materials that are generally assumed to reflect and absorb MWs, respectively. This will therefore inevitably lead to the distortion of the MW field, and potentially lead to further uneven distribution of MWs, and subsequently uneven heating of the composite part. *Arcing* could also be a possibility.
- *Part quality and understanding of MW effects on the composite material*. Due to the inherent heating nature of MWs, the cause and effect MWs have on the eventual composite material's properties is yet not fully understood. As mentioned above, in a carbon-epoxy composite for example, the heating will be dominated by the carbon fibres, and additionally a certain volume through the thickness will be heated at the same time, which are key differences compared with conventional heating methods. Additionally, the heating and cooling rates achievable with MW heating are also greater than using conventional methods. Because of these reasons, some changes in mechanical properties are to be expected by changing from conventional curing methods to MW. The effects MW curing has on the short and long term material properties needs to be better understood.

These challenges need to be addressed before MW curing of composites can be considered for structural industrial applications.

The aim of the present work is to provide further insight into MW curing of carbon-epoxy composites and to understand the influence of this curing technology on their physical and mechanical performance. The current study employs a system with a high MW field homogeneity, and therefore the results obtained were expected to be as consistent as, and with at least equal mechanical performance compared with conventionally-cured composites at a significantly reduced time. The individual objectives were:

- Review the current state of the art in rapid curing of composites, including MW.
- Establish a methodology to measure MW penetration depth in composites.
- Establish a reliable methodology to cure carbon-epoxy composites in a MW environment.
- Investigate the physical properties of MW-cured composites using differential scanning calorimetry (DSC) and image analysis, and compare the results with conventionally-cured composites.
- Investigate the mechanical properties of MW-cured composites under tension, compression, in-plane shear (IPS), mode I interlaminar fracture, matrix nano-indentation and fibre push-out, and compare the results with conventionally-cured composites.
- Propose an explanation for any differences in the physical and mechanical properties of MW-cured and conventionally-cured composite materials.

Chapter 2 presents a summary of the current technologies used for rapid curing of composites, as well as key concepts and theories related to MWs and MW curing of composite materials. This is then followed by a literature review on the past work in the field of MW heating of composites, with particular focus on carbon-epoxy composites.

Chapter 3 provides some basic information on the MW equipment, materials and consumables used in the investigation. This is then followed by the description of the experimental work, including the processing parameters, details of the physical and mechanical tests that were carried out to compare and evaluate the performance of MW-cured against conventionally cured composites. The tests included standardised mechanical tests (including tension, compression, in-plane shear, mode I

interlaminar fracture), non-standardised mechanical tests (i.e. fibre push-out testing to measure the fibre-matrix interfacial shear strength (IFSS) and matrix nano-indentation), and thermo-physical tests (differential scanning calorimetry (DSC)) to assess the degree of cure. Observations of the fracture surfaces using scanning electron microscopy (SEM) are also reported.

The results of the experimental work are reported in chapter 4, with discussions presented in chapter 5. The overall conclusions and recommendations for future work can be found in chapters 6 and 7 respectively.

Chapter 2

Literature Review

This chapter starts with a summary of alternative heating methods for the fast curing of composites that are currently under development or are being used for specific applications. This is then followed by an introduction to basic principles and theory of MW heating, placing focus on factors most relevant for MW heating of carbon fibre reinforced polymers (CFRPs). The chapter concludes with a review of the published literature in MW curing of CFRPs.

2.1 Alternative Heating Methods

As mentioned in chapter 1, ovens and autoclaves are the conventional devices used to achieve heating for the cure of polymer matrix composites (PMCs) and because of their reliance on conductive heating of a gas medium, there is little scope for reducing the process cycle time. The current section examines alternative heating methods that are being used or are under development for curing composite parts.

2.1.1 Quickstep

Quickstep is possibly, from a conceptual and practical point of view, the most similar method to existing curing methods of composite materials, and could be considered an incremental improvement as opposed to a step change. The process was invented and patented by Australian company Quickstep Pty Ltd [29]. The gas medium that is normally present in conventional ovens and autoclaves for curing was replaced with a liquid medium (referred to as a heat transfer fluid (HTF) in

Figure 2.1) to improve the process efficiency by taking advantage of the higher thermal conductivity of the liquid. Flexible bladders are used to act as the interface between the part, the mould and the liquid medium. These bladders are sealed in order to provide the application of pressure (Figure 2.1). Liquid media at different temperatures are introduced at different intervals during the heating cycle for the part to achieve the required temperature. As in conventional ovens, the hot medium and the pressure are continuously applied until the end of the dwell cycle. Once the dwell cycle is complete, the hot medium is exchanged with a lower temperature medium until room temperature is achieved. The process is then complete and the part is then removed.

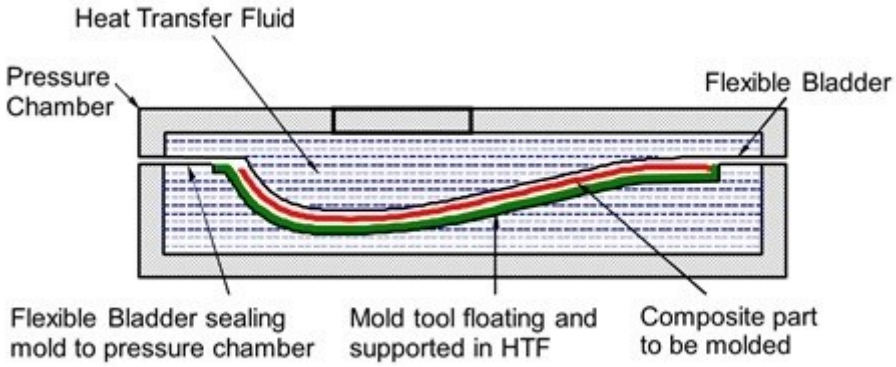


Figure 2.1 Schematic of the Quickstep process [29]

Quickstep cured composites were reported to have similar glass transition temperature (T_g) and interlaminar shear strength (ILSS) compared with press-cured and autoclave-cured methods by Tian *et al*. [30] and Khan *et al*. [31] respectively. Khan *et al*. [31] reported an approximately 10% reduction in flexural strength, with similar reduction in the aforementioned properties compared with autoclave-cured composites when aged in water. Khan *et al.*'s [31] heating rate was 10 °C/min, and obtained a cure cycle reduction of approximately one third compared with the material manufacturer's recommended autoclave cure cycle.

One of the main advantages of the Quickstep process is that no modifications are required to the composite materials as these are heated using conduction means as with conventional ovens and autoclaves. This could be important for aerospace companies since the qualification procedure would be significantly less arduous than for a new process also requiring new materials to be used.

Additionally, because the liquid medium is pre-heated in separate tanks prior to being introduced into the chamber, the process is quick and the time taken to cure the part is purely dependent on the material and part geometry. However, the energy required to heat and maintain temperature of the entire volume is very high, and therefore a significant amount of energy is still wasted. Furthermore, it is difficult to expect any additional increment in process efficiency as the process still relies on conduction to cure the composite part.

In July 2013 Quickstep Pty Ltd. received the first commercial order of its patented Quickstep process from ORPE Technologiya in Russia. It is said that the Russian company intend to use the Quickstep process to produce composite parts of a satellite launcher. Quickstep Pty Ltd. is also actively pursuing to sell its technology to the automotive industry, aimed at producing body panels made of composite materials [32].

2.1.2 Laser curing

A laser is a man-made type of EM radiation, with very unique characteristics as they are monochromatic (i.e. one wavelength), coherent (i.e. all wavelengths are in phase) and collimated (i.e. parallel in the same direction). Lasers can be in almost any frequency (e.g. X-ray laser, ultra-violet (UV) laser, infra-red (IR) laser, MW laser), and not only in the visible light range.

The use of lasers for different applications has grown substantially in the last few years mainly due to the developments in lasers and the significant reduction in capital and operational costs. In the field of composite materials, the concept of using laser-assisted AFPs and ATLs to manufacture composite parts dates back to 1990 [33]. However the successful industrialisation and commercialisation of the technology is more recent [34].

AFP and ATL are similar processes currently used in both commercial and military aircraft applications to produce wing skins and aircraft fuselage [35], where unidirectional (UD) carbon-epoxy tape is supplied in roll form on backing paper and typically comes in 75, 150, and 300 mm

widths. The roll of material is loaded into the tape-laying head, and the tape head is mounted on a 4-axis gantry for flat applications or a 5-axis gantry for contour applications. The gantry positions the tape head over and onto flat or contour moulds for lay-up.

As the material is placed on the mould, it is heated and compacted while the automated robotic head moves along a pre-determined path. Heating methods include hot air, IR, direct flame, and more recently, laser. These systems will usually have a closed-loop feedback system which means that overheating the material can be avoided by using a control system which measures the local material temperature and modifies the heat output by using a predetermined relationship between the head speed and the heat output. The key advantages of AFP and ATL are speed, accuracy, consistency and reduced scrap. One drawback however is the geometrical limitations of the components it can be produced using these techniques [36].

The use of lasers in AFP or ATL provides one key advantage over other heating methods such as the aforementioned hot air, IR and direct flame, since lasers can provide very simple, local and quick energy control, while at the same time producing composite laminates with comparable mechanical properties [36]. One example is the work done by Funck and Netizel [37], where a 1.2k W CO_2 laser was used to assist in rapid heating during the filament winding process. The system consisted of a laser, a conventional oven, a four-axis winding device, a mandrel and a spool with prepreg material. In order to assist in process speed, the laser was defocused, thus produced an elliptical beam shape (i.e. achieved a larger heating area in a single pass). The process consisted of four steps; (i) pre-heating of the prepreg tape in a conventional oven, (ii) heating of the prepreg tape using laser, (iii) temperature measurement of the prepreg tape, and, (iv) winding of the prepreg onto the mandrel. The pre-heating of the tape together with the temperature measurement allowed accurate temperature control, and the temperature feedback loop that exists with the laser meant that the laser power could be adjusted accordingly to ensure the prepreg was at the optimum winding temperature. The laser method provided the highest energy density and efficiency compared with IR, hot gas and direct flame, and the lowest response time of only a few milliseconds. However, the high capital cost in comparison to the other heating methods was a major drawback.

More recently Automated Dynamics industrialised a laser-based AFP heating system for thermoplastic or thermoset composites, thus replacing the IR heating systems usually present when curing thermoset-based prepregs, and hot-gas systems which are typically used for thermoplastic-based systems [34]. Similarly, the Fraunhofer Institute for Production Technology in Germany has been investigating both in-situ and two-step curing processes, where investigations are on-going to identify the right level of consolidation by simultaneously controlling the temperature, pressure and time to achieve the maximum material throughput with minimum residual stress build-up [33].

However, in-situ fabrication of thermoset or thermoplastic-based composite components is not commercially available yet [33]. At present, in commercially available systems the laser is only used to soften the prepreg to increase the tackiness of the material, and it is not used to cure the material. Therefore, the biggest limitation with laser-assisted, in-situ curing of thermoset-based composites is related to process speed, which is hindered by the matrix resin chemistry. Thermoset resins, especially those designated as aerospace grade, require a high temperature – typically 180°C – and a long duration of time – typically eight or more hours – in order to cure. Therefore, even if the laser was used in conjunction with AFP or ATL, the bottleneck in the curing process will be the material's curing time. This is the reason why laser-assisted AFP or ATL is commonly used in a two-stage process, i.e. partial heating during the AFP or ATL consolidation stage, and a second stage in a conventional hot-press, oven or autoclave, and this is unlikely to change in the near future [33]. Therefore, the process time reduction is predominantly due to the automation of the process, not the reduction in curing time. Additionally, even if a rapid cure resin with mechanical performance suitable for structural applications is developed, the following challenges for in-situ curing laser-assisted AFP or ATL remains:

- Curing on a single pass is, at least at present, unrealistic and therefore the laser needs to be able to penetrate past the first ply, maybe even the second, third, or more plies in order to make in-situ curing a possibility. Penetration depth of the laser needs to be investigated as a function of the heating ability of the material.

- Given the above, assess how many passes are required to cure the part, taking into account that multiple heating and cooling passes may lead to sub-par performance of the material.
- Assess the short and long-term mechanical performance of in-situ laser-cured composites.

2.1.3 Electron Beam (EB) curing

EB curing of composites has been around for over 30 years [38]. The technology relies on the Coulomb heating caused by the fast electron movement in the resin as it interacts with the electrons from the EB, which are released through an accelerator.

The material properties of EB-cured composites with epoxy matrix show both improvements and deterioration compared with conventionally-cured composites. The tensile modulus and T_g of EB-cured neat resin have been reported to be equivalent or better than conventionally-cured resins [39-41]. Lopata *et al.* [42] has shown that EB-cured composite materials can have relatively low V_v (void volume content) and comparable flexural, tensile and compressive mechanical properties. However Lopata *et al.* reported a decrease in neat resin toughness and low composite ILSS by approximately 30% to 50% for the latter. It is believed that the reduced ILSS was mainly due to poor fibre-matrix adhesion [38,39]. A table summarising Lopata *et al*'s results can be seen in Table 2.1.

Table 2.1 Physical and mechanical properties of conventionally-cured and EB-cured composites [38,43].

Property	**Thermally cured Cytec 977-2**	**EB cured 8H***	**EB cured 3K***
Cure conditions	Autoclave (6 h, 177°C)	250 kGy (25°C)	150 kGy (25°C)
V_v (%)	Not reported	1.77	0.64
T_g (°C)	200	396	212
0° tensile modulus (GPa)	166	168	157
0° tensile strength (MPa)	2537	1869	2200
0° flexural modulus (GPa)	147	196	154
0° flexural strength (MPa)	1641	1986	1765
0° compressive modulus (GPa)	152	149	Not reported
0° compressive strength (MPa)	1580	1683	1428
0° interlaminar shear strength (MPa)	110	77	89

*Proprietary resin formulation

The first company to ever use EB curing of composites at an industrial level was Aerospatiale from France, where EB was used for manufacturing missile fuel tanks [44,45]. Since then, Air Canada Winnipeg Maintenance Base and Acsion Industries have successfully used EB curing to repair secondary composite structures (i.e. lower rear fairing and wing-to-body fairing) in Air Canada's Airbus A319, A320 and A340s [38,39]. Through the use of small, portable EB accelerators and a proprietary EB-curable epoxy resin called 1L0, the Acsion-Air Canada joint development managed to repair the fairing at the lower rear of the aircraft fuselage using EB, thus becoming the first commercial airline application. This repair was in service on the aircraft for 900 landing and take-off cycles for a period in excess of 16 months [38].

EB curing has many advantages such as speed, control and penetration depth – up to 40 mm thick composites when cured using a double-sided irradiation process. Drawbacks include cost – an electron generator typically costs between €2-4 million [38], beam size, and the need for a vacuum between the accelerator nozzle and the part to be cured in order to avoid divergence of the beam. However, in the Air Canada case, EB was successful due to its portability and because it was used for repair and not production of a full component. The aircrafts could be repaired quickly, meaning that using a more expensive technique could ultimately save time and costs. However, it is believed that in production cases, i.e. not repair, where needs are to cure a whole section, not parts of it, beams may eventually take longer to carry out the task compared with MWs. Additionally, resins need to be

modified to absorb the free electrons from the EB, which requires additional work and additional research (as well as time and costs for qualification). However this last point provides a distinctive advantage over other typical thermal-cure resins. As the resin is specifically designed to cure using EB, the resin does not polymerise by itself at ambient temperature, and therefore will provide a significantly longer shelf life compared with standard resins [38].

2.1.4 Induction

Induction heating of electrically conductive or ferromagnetic materials is possible when these types of materials are exposed to an alternating EM field typically within the 100 kHz to 10 MHz frequency range. The induced eddy currents and magnetic polarisation generates heat. In most cases, heating due to eddy currents will dominate over the magnetic effects [46]. However in order to induce eddy currents in this frequency range, an electrically conducting closed loop is required, thus for composite applications, woven carbon fabrics are preferred for induction heating.

One of the best examples of this technology is demonstrated by the French company Roctool [47] – Roctool patents include US2004058027 (A1) and WO2009125079 (A2). Although there are a few variations to the original Roctool concept, the Roctool method mainly relies on the design and production of moulds that can be heated using induction, where only the thin (approximately 0.2 mm thick [48]) magnetic steel surface of the mould is heated, and therefore maintains the rest of the mould cooler than the surface of the mould where the composite is placed. Cooling of the mould is then achieved by circulating a coolant. The composite material is laid on the female mould, and the pressure is applied using the male mould. The technique is known for producing a Class-A surface finish, and the high heating rate – Roctool claims its technology can achieve 280°C in 45 to 90 seconds depending on the size of the part with no pre-heating [49] – makes the technology attractive for applications where high production rates are required.

Although the Roctool induction heating technique is very quick and can manufacture composite components such as an average-sized automotive bonnet in less than 5 minutes, the electrical power required is very high – 300 kW was required in the aforementioned automotive bonnet example [50]).

Additionally, the cost of purchasing these moulds is very high and a small redesign of the mould will most likely lead to the purchasing of a new mould, which will be very costly. It has also been reported that the operational life of the mould is dependent on the life of the mould surface, which requires repair or replacement after only approximately 100 cycles [48], thus further increasing costs. Additionally, from an industrial point of view, having a sole mould supplier may be a significant concern.

The Roctool technique is more widely used for thermoplastic-based composites than thermoset based, such as in consumer electronics [51]. A good example is Taiwan-based company Ju Teng, which produced more than one million parts of composite mobile phone casings in the last quarter of 2013 using Roctool technology. The author has been unable to find any literature describing the mechanical performance of composite parts manufactured using this technology. It is believed this may be because the parts made using Roctool are, at present, mainly structurally non-critical, e.g. car body panels and consumer electronic casings. There are no known reports where Roctool was used to manufacture key primary structural components such as vehicle chassis or primary, or even secondary, aircraft structures.

2.1.5 Microwave (MW)

There are various MW frequency bands which are allocated for Industrial, Scientific and Medical (ISM) use, and the frequencies of interest for heating are 0.869 GHz (UK only), 0.915 GHz (US only), 2.45 GHz, 5.80 GHz and 22.0 GHz [9]. Significant progress has been made in MW technology since its invention shortly after the Second World War, however two major obstacles have limited the application of MWs for heating and curing composite materials, namely; i) difficulty in achieving a homogeneous MW field distribution and subsequent even heating, and, ii) arcing at the tips of the carbon fibres. These two reasons led to negative conclusions related to the use of this technology for curing composite materials, especially CFRPs.

Four different methods were developed by different organisations in order to tackle these problems;

- Vötsch Hephaistos Microwave (VHM): It could be argued that the VHM is the current state-of-the-art in unpressurised fixed frequency MW systems due to its highly homogeneous MW field, potential for up-scaling and operational control. The VHM relies on three key factors to achieve a high MW field homogeneity, namely; i) hexagonal cavity, ii) waveguide design and its even distribution around the cavity (i.e. two on each side of the hexagon), and, iii) random magnetron firing sequence. Further details are described in Section 3.1.3.

  The VHM was specifically designed with composites processing in mind, therefore the typical bench that is seen in conventional ovens and autoclaves is present, metallic moulds can be used, and holes around the cavity for the vacuum hose is also present – causing no MW leakage. Therefore, the setup required to cure a composite laminate does not need to be very different to the typical setup used in the composites industry. However, due to the nature of MWs, arcing and uneven MW field distribution is still a possibility in certain cases, albeit far less likely than in other conventional fixed frequency MW systems, and therefore care is needed when preparing and curing a laminate in the VHM.

- MW-assisted ATL: MW heating of materials in general has always been a relatively complex matter because of the way MWs interact with materials. Unlike lasers or EB where the energy is focussed on the area of interest, the part is normally introduced in an applicator and heated, as it is normally done in a conventional oven. However, because MWs interact directly with the material, the MW field inevitably changes according to the cavity geometry, part geometry and other factors described in Section 2.2, and since dielectric, magnetic and electrical properties of the material also change with temperature, the MW field-material interaction changes accordingly too. This eventually leads to a very complex, continuously changing MW field throughout the process. The method developed and patented by Airbus Operations Spain [52] with patent number US 2008/0023130 (A1), has attempted to overcome this issue by focussing MWs in the area of interest, as with lasers and EB, using an ATL machine to place and compact the layers of composite material in conjunction with a MW head to locally heat the material. The automated process makes the technique very attractive, but local heating of the material may lead to a lengthy and costly process

depending on the size of the part. Additionally, because the part sees multiple MW passes, the heat experienced by the first layer may differ to the heat experienced by the outer layers. The author has been unable to find any published literature other than the patent on this technique.

- Variable Frequency Microwave (VFM): In VFM systems, the magnetrons would typically be designed to operate by continuously fluctuating between two set frequencies, thus changing and distributing the MW field inside the cavity. Although technically very useful, the capital and running costs are significantly greater than similarly sized fixed frequency MW systems. A VFM system with an applicator the size of a domestic MW could cost similar to a fixed frequency MW system with a 1 m^3 volume, or even larger. The typical life of variable frequency magnetrons are also far shorter.
- A pressurised MW, i.e. a MW autoclave, using a fixed frequency of 2.45 GHz particularly targeted for the aerospace industry was developed by DLR [53]. The system relies on having multiple (i.e. 96) magnetrons evenly distributed around a cylindrical cavity. Unfortunately, the article does not provide details regarding the performance of the materials produced, nor whether the process was a success. There has not been any application of such technology for real parts and since the article was published [53], there has not been any further publication.
- Microwave Assisted Curing in resin transfer moulding (MAC-RTM) [54]: A project funded by the European Commission under the 7^{th} framework programme (FP7), the concept consisted of MW curing composite materials with thermoset matrices such as vinylester, polyester and epoxy, in an RTM process. Electrically steering antenna systems were used to direct the MW energy to the required regions, and direct current (DC) curing sensors were used to monitor the live degree of cure of the component. The project consortium reported comparable mechanical properties with conventionally cured parts, with a reduction in curing time of 40%.

Details regarding MW theory and MW heating of composites are described in Section 2.2.

2.2 Microwaves and Microwave Heating

2.2.1 Fundamentals of Microwaves

MWs lie in the 300 MHz to 300 GHz range in the electromagnetic (EM) spectrum [9,55-57], with wavelengths ranging from 1 mm to 1 m in a vacuum (Figure 2.2). The speed at which EM waves can travel depends on the medium in which it is travelling, reaching its maximum speed when travelling through free space (i.e. perfect vacuum) at the speed of light (~3×10^8 m/s).

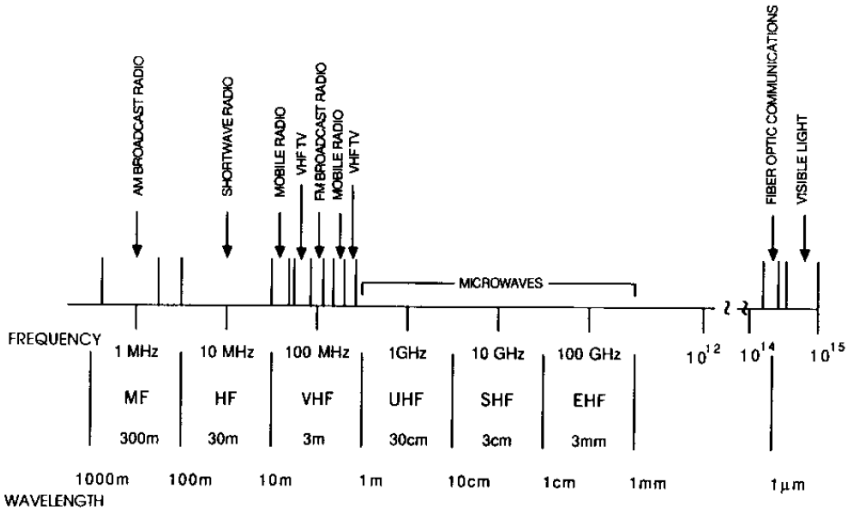


Figure 2.2 The electromagnetic spectrum [58].

All MWs have an electric field *E* and magnetic field *H*, whereby the field intensity at any point in space is based on a sine or cosine function varying with time, and the component electric and magnetic waves travel in the same direction at all points in space. *E* and *H* are perpendicular to each other along the direction of propagation [59,60] as seen in Figure 2.3.

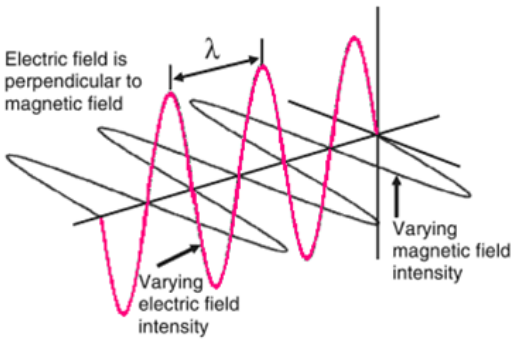


Figure 2.3 A schematic of an electromagnetic wave (λ = wavelength) [58].

2.2.2 Fundamentals of Microwave Heating

In isotropic dielectric materials, the phenomena of MW heating can be explained by the displacement of positive and negative charges under an alternating MW field causing particles to re-orientate, thus generating heat. This mechanism of charge displacement (i.e. polarisation) is dependent on the type of material and the frequency of the applied MW field. The main type of polarisation applicable to the MW range in the EM spectrum is orientation polarisation. Maxwell-Wagner polarisation (also called interfacial or space charge polarisation) can also be found in heterogeneous materials such as composites, however this phenomena is normally attributed to low EM frequency, typically at frequencies less than 5×10^7 Hz, and therefore, it is uncertain whether this has a noticeable effect in the MW range. Typically, these two mechanisms, together with resistance heating, form the basis of MW heating of CFRPs [9,61].

The material properties that affect the aforementioned heating mechanisms are:

Electrical conductivity (σ_{ec}): With electrically conducting materials, eddy currents can be induced by the time-varying MW field, similar to what is observed in low frequency induction heating. These eddy currents are dissipated as heat due to the electrical resistance of the material and the heat generation is proportional to the electrical resistivity of the material. However, if the material's electrical conductivity is very high (e.g. metals), the induced currents could produce a magnetic field in the sample that repels the MW's magnetic field, thus limiting the dissipation of MWs through the sample (i.e. no heating generated within the sample) [63]. This is a very important factor to take into account when heating CFRPs, as it infers that the fibre orientation and the lay-up sequence will have a significant impact on the ability to heat the material with MWs.

Complex dielectric constant (ε^*): A dielectric material is a material that has the ability to store energy when an external electric field is applied. As MWs enter the material and transmit energy, heat is generated within the material. The complex dielectric constant can be expressed as:

$$\varepsilon^* = \varepsilon' - j\varepsilon'' \quad \text{(Eq. 2.1)}$$

where ε' and ε'' are the dielectric constant and dielectric loss, respectively.

The dielectric constant (ε') describes the penetration of MWs into the material and is a measure of how much electrical energy from an external electric field is stored in the material. The imaginary part of the complex dielectric constant is the loss factor (ε'') and represents the material's ability to turn energy into heat when an external EM field is applied.

The dielectric loss tangent $\tan\delta_{dielectric}$ is another common term used to describe the dielectric response and expresses the efficiency of the material to convert absorbed energy into heat. The loss tangent (in which $\delta_{dielectric}$ is the phase difference between the oscillating electric field and the polarisation of the material) is calculated as the ratio of the imaginary part of the complex dielectric constant ε'' to the real part ε':

$$tan\delta_{dielectric} = \frac{\varepsilon''}{\varepsilon'} \qquad \text{(Eq. 2.2)}$$

Table 2.2 provides the dielectric properties for some common materials at specific frequencies and temperatures.

Table 2.2 The dielectric constants of some common materials [64,65].

Material	**Remarks**	**Temperature (°C)**	**Frequency**	**Dielectric constant (ε')**	**Dielectric loss (ε'')***	**$\tan\delta_{dielectric}$**
Alumina*	Pure	20	3 GHz	8.90	0.01	0.001
Borosilicate Glass	Normal	20	1 MHz	5.3	0.0047	0.0009
Diamond	-	20	100 MHz	5.5	Not available	
Epoxy*	Araldite	25	3 GHz	3.14	0.076	0.024
Ice*	-	-12	3 GHz	3.2	0.003	0.001
Polyethylene (PE)*	-	20	3 GHz	2.3	0.0026	0.001
Polypropylene (PP)	-	20	1 MHz	2.2	0.0004	0.0002
Poly-tetra-fluoro-ethylene (PTFE)*	Teflon®	20	3 GHz	2.1	0.0003	0.0001
Silicone*	Unfilled	25	3 GHz	7.8	0.48	0.062
Water*	Distilled	20	3 GHz	76.7	12	0.156
Wood	Balsa	20	30 GHz	1.2	Not available	

*Von Hippel [65]

Many different variables influence the dielectric properties of a material under MW exposure. Temperature, MW frequency and moisture content are some of the typical factors which need to be taken into account, making MW absorption and material behaviour very complex and leading to a unique process that has to be tailored specifically for individual applications. Some of these factors are described below.

i) Influence of Temperature

The dependence of the dielectric constant (ε') and dielectric loss (ε'') of water on temperature at different frequencies is shown in Figure 2.4, where the dotted line sections represent a theoretical plot, and the continuous lines represent data from experimental results. It can be seen that both ε' and ε'' achieve maxima within the temperature range considered. At 2.45 GHz, these maxima occur at ~0 °C

and ~-30 °C for ε' and ε'' respectively. After reaching its peak, ε' and ε'' keep decreasing with temperature, but for the latter the decay after ~40 °C is minimal as it reaches a plateau.

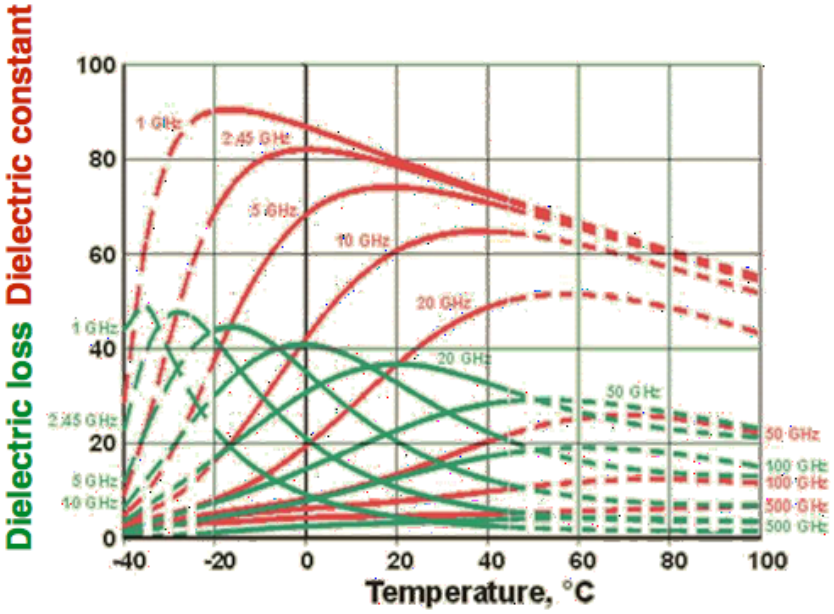


Figure 2.4 Relation between dielectric constant, dielectric loss, frequency and temperature of water [66]. Continuous and dotted lines taken from experimental and theoretical data respectively.

Zong *et al.* [67] carried out a similar investigation for an epoxy-amine system at 2.45 GHz between the temperatures of 20 °C and 90 °C, and degree of cure from zero to 82%. It was shown that both ε' and ε'' increased with temperature and decreased with degree of cure (Figure 2.5 and Figure 2.6), and were highly affected by the number of polar groups (i.e. greater number of polar groups when the resin has a low degree of cure), and resin viscosity (i.e. greater molecule mobility at a low degree of cure).

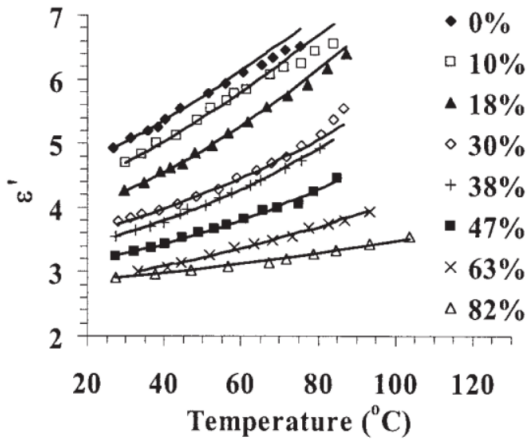


Figure 2.5 Theoretical (lines) and experimental (points) dielectric constant of epoxy as a function of temperature and degree of cure [67].

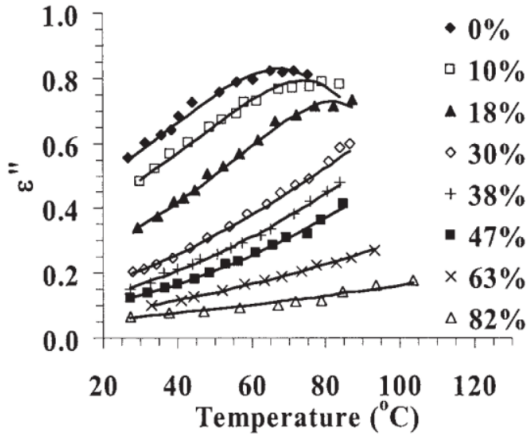


Figure 2.6 Theoretical (lines) and experimental (points) dielectric loss of epoxy as a function of temperature and degree of cure [67].

In the case of thermoplastic materials, the initial loss factor is very low (Figure 2.7), and ε' and ε'' increase with increasing temperature due to the increasing mobility of the molecules as it approaches the material's softening and melting temperatures. This can have a detrimental effect when attempting to heat a material in a non-homogeneous MW field, as the region with the high temperature will continue increasing in temperature at a faster rate than the rest of the part, thus risking over-heating certain regions and under-heating other regions [9].

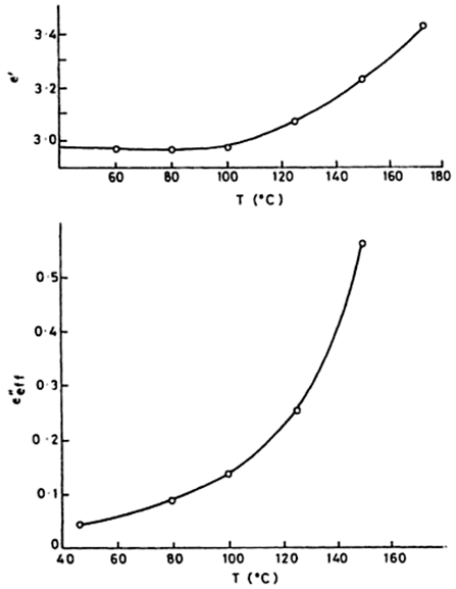


Figure 2.7 Dielectric properties of Nylon 66 at 3 GHz [68].

ii) Influence of Microwave Frequency

The frequency of the MW not only contributes directly to the dissipation of the MWs through the material, but also has the ability to influence the dielectric constant [68]. For water the relation between the dielectric properties and MW frequency can be seen in Figure 2.8, which shows the dielectric constant to be high and constant up to ~8 GHz, then undergoes a steep decrease as the frequency increases further. Dielectric loss on the other hand is low at 0.8 GHz and shows a steady increase, having a peak dielectric loss value at ~20 GHz.

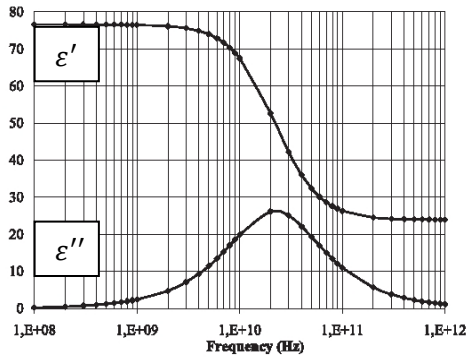


Figure 2.8 Dielectric constant and dielectric loss of water as a function of MW frequency [69].

A similar trend is observed for epoxies prior to the initiation of the curing process, as seen in Figure 2.9. What this shows is that materials will typically have a frequency at which the dielectric constant is highest, and another frequency at which the dielectric loss is highest, thus requiring a compromise to obtain the highest heating efficiency (i.e. $\tan\delta_{dielectric}$) for the material and part under investigation.

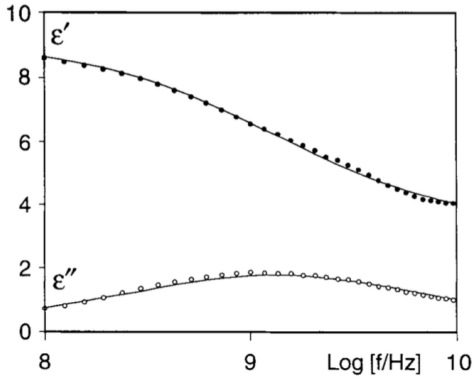


Figure 2.9 Theoretical (line) and experimental (points) dielectric constant (ε') and dielectric loss (ε'') of uncured epoxy as a function of frequency at constant temperature 70°C [70].

iii) Influence of Moisture content

Dielectric properties are greatly affected by the content of moisture in a material since water has a very high dielectric constant and loss (approximately 77 and 12 respectively [65]). Usually, the dielectric constant and loss of the material to be processed has a much lower value, e.g. 3.1 and 0.076 respectively for epoxy [65], thus the dielectric constant would increase if water is added to the material [71,72].

However, moisture can decrease a polymer's physical and mechanical properties [22], and so adding water into a resin to improve the MW heating characteristics is not a viable option. Unfortunately, some materials can contain moisture due to absorption from the atmosphere. The degree of absorption will depend on the material type (e.g. Nylon is known to have a high water absorption) and condition (e.g. degree of cure of thermosetting resins), and this needs to be taken into consideration if the material is to be MW heated by ensuring a consistent environment when handling, storing and processing the material.

iv) Influence of other variables

- MW power: As the power increases, the electric field increases and the number of polarised dipoles also increases. Therefore, the dielectric loss factor increases as MW power increases [71,72]. However, the heating will only continue to increase as long as there are 'free' dipoles available capable of interacting with the additional MWs (i.e. the material has a limited capacity to absorb MWs) and thus also has a limitation to transfer this energy to heat.
- Material composition: For composite materials in particular, where the material is composed of two or more constituents, the volume content and orientation of the reinforcement plays also a key role [9,73]. This is particularly critical for materials that highly absorb MWs such as carbon fibres as these will dominate the MW heating process. For example, a UD laminate will absorb MWs and heat differently compared with ±45° or 0°/90° laminates (assuming a homogeneous MW field, where the direction of the excitation field is constant across the volume of the laminate).

The existence of all these complexities mean that significant work is required to fully simulate the MW heating of materials, particularly for the heating of CFRPs.

Complex permeability (μ)*: In a manner analogous to the complex dielectric constant, the complex permeability can be described as:

$$\mu^* = \mu' - j\mu'' \quad \text{(Eq. 2.3)}$$

where μ' is the magnetic permeability and μ'' is the magnetic loss factor under the influence of the alternating magnetic field [9]. Again, similar to the case of ε' and ε'', heating is due to hysteresis losses caused by the time-varying magnetic field.

In the case of carbon-epoxy composites, the value of permeability is low (approximately 1.26×10^{-6} H/m [65]. However, it is necessary to include this variable as this is a requirement to calculate the penetration depth (more details regarding penetration depth in Section 2.2.4).

2.2.3 Arcing/Electric Discharge

One undesirable effect on the application of MWs to heat CFRPs is the possibility of a phenomenon commonly referred to as arcing (also called electric discharge). Arcing is the release and transmission of electricity in an applied electric field through a medium [60], e.g. gas, and is likely to occur when electrically conducting parts are close to one another in a region where the MW field is very high [61], and can cause material, mould, applicator, magnetron damage, [62] and in the worst cases, even fire. At atmospheric pressure, the breakdown field (i.e. the electric field necessary to cause arcing) is approximately 10^6 V/m (i.e. 10 V/μm). In a domestic MW with a frequency of 2.45 GHz and 700 W of power, the field does not exceed 5300 V/m, which explains why there is no arcing when MWs are launched into an empty metallic cavity, except when sharp electrically conducting items (e.g. metallic fork) are introduced [61]. Therefore, when taking into account that the diameter of carbon fibres and the spacing between them is less than 10×10^{-6} m in typical CFRP composites, in theory only a small potential difference (i.e. voltage) of only 10 V at the tips of the carbon fibres is sufficient to cause arcing.

The highly homogeneous MW field in the VHM helps in minimising arcing by constantly changing the MW field, minimising the probability of fixed wave patterns in the applicator. This in turn minimises the charge build-up at the tips of the carbon fibres, which is the cause of arcing as mentioned above. The methodology used to avoid arcing when curing CFRP composites is described in Section 3.1.3 and 3.3.1.

2.2.4 Penetration/Skin Depth

EM energy is converted to heat as a result of the loss (dielectric and resistive) properties of the materials. As MWs penetrate deeper into the material, more energy is transferred to the material,

causing a decrease in MW energy, i.e. there is an inverse relationship between heating ability and MW penetration.

In general, when an EM wave is incident on a plane surface of a material, a substantial amount of energy is reflected at the air-sample interface and the remaining energy enter the material with a change of direction (i.e. refraction). The energy transmitted into the material is progressively absorbed, decreasing the magnitude of the MW energy as it penetrates into the material. The theoretical value of penetration depth for carbon-epoxy composites can be obtained by using eq. 2.5 [73]:

$$D_p = \sqrt{\frac{1}{\pi \cdot f \cdot \mu\prime \cdot \sigma_{ec}}} \qquad \text{(Eq. 2.5)}$$

where f is frequency (Hz), μ' is magnetic permeability (H/m), and σ_{ec} is electrical conductivity (S/m). Assuming a μ' of 1.26×10^{-6} H/m, σ_{ec} of either 2×10^{4} S/m or 100 S/m for waves parallel and orthogonal to the carbon fibre direction respectively of a CFRP, and MW frequency of 2.45×10^{9} Hz, a penetration depth of ~1 mm and less than 0.1 mm for orthogonal and parallel polarisation respectively is obtained [73].

2.3 Influence of IFSS on Mechanical Properties of Composite Materials

It has long been known that the mechanical properties of composite materials are highly dependent on its individual constituents, i.e. fibre and matrix. However, the role of the interface plays also a key part [74-82], since the interface is responsible for transferring the load from the matrix to the fibres. It has generally been accepted that poor fibre-matrix adhesion leads to poor composite properties [80]. Madhukar and Drzal [75-78] carried out an extensive investigation into the effect of fibre-matrix IFSS on the mechanical properties of conventionally-cured CFRPs by creating three composite systems, i.e. untreated (AU-4), surface treated (AS-4) and surface treated and sized (AS-4C). They showed that the strength, modulus and Poisson's ratio in 0° tension was unaffected by the surface treatments, however, the strength and strain to failure were highly affected by the surface treatment when tested perpendicular to the fibre direction, with the strength increasing with increasing IFSS. The 90° tension

tests showed a change in failure mode [75]. When tested in 0° compression, an increase in IFSS of 119% increased the compression strength and strain to failure by ~69% and 49% respectively [76]. In addition, under in-plane shear testing (i.e. ±45° tensile test), it was shown that the modulus was insensitive to the changes in IFSS, however the strength increased by 162% when the IFSS increased by 118% [77]. Mode I interlaminar fracture toughness increased almost linearly with IFSS – an increase in IFSS of 19% led to a subsequent increase in interlaminar fracture toughness G_{1C} (using double cantilever beam (DCB) testing) by 17% [78].

2.4 Microwave Processing of Polymer Matrix Composites – Past Work

Many papers have been published in the field of MW heating of materials, such as plywood [83], rubber [84], polymers [26,85-89] and polymer composites [11-25,27,28,90-103], just to name a few. The current review will only focus on MW heating of CFRP composites, and more specifically carbon fibre reinforced thermosetting composites, as these present a set of specific challenges (i.e. arcing, selective heating and exothermic reaction) which other types of materials (e.g. thermosetting polymers, thermoplastics, glass-reinforced polymers) do not experience. The existence of these unresolved challenges may be the reason why there are relatively few publications on MW curing of carbon fibre reinforced thermosetting composites. This also explains why the results presented in the past were highly scattered, and why little work was done on process reliability [7].

One of the first factors that need to be assessed is the equipment and the methodology that was used to manufacture the composite laminates by previous investigators. Normally the manufacturing equipment used is considered merely as a tool to produce test samples. In the case of MW curing of composites, the equipment used will influence the setup and the operational procedure, which in turn will affect the material's performance. Additionally, because the material's performance will be greatly influenced by the MW field homogeneity, it is important to assess the results obtained in relation to the equipment and methodology used. This is more so when considering that some early test results were based on samples manufactured using domestic MW equipment [25,93,95], which

most likely had a low probability of obtaining a highly homogeneous MW field, as well as lacking power and temperature control, and the application of vacuum pressure on the sample during curing was not possible.

MW field homogeneity is a big concern, particularly for the studies carried out using fixed frequency systems [13-15,25,34,93-95,98,99], since MW field homogeneity is related to cure homogeneity. None of the reviewed literature reported studies to investigate the degree of MW field homogeneity within their respective cavities, and based on the dimensions of the samples produced (i.e. less than 100 mm ×100 mm, which is less than one MW wavelength) using a fixed frequency of 2.45 GHz, it suggests that the field was not homogeneous, thus agreeing with the criticisms related to difficulties in up-scaling the MW heating process [100]. These drawbacks however are not limited to only domestic MW equipment, since the samples produced using custom-built systems [13-15,34,94,98,99] were of similar dimensions, with the exceptions of Papargyris [16] and Paulauskas [97], who used VFM equipment and produced 200 mm × 200 mm (fluctuating frequency between 4 and 8 GHz) and 150 mm × 150 mm laminates respectively (varying frequencies of 5±1 GHz, and 13.8±1 GHz).

The lack of temperature control was common for most of the aforementioned work [12,14,15,25,34,94,95,97-99], and therefore power was not controlled as a function of time or temperature in order to obtain a constant heating rate, nor a fixed dwelling temperature. In these cases, the laminates were cured by setting ‘x’ MW power for ‘y’ time. One exception was Lee [93], who controlled the power manually when the temperature of the sample reached the desired dwell temperature, and Papargyris [16] who used an automated temperature-power feedback control.

Lack of pressure was also common for most of the aforementioned work [13-15,34,94,97-99], for the exceptions of Lee [93], who applied a positive pressure of approximately 4.5 bar (with no vacuum bagging however), and Nightingale [95], who applied a PTFE sleeve around the composite laminate, also without vacuum bagging. Nightingale [96] reported arcing problems, which is not surprising taking into account that Lee [93] was the only author suggesting and implementing a methodology to

avoid arcing at the tips of the carbon fibres. The method consisted of using perforated aluminium tape at the edges of the laminate. The use of aluminium tape is an effective way to avoid accumulation of charges at the tips of the carbon fibres, however it has a number of drawbacks. Firstly, the aluminium tape will reflect the MWs that are incident on the tape, thus reducing process efficiency and generating a more complex MW field. Secondly, the high thermal conductivity of aluminium will lead to the heat loss from the composite to the aluminium tape, and thirdly, the combination of the two aforementioned effects will cause a complex heating pattern between the aluminium tape and the composite, thus making the process more unpredictable and inconsistent.

One final remark regarding the methodology employed by previous researchers is the use of non-metallic moulds, such as PTFE [15,34,93-95,99], glass-reinforced PTFE [93], PP [93], Macor® [16] and Quartz [97]. The materials chosen were materials with low dielectric properties with a maximum operating temperature above the curing temperature of the respective composite material. There are however risks associated with PTFE, as it is known that PTFE produces a toxic bi-product, i.e. carbonyl fluoride, when decomposed at high temperature (~450 °C).

The samples investigated in the past were in the form of UD [15,34,93,94,97,99] and multi-directional (MD) [15,16,93,94,97] laminates, and some tests were also done with single fibre model composites [13,14,25,98]. The thickest laminate investigated was 38 mm [94], however MW heating was used for post-curing only. Lee [93] and Paulauskas [97] did not succeed in curing woven composite laminates using a fixed frequency of 2.45 GHz, and variable frequencies of 5±1 GHz and 13.8±1 GHz, respectively. The remaining authors cured UD laminates and single fibre model composites, with varying degrees of success.

The authors that managed to MW cure carbon fibre reinforced thermosetting composites reported a significant decrease in cure cycle [13,16,95,97-99,101,102] in comparison with conventional curing methods. As an idea in terms of the magnitude of the reduction in cure cycle, Agrawal [13] achieved MW curing in 15 minutes as opposed to the conventional five hours, Nightingale [95] achieved MW

curing in 40 minutes compared with the 200 minutes required conventionally, and Paulauskas [97] achieved MW curing in two hours compared with the typical 4.5 hours. These results show a significant variation in cure cycle reduction, which is believed to be due to the different equipment and methodologies, in addition to the different materials used. For example, when a small sample is heated in a small MW applicator, it has the advantage that the setup can be designed so that MWs can be almost entirely focussed on the sample, thus concentrating the energy and therefore achieving a high heating rate. The drawback however is that hot-spots will be unavoidable with larger samples. On the other hand, dispersing the energy across a larger applicator and sample allows a more homogeneous heating, but possibly at the expense of heating rate. However this could be less problematic since MW power could be increased.

Mijovic *et al*'s [10] investigation on epoxy resin was the only publication that reported a decrease in curing rate using MWs compared with conventional methods. This was despite the fact that no differences were observed in reaction kinetics.

In terms of mechanical performance of MW-cured composites, Paulauskas [97] was the only author to report a decrease in T_g (~20%), 0° ultimate tensile strength (UTS) (~9%) and 90° UTS (~9%) at both 5±1.0 GHz and 13.8±1.0 GHz. On the other hand, Papargyris [16] and Nightingale [95] reported similar flexural strength and modulus values when laminates were cured using MWs, Wei *et al.* [34,94,99] reported an increase in flexural strength and modulus, and Fang [91] reported similar flexural strength and modulus values at room temperature, but higher values at 177°C when cured using MWs. In addition, ILSS values presented by Nightingale [95] and Papargyris [16] using short beam shear (SBS) tests showed similar, and a 9% increase, with MW-cured laminates respectively.

Subsequently, Agrawal and Drzal [13], Wei *et al.* [15], Papargyris [16] and Day [25] all investigated the effect of MW curing on the fibre-matrix interface. They all reported an improved fibre-matrix bond, and attributed the increase in mechanical properties primarily to this factor. However, Agrawal [13] and Day's [25] publications are the only ones that provide quantitative values of increase in IFSS

(70% and 20% respectively), but these were obtained by testing single fibre model composites only. The remaining publications [15,16] were based on failure mode investigation using SEM, where the failure mode changed from interface-dominated to matrix-dominated.

Based on the MW curing results on single fibre composites, Agrawal [13] stated that the conductive nature of carbon fibres led to a concentration of energy, and therefore heat, at the fibre-matrix interface, thus causing an unidentified phenomenon, which could have led to:

- Differences in physical and mechanical properties at the interface in comparison with the bulk matrix due to the high temperature.
- MWs causing chemical changes of the fibre sizing.
- Sharp temperature gradient from the fibre to the matrix affecting the properties of the bulk matrix.
- Since the carbon fibres absorb most of the MWs, the heat will predominantly go from the fibre to the matrix, thus curing the interface before the bulk matrix, and hence producing a stress-free interface with improved adhesion.

Thostenson [103] suggested that the changes may be chemical, with MWs potentially initiating chemical reactions that are not possible using conventional heating methods.

2.5 Literature Review – Summary

The following topics were presented in chapter 2;

- *Alternative manufacturing methods*. It has been shown that several alternative manufacturing methods exist today as potential replacements of existing conventional oven and autoclave systems. There is no evidence however that one technology will dominate over the others, as there are no indications that a ‘one size fits all’ solution is actually possible or beneficial. It is expected that in the future, manufacturers of composite parts will be faced with a greater number of possibilities in terms of curing methods and material systems, and therefore the

procedure of selecting a manufacturing method for a specific application using a specific material system will be more complex. However, this will only be possible once a better understanding is obtained of the various alternative processes, and its impact on material performance and overall process efficiency (i.e. financial impact).

In this sense, MWs could offer rapid heating (although potentially not as fast as induction), reduced tooling costs, especially when compared with induction, relatively low capital and running costs, especially if using common frequencies such as 2.45 GHz, thus potentially providing a highly efficient process. In addition, if the improvement in mechanical properties is confirmed, then this could also be a big added bonus. However, as mentioned previously, these advantages will be application-dependent, and it is assuming that arcing and uneven MW distribution issues are resolved, thus producing consistent results.

- *MW heating theory*. The key parameters to take into account when considering the use of MWs for heating composite materials are its MW absorption and loss properties which in the case of CFRPs is fibre-dominated. The penetration depth is a result of the MW absorption of the material. The calculation of such parameters for standard isotropic materials is relatively simple, as demonstrated by the large dielectric property value database provided by von Hippel [59] for example. However, the calculation for anisotropic materials with low electrical conductivity such as CFRPs is more difficult to carry out due to the many variables involved, and the uncertainty regarding the interaction of the different effects.
- *Literature review of MW heating of carbon-epoxy composites*. In most cases, it is difficult to directly compare the different studies that have led to uncertainties regarding the technology. The only conclusion that could be obtained from the literature review is that MWs reduce the time to cure composites. However, even this conclusion could be challenged if taking into account only the literature available to date.

The information presented in the literature review leaves little doubt that the curing conditions were far from ideal and therefore an improvement in process methodology is required to produce good

quality laminates in a reliable and consistent manner with dimensions large enough to follow the relevant mechanical test standards in order to verify the results and conclusions provided in the past.

Based on the literature review, the discrepancies in the results presented in the past by other investigators [9-16,18,25,27,28,73,90,91,93-103] are believed to be mainly due to;

i) *Significant differences in hardware design*: MW systems require careful design, as achieving a high MW field homogeneity is of critical importance to achieve a highly homogeneous heating throughout the material. The MW systems used in the past were relatively simple systems, and therefore it would seem unlikely these systems could avoid cold and hot spots across the sample, as evidenced by the scepticism that has existed and exists even today regarding MW heating of CFRP composites.

ii) *Different methodologies used to define the process cycle*: Most of the aforementioned MW systems lacked temperature control, thus the processing methodology was typically 'x' MW power for 'y' time. Such a heating profile would have produced a variation in heating rate as a function of time, and a fixed dwell temperature would have been unlikely. This would have inevitably led to a very different cure cycle to the one which thermosetting resins are normally designed to follow. Additionally, in conjunction with point i), different MW cavity designs, and waveguide design (or lack of), probably had a different effect on the material (even if they were set at the same MW power) due to the different MW field distributions present in the cavities, i.e. the reproducibility of the heating process and subsequent material test results are unlikely. Additionally, vacuum bagging was not present in past investigations, possibly due to arcing problems, and therefore the laminate quality is questionable.

iii) *Exposed carbon fibres cause arcing*: Arcing causes three very undesirable effects; first is the detrimental damage on the material, second is that vacuum bagging becomes unfeasible, thus leading to high void content, and finally, the health and safety implications. The probability of arcing is greater in inhomogeneous MW systems. Only Lee [93] presented a method to avoid arcing using perforated aluminium tape, however no author referenced this methodology, nor investigated other methods to avoid arcing.

This could potentially mean that the other authors attempted the methodology however still did not succeed in avoiding arcing.

iv) *Mechanical tests carried out on samples with non-standardised dimensions*: In the past, sample dimensions produced using MWs were typically less than one wavelength (i.e. 125 mm at 2.45 GHz frequency) and smaller than the dimensions recommended by the relevant test standards such as American Society for Testing and Materials (ASTM) D3039 [104], ASTM D6641 [105] and ASTM D3518 [106], possibly due to the difficulty in obtaining a highly homogeneous MW field over the standard specimen volume, or arcing. The fact that testing of MW-cured composites were only carried out for tension, interlaminar shear (using short beam shear method) and flexure tests (i.e. tests which do not require specific test jigs and can be done with relatively short coupons) is an indication of the serious difficulties that past researchers experienced to produce samples sufficiently large to enable characterisation with a range of standard specimens. Therefore it is not unsurprising that tests under compression loading for example were not carried out, even when compressive properties are possibly, together with fracture, two of the most important mechanical properties of composite materials used in structural applications. As an analogy, when CFRPs are cured in a conventional oven and undergoes excessive thermal runaway (i.e. uncontrolled temperature increase due to the resin's exothermic reaction that leads to material degradation) for example, the material is disposed rather than tested, since the material has undergone an unsuitable cure cycle and the material is not in an acceptable condition. Likewise, knowing that MW heating of CFRPs in the past was not consistent, homogeneous, nor followed a suitable procedure, it is difficult to assume the results in the literature are representative of suitably cured materials. For all these reasons, it can be said that the scepticism that exists today regarding the technology is possibly well justified.

Chapter 3

Experimental Procedure

This chapter provides a description of the materials, consumables and the VHM MW equipment. This is then followed by a description of the operational procedure for curing carbon-epoxy composites in a MW environment without arcing, and a proposed methodology for measuring the MW penetration depth in composites. Subsequently, the different methodologies used for physical and mechanical testing of the manufactured composite samples are reported, and the chapter concludes with a description of the methodology used for material failure assessment.

3.1 Materials, Consumables and Equipment

3.1.1 Carbon-Epoxy Composite Material and Lay-up Sequence

Only a single, well-characterised material was used throughout the present study for consistency purposes. The material chosen was Gurit OoA continuous UD 600 g/m^2 carbon fibre reinforced epoxy SPARPREG [107] composite pre-preg (here onwards referred to as 'SPARPREG'), which has a poly-acrylonitrile (PAN) based carbon fibre with an elastic modulus of 255 GPa, tensile strength of 4.3 GPa, fibre density of 1.8 g/cm^3 and a cured ply thickness (CPT) of 0.6 mm. A material in pre-preg form was chosen in order to ensure material consistency and quality, with the aim to minimise the effects caused by inconsistencies, which could be present in other form of materials, for example composites produced by resin infusion techniques.

Table 3.1 shows the cure cycle options provided by the material manufacturer (at a heating rate of 2° C/min), in addition to other cure cycles used in this study.

Table 3.1 SPARPREG cure cycles recommended by Gurit* [107], and MW cure cycles used in the present study.

	Time to 95% Cure (Minutes)		
Cure Temp. (°C)	Incl. ramp-up @ 0.3°C/min from 20°C	Incl. ramp-up @ 2°C/min from 20°C*	Incl. ramp-up @ 10°C/min from 20°C
85	817	632.5	592.5
90	633	395	355
100	447	220	180
110	390	135	95
120	378	95	55

*Manufacturer's recommended cure cycle (MRCC).

The resin used to cover the edges of the carbon fibres was SP9435 [108] from Gurit, which is a monocomponent epoxy resin, which was chosen specifically due to its similarity with the SPARPREG's matrix as suggested by Gurit.

3.1.2 Consumables

Standard vacuum bagging consumables from Cytec [109] (formerly Richmond Aerovac) were used to manufacture composite materials throughout the present work for both MW curing and conventional oven curing. The individual items are described below.

Vacuum bagging film: 526260SHEET – Capran 526, heat stabilised high temperature Nylon 6/6 bagging film. 50 μm thick, flat sheet.

Vacuum bagging sealant tape: SM5143 – General-purpose sealant tape, 3 mm thick.

Release film: A6000BNP1515 – A6000, non-perforated ethylene-tetra-fluoro-ethylene (ETFE) release film, 15 μm thick.

Bleeder/breather fabric: AB33N60 – Heavy weight 340 g/m^2 nylon/polyester non-woven blended breather fabric, 1.52 m wide.

Release fabric/peel ply: B444460 – 60 g/m² silicone release coated Nylon peel ply.

Flashtape: FT10572 – Flashtape 1, 12.5 mm wide.

3.1.3 Vötsch Hephaistos Microwave (VHM) System

A VHM 100/100 system as seen in Figure 3.1 was used in this study. It has a hexagonal cavity with 12 magnetrons symmetrically located around the cavity with two magnetrons on each side of the hexagon. Each magnetron is capable of producing a maximum MW power output of 0.85 kW at a fixed frequency of 2.45 GHz. The power output of this system can be adjusted from 0.51 kW (5%) to 10.2 kW with a minimum resolution of 10 W [110]. One fibre optic probe connected to the VHM was used to provide the temperature feedback loop to control the MW power. This probe was labelled as T_{mw} throughout this study.

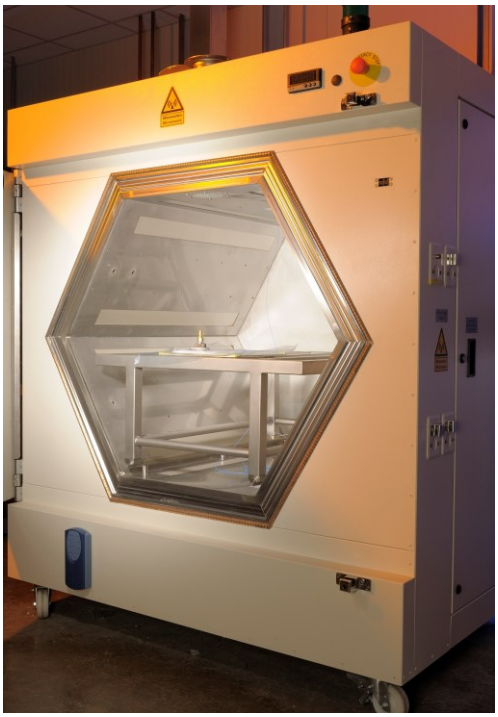


Figure 3.1 VHM 100/100 system located in TWI North-East (Middlesbrough).

The main difference between the VHM system and other systems used in the past to cure composite materials (i.e. domestic and custom-built MW systems [8-22,24,25,87-100]) is that the VHM was purposely designed to achieve a very homogeneous MW field. This was achieved through the development of:

i. Hexagonal cavity: A hexagonal cavity provides six sides, with two magnetrons on each side, thus releasing MWs at six different angles, and equally encourages MWs to reflect at a

minimum of six different angles in the cavity, thus assisting in dispersing MWs in different directions.

ii. Waveguide design: The waveguide design is unique, where the multiple slots (which the MWs use to exit the waveguide and enter the cavity) have different widths (labelled as y_2 in Figure 3.2) and are offset by varying distances from one another (labelled as y_1 in Figure 3.2) in order to create different MW release points. Figure 3.2 shows a schematic of the waveguides used in the VHM. It was not possible to include the original engineering drawing due to confidentiality reasons.

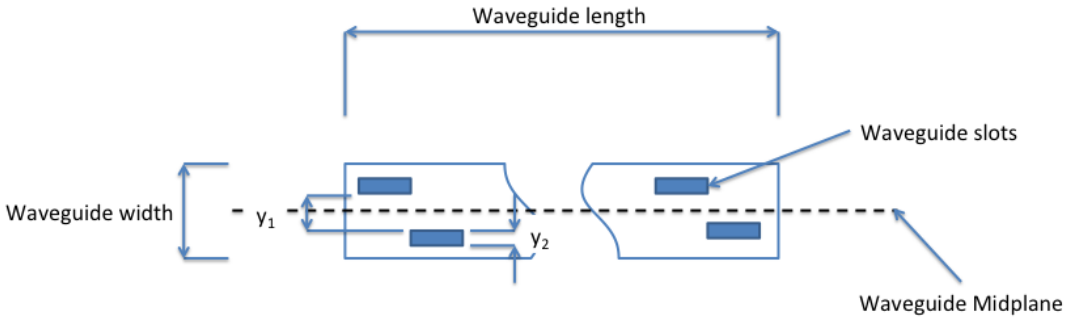


Figure 3.2 Schematic drawing of waveguides used in VHM 100/100.

iii. Firing sequence: A continuously varying MW firing (i.e. magnetron activation) sequence creates a different EM field per rotation (the term rotation is used here based on the assumption that all magnetrons 1 to 12, irrespective of its sequence, will activate once before being activated a second time), thus leading to a constantly changing MW field.

iv. Combination of the above: The VHM's 2.45 GHz fixed frequency system means that the wavelength is also fixed (~125 mm) and, therefore, the EM field pattern that can be achieved is limited. The way the VHM system produces a homogeneous MW field is through a combination of all the points above (i-iii, pages 39-40). The method to achieve a high MW field homogeneity is by means of mixing the EM waves as much as possible by offsetting the location of the release of the MWs, encouraging more even MW release and reflection using all the sides of the hexagon, and finally the change in firing sequence enhances the disruption of the MW field and therefore encourage even further the enhancement of the MW field distribution.

Figure 3.3 [110] shows the result of the above, where the green, yellow, orange and red colours describe the MW field. The green and red colours represent the lowest and highest MW field densities respectively. According to this figure, the hexagonal applicator shows very few intensity peaks in the MW field, whereas the circular applicator has a clear high intensity MW field region (represented by the orange-red colour range). Figure 3.3 is only a snapshot, and although the EM fields typically change as a function of time, it is expected that the MW field density will remain relatively constant with time (assuming an empty applicator). Additionally, the MW field density pattern is expected to remain constant, but rotating from the centre of the circle as a function of time.

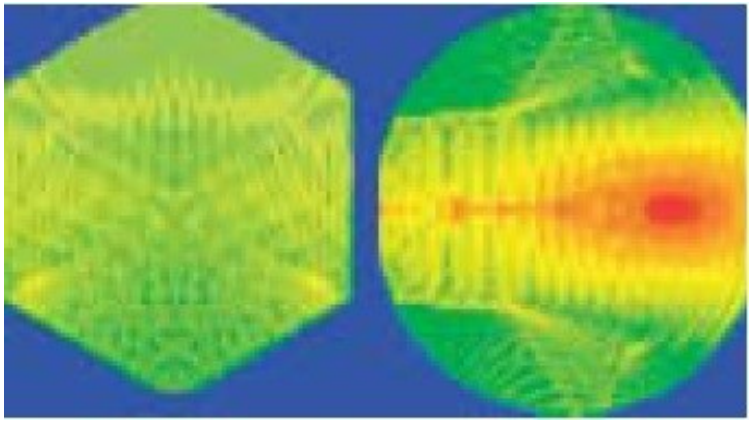


Figure 3.3 MW field distribution simulation [110]. Left: hexagonal cavity, right: circular cavity.

Programming of the heating cycle and control of the MW power was done via S!MPATI, a software developed in-house by the equipment manufacturer. S!MPATI was used throughout the present investigation in order to set the desired heating programme. This software is not specific for the VHM only, but is a modification to the existing software used to program conventional ovens produced by the same manufacturer.

Fibre-optic probes (TS3/4 and TS-Nano) connected to a 4-channel FOTEMP4-16" data logger were used to monitor and record the temperature. These were supplied by Optocon AG (Dresden, Germany). The TS3 probes are safe to operate between -200 to +300 °C and have a resolution of ± 0.2 °C and a response time of ≤ 2 s. The TS4 operate between -200 to +200 °C and has the same resolution and response time as the TS3. The TS-Nano has the same temperature range as the TS4 but a resolution of

± 1 °C, and a response time of ≤10 s. All three types of probes were coated with a PTFE sleeve for protection and ease of removal after curing of the laminates.

The VHM has several safety features installed in order to ensure the safe operation of the system, both for the users and the equipment. The four key safety features are; i) Multiple MW leak detectors that continuously monitor the absence of the EM field between the cavity and the outer enclosure of the system. The equipment shuts down if the MW leak detectors detect high EM fields, ii) The VHM does not activate the magnetrons until the two locking mechanisms attached to the door are appropriately secured, iii) The MW field densities reflected back into the waveguides are also continuously monitored and the system shuts down if the level is above a defined threshold, and iv) the VHM can be programmed so that the equipment shuts down if the sample temperature (detected by the probe connected to the VHM), or the MW power, exceeds a pre-defined limit.

3.2 MW Heating of Water

The MW distribution within the VHM was assessed prior to MW curing of CFRPs by carrying out some basic heating tests of water (Figure 3.4) in order to gain some confidence regarding the MW field distribution within the VHM cavity. Two polypropylene (PP) beakers containing approximately 500 mL of water were placed on top of PTFE sheets at different locations within the MW chamber. The locations chosen were an attempt to resemble the worst-case scenario, i.e. in close vicinity to the edge where a composite laminate could potentially be placed. Additionally, one of the tests, i.e. test ‘e’, was carried without the metallic bench to simulate the case when a large part is introduced into the cavity, and thus resembles the scenario seen in Figure 3.3.

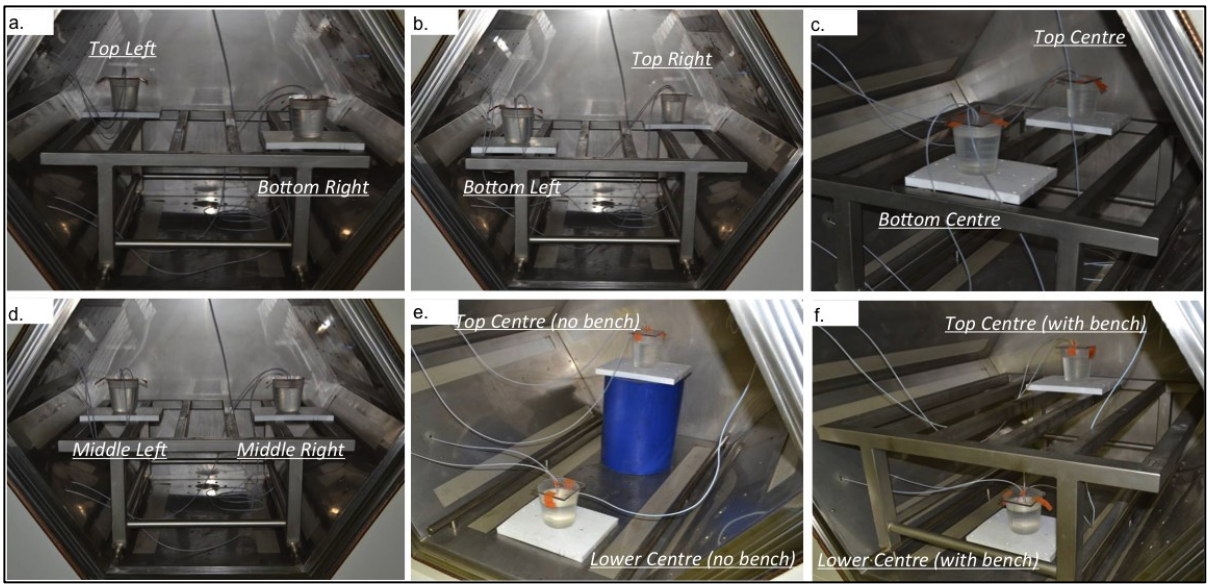


Figure 3.4 PP beakers containing water in six different configurations to assess the MW distribution.
a. Top left and bottom right, b. top right and bottom left, c. top centre and bottom centre, d. middle left and middle right, e. top centre and lower centre (no bench), f. top centre and lower centre (with bench).

Four fibre-optic temperature probes (two in each beaker) were used to monitor and record the change in temperature. 5% MW power (i.e. 0.51 kW) was used throughout the process, and heating was stopped when the water temperature reached 90 °C. The tips of the fibre optic probes were positioned at the 250 ml mark in all cases. The results (Section 4.1) obtained provided the necessary confidence regarding the MW field distribution of the VHM system in order to move on to curing of CFRPs.

3.3 Curing Methods and Procedures

3.3.1 MW Curing of Carbon-Epoxy SPARPREG

The MW curing setup and procedure in the present study was kept as consistent as possible with existing ones in the composites industry (Figure 3.5 [111]) to allow a fair comparison with conventionally-cured laminates. Typical consumables (described in Section 3.1.2) employed for oven curing of composites were used, such as breather/bleeder cloth, release ply and vacuum bag.

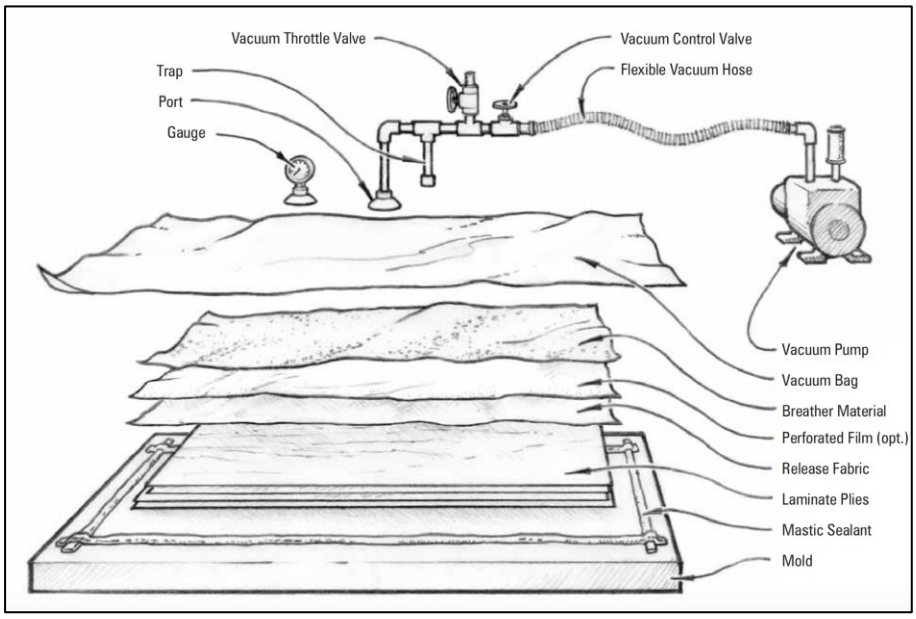


Figure 3.5 Schematic of vacuum bagging setup used [111].

The SPARPREG prepreg material was removed from the freezer and stored at ambient conditions (i.e. maximum 20 °C and 60% maximum RH, as defined in the Composite Materials Handbook [112]) 24 hours prior to handling and cutting. Cutting was carried out manually using a Stanley knife and an aluminium template with dimensions of 300 mm × 300 mm.

Two laminates with two plies each were laminated manually and then debulked in a vacuum table for 30 mins. The two-ply laminates were then laminated to produce a single four-ply laminate, and was then further debulked for an additional hour. The laminating and debulking process was repeated until the desired number of plies was achieved.

Four plies were laminated to produce 2.4 mm thick laminates for tension, compression and IPS testing coupons. Eight plies were laminated to produce the mode I interlaminar fracture coupons, and 100 plies were laminated to produce the 60 mm thick laminates.

An ETFE film (described in Section 3.1.2) with dimensions of 100 mm × 300 mm was introduced in the laminate between plies four and five prior to debulking in order to produce the mode I interlaminar fracture coupons. The edge of the ETFE film that was embedded in the laminate created the crack initiation point for the mode I interlaminar fracture testing.

In the case of the 60 mm thick laminate, the bottom and top sub-laminates were comprised of two plies each, whereas the remaining 12 sub-laminates were comprised of eight plies each, (separated with peel plies between each sub-laminate to allow easy removal of the sub-laminates for testing after curing) with an ETFE layer in between the plies four and five of each of the sub-laminates to create the crack initiation point for the mode I interlaminar fracture testing. An aluminium plate was used as the mould for curing the 2.4 mm and 4.8 mm thick laminates, whereas a cordierite (i.e. a machinable engineering ceramic) mould was used for the 60 mm thick laminate. Both the aluminium plate and the cordierite mould had dimensions of 400 mm × 400 mm.

The most distinctive aspect of the setup and process methodology compared with studies from other authors [12,14-16,25,34,93-95,97-99] was the shielding of the ends of the carbon fibres using epoxy resin to avoid exposed carbon fibres – this is imperative as without the shielding of carbon fibres the vacuum bag will be punctured (i.e. not allowing full consolidation) and the material will be damaged due to arcing. The health and safety implications of arcing (i.e. combustion of material and consumables) should also not be forgotten. Figure 3.6 shows a CFRP laminate where multiple areas, particularly the corners, were burnt. This was the result of the laminate being heated in the VHM 100/100 cavity for two minutes at the minimum MW power of 510 Watts with no shielding.



Figure 3.6 A burnt CFRP laminate when heated in the VHM 100/100 with no shielding at the edges of the laminate.

The author has identified two different ways to avoid arcing; through the use of aluminium tape, or epoxy resin. The aluminium tape was used to earth the fibres, where the excess current at the carbon fibre ends was transferred to the aluminium tape, and then to the mould and the metallic bench, and ultimately to the walls of the MW cavity, thus avoiding charge build up and arcing. The main drawback of using aluminium tape for shielding was the difficulty in ensuring an even current (and therefore heat) distribution. The overlap area between the tape and the laminate needed to be identical on all four sides to ensure an even and consistent heating of the laminate. An additional disadvantage of using this technique is that in certain cases, excessive current was lost, leading to an increase in MW power and, therefore, ultimately making the process less energy efficient or even unsuccessful. It is also believed that aluminium tape restricts the consolidation process, since the tape completely covered the edges of the laminate, thus limiting the removal of trapped air in between the plies and subsequently increasing the laminate void content.

On the other hand, the epoxy resin's dielectric properties absorbs some of the incident MWs, and also minimises the risk of charge accumulation at the tips of the carbon fibres as these were fully covered by the resin and therefore a higher voltage would be required to cause arcing. Therefore, the use of epoxy resin provided more consistent results, with significantly lower energy usage compared with aluminium tape, as the heat was retained within the laminate, and not dissipated to the mould as with the aluminium tape. Removing a MW reflecting material (i.e. aluminium) as a mould and replacing this with a MW transparent material (e.g. thermoplastics, ceramics) is advantageous too as this further increases the process efficiency as the aluminium mould inevitably blocks MWs from the lower half of the VHM applicator to reach the material, whereas the use of a MW transparent mould allows heating through both the top and bottom surfaces of the laminate and therefore can process thicker parts more efficiently. A material with high thermal conductivity such as aluminium is also disadvantageous as it acts as a heat sink. This is not an issue in conventional heating processes as the entire chamber is at the same temperature, however in a MW environment, where only the component is heated, losing heat to the mould and the rest of the cavity can be an enormous loss, thus requiring more energy than is necessary. This is particularly the case when taking into account that the volume of the sample to be processed will always be much smaller than the volume of the cavity.

Shielding the edges of the laminate using epoxy resin was carried out after debulking four plies for the four-ply 2.4 mm thick laminate, and after debulking eight plies for the eight-ply 4.8 mm thick and 100-ply 60 mm thick laminates. Once the shielding procedure was complete, the laminates were debulked one last time for 30 minutes (i.e. epoxy resin underwent debulking too). The remaining setup, i.e. vacuum bagging and use of consumables, were in line with those employed for the production of the oven-cured reference laminate. The laminates were then introduced into the cavity to be cured. A vacuum of 0.9 bar was kept throughout the cure cycle to produce both the oven-cured and MW-cured laminates. The 16 laminates produced using MWs are listed in Table 3.2.

Table 3.2 MW-cured laminates showing curing dwell time defined as S(laminate number)_MW(dwell time at 120°C), laminate size, lay-up sequence, test method and laminate number.

Dwell Time (Minutes)	Laminate Dimension (mm)	Laminate Lay-up	Test Method	Laminate Number
30	300×300×2.4	UD	Tension, 0°	S11_MW30
			Tension, 90°	S12_MW30
			Compression, 0°	S1_MW30
35		UD	Tension, 0°	S4_MW35
			Tension, 90°	S5_MW35
			Compression, 0°	S13_MW35
40		UD	Tension, 0°	S7_MW40
			Tension, 90°	S6_MW40
			Compression, 0°	S8_MW40
		±45°	IPS, ±45°	S28_MW40
	300×300×4.8	UD	Fracture, Mode I	S23_MW40
45	300×300×2.4	UD	Tension, 0°	S15_MW45
			Tension, 90°	S16_MW45
			Compression, 0°	S18_MW45
		±45°	IPS, ±45°	S29_MW45
90	300×300×60	UD	Fracture, Mode I	S25_MW90

Note: Laminates S2, S3, S9, S10, S14, S17 and S19 were used for DSC and optical microscopy and therefore have not been included. The oven-cured laminates are listed in Table 3.3.

Five temperature probes were used to measure the temperature of the 2.4 mm thick laminate when cured using MWs (labelled T1, T2, T3, T4 and T_{MW} in Figure 3.7). Two probes (T3 and T4) were on the top surface of the laminate, and the remaining probes were on the bottom surface of the laminate (i.e. in between the laminate and the mould). T_{MW} provided the temperature feedback to the S!MPATI software, which then controlled the MW power. T1 and T3 were positioned 25 mm inboard from the left edge of the laminate and 150 mm inboard from the horizontal edge (in reference to Figure 3.7). T2 and T4 were positioned 25 mm inboard from the right edge of the laminate and 150 mm inboard from the horizontal edge (also in reference to Figure 3.7). T_{MW} was positioned in the middle of the laminate, i.e. 150 mm × 150 mm inboard from the edges, and linked to the VHM computer.

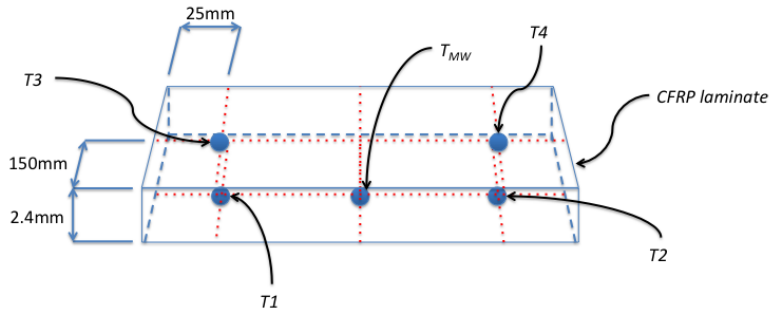


Figure 3.7 Position of the five fibre optic probes that were used to record temperature in the VHM.

300 mm square laminates were produced with; a) thickness of 2.4 mm for tension, compression and IPS tests, b) thickness of 4.8 mm for mode I interlaminar fracture tests, and c) thickness of 60 mm for thick laminate interlaminar fracture tests, however the latter were subdivided into 4.8 mm thick laminate sections using a release film (Figure 3.8). The heating rates for the 2.4 and 4.8 mm laminates were set to 10 °C/min for the MW-cured laminates. The 60 mm thick fracture laminate was heated at a rate of 2 °C/min and a dwell time of 90 minutes for the MW-cured laminates with dwell times of 30, 35, 40 and 45 minutes for the 2.4 mm thick laminates, and 40 minutes for the 4.8 mm thick laminate. The S!MPATI software was used to set a maximum temperature deviation of 1 °C between the set temperature and the actual temperature recorded by the T_{MW} probe, i.e. the probe with the feedback loop.

In order to enable a fair comparison with the oven-cured laminate S26_O90, the temperature was recorded at five different locations through the thickness of the laminate using fibre optic probes. Metallic thermocouples were not used to avoid any potential interference with MWs. The reference temperature (i.e. the probe which provided the temperature feedback to the VHM computer) was positioned at sub-laminate 10 (labelled T_{mw}). A vacuum of 0.9 bar was kept throughout the cycle and a 17 mm thick engineering ceramic plate (i.e. cordierite) was used as mould to produce the 60 mm thick laminates.

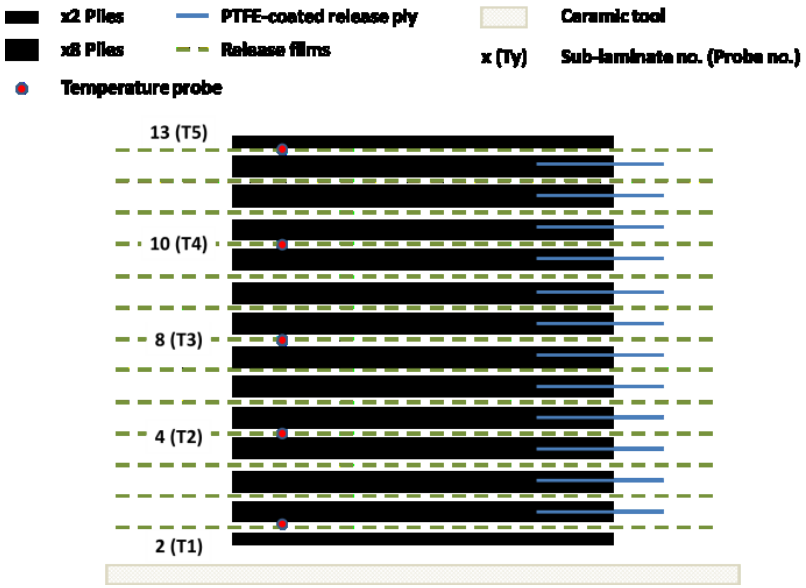


Figure 3.8 Schematic of the layup used for curing thick laminates (For test S25_MW90, T4 was labelled T_{MW}, and T5 was T4).

3.3.2 Conventional Oven Curing of Carbon-Epoxy SPARPREG

The oven-cured laminates were produced using a single-sided aluminium mould for the 2.4 mm and 4.8 mm thick laminates, whereas a cordierite mould was used for the 60 mm thick laminate, by means of OoA vacuum bagging, using typical consumables and curing methodologies used in the composites industry, with the same cutting, laminating and debulking processes as with the MW-cured laminates described in Section 3.3.1. The six laminates produced using a conventional oven are listed in Table 3.3.

Table 3.3 Oven-cured laminates showing curing dwell time, laminate size, lay-up sequence, test method and laminate number.

Dwell Time (Minutes)	Laminate Dimension (mm)	Laminate Lay-up	Test Method	Laminate Number
45	300×300×2.4	UD	Tension, 0°	S21_O45
			Tension, 90°	S22_O45
			Compression, 0°	S20_O45
		±45°	IPS, ±45°	S27_O45
	300×300×4.8	UD	Fracture, Mode I	S24_O45
100	300×300×60	UD	Fracture, Mode I	S26_O90

The 4.8 mm thick laminate S24_O45 followed the manufacturer's recommended cure cycle (MRCC), with a heating rate of 2 °C/min with a dwell time of 45 min at 120 °C. Four type N thermocouples were used to measure the temperatures of each laminate. The position of the thermocouples for curing laminate S27_O45 were the same as those seen in Figure 3.6 (T1 to T5, T_{MW} not present in conventional oven curing).

The 2.4 mm thick laminates S20_O45-S22_O45 and S27_O45 were produced with a heating rate of 4 °C/min from 20 °C to 100 °C, and then reduced to 1 °C/min from 100 °C to 120 °C, i.e. an average of 2.5 °C/min. The higher initial heating rate was used in order to provide a more direct comparison with the MW-cured laminates. The 4 °C/min heating rate was the oven's limit.

Laminates S20_O45-S22_O45 and S27_O45 were cured in the oven simultaneously. Four type N thermocouples were used to measure the temperatures of each laminate (labelled T1, T2, T3 and T4 in Figure 3.9). The thermocouple was placed in the middle of each laminate (i.e. 150 mm × 150 mm from the edges), in between the laminate surface and the mould.

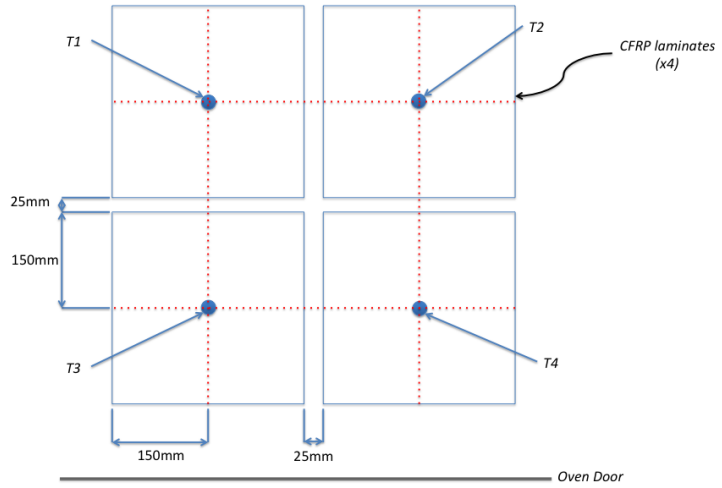


Figure 3.9 Location of the four thermocouples that were used to record temperature in the conventional oven to cure the 2.4 mm thick laminates S19 to S22_O45.

The 60 mm thick laminate (i.e. S26_O90) was also originally set to cure according to the MRCC of 45 min at 120°C, however the thermal runaway and the high oven temperature led to a dwell time of more than 100 min. Therefore, the heating rate was set to 0.2°C/min from 20 to 30°C and 0.4°C/min from 30 to 120°C (i.e. average heating rate of 0.3°C/min) to avoid excessive thermal runaway and to minimise the associated material degradation. Cooling was carried out by switching the oven power off and leaving the laminate in the oven until it reached ~40°C. The temperature was monitored throughout the curing process at five different sub-laminates at 2, 4, 8, 10 and 13 (i.e. the same as with the MW curing setup used to produce laminate S25_MW90) – counting from the mould upwards (Figure 3.8) through the thickness.

The temperature control criteria in the oven was set so that the temperature deviation between the minimum and the target temperature was less than 2°C.

A vacuum of 0.9 bar was kept throughout the cycle for all the oven-cured cases. This was the same as with the MW-cured cases.

3.4 Degree of Cure

A Perkin Elmer DSC 6000 with Pyris software was used to identify the material's T_g and degree of cure. Differential scanning calorimetry (DSC) was carried out across laminates at three different locations per laminate and four samples per location, in order to identify the degree of cure and consequently to assess the property variation across and through the thickness (the latter only applicable to the 60 mm thick laminates) of the laminate from its respective curing method.

The degree of cure was calculated by comparing a reference enthalpy ΔH value obtained from a semi-cured (the term 'semi-cured' describes the prepreg's stage of cure) sample with the enthalpy measured for a cured sample. The sample was heated from 20 °C to 250 °C at a rate of 10 °C/min and the thermograph was recorded (see Figure 3.10).

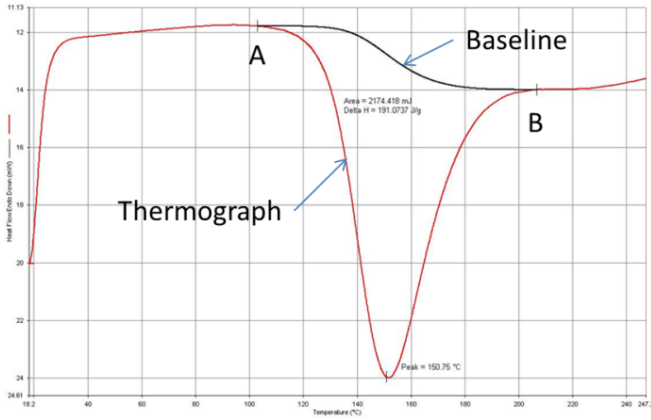


Figure 3.10 DSC result of a typical of semi-cured sample.

Using the heat flow curve obtained, the peak area was calculated between points A and B using a sigmoidal baseline with the start and end points approximately between the two horizontal sections of the thermograph before and after the valley. Points A and B are locations where the heat flow curve flattens to produce a horizontal tangent. The reference enthalpy ΔH was determined to be ~191 J/g. and was chosen for the calculation of degree of cure. ΔH was also measured for cured samples using the same dynamic analysis as the reference sample. It was assumed that a lack of exothermic reaction after point 'B' was an indication of a highly cured sample. A representative thermograph is shown in Figure 3.11.

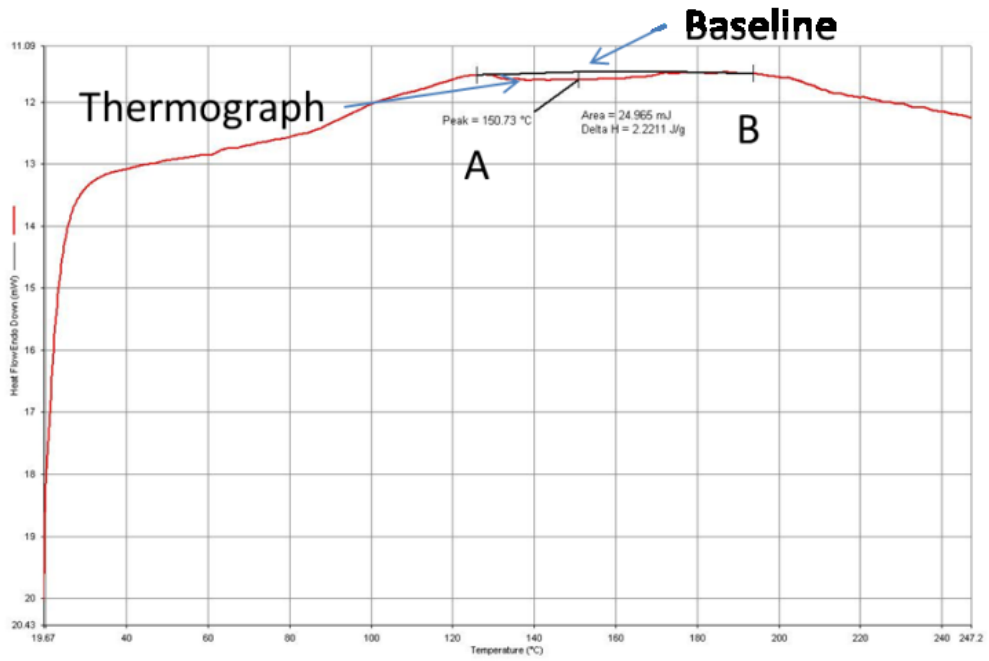


Figure 3.11 DSC result of a typical MW-cured sample (Sample S15_MW45, 45 mins dwell at 120°C).

ΔH for the cured sample was determined using the same procedure as for the reference sample; in this case ΔH for the cured sample shown in Figure 3.11 was ~2.2 J/g.

In order to obtain the degree of cure of sample 'x', ΔH measured from the sample 'x' was compared to the reference sample's ΔH.

$$Degree\ of\ cure\ (x) = \left(1 - \frac{\Delta H\ (x)}{\Delta H\ (Reference)}\right) \times 100 \qquad \text{(Eq. 3.1)}$$

3.5 Determination of the Fibre Volume (V_f) and Void Volume (V_v) Content

Optical microscopy and image analysis was used to determine the V_f and V_v contents based on ASTM E2109-01 (2007) [113]. Three sections of each of the 4.8 mm sub-laminates (i.e. S23_MW40~S26_O90) were prepared by cutting small samples (~20 mm × 20 mm) using a Dremel hand tool with a diamond-coated disc. The samples were then individually placed in a PP pot with the surface of interest facing downwards in contact with the inside bottom surface of the pot. The pot was

then filled with room temperature curing polyester resin and left to cure for 24 hours. Once cured, the polyester block containing the sample was removed from the pot. The polyester and the sample block was then polished using discs with grit sizes in the following sequence of 1200 μm, 600 μm, 320 μm, 3 μm, and 1 μm, with water used as a coolant. The process was finished with a 0.25 μm polishing disc with water-based colloidal silica suspension. Once complete, the samples were placed under an Olympus BX51M microscope and a Leica DFC295 camera was used to obtain the images. Six non-overlapping images from each position covering the top, bottom and centre of the individual laminate sections were taken to measure the V_f and V_v. Therefore, a total of 18 images were used to obtain the V_f and V_v values of each 60 mm thick laminate (i.e. S25_MW90 and S26_O90), which equates to a total of 108 images for the oven-cured laminates, and 108 images for the MW-cured laminates. Representative images used for the measurement of V_f and V_v are shown in Figure 3.12.

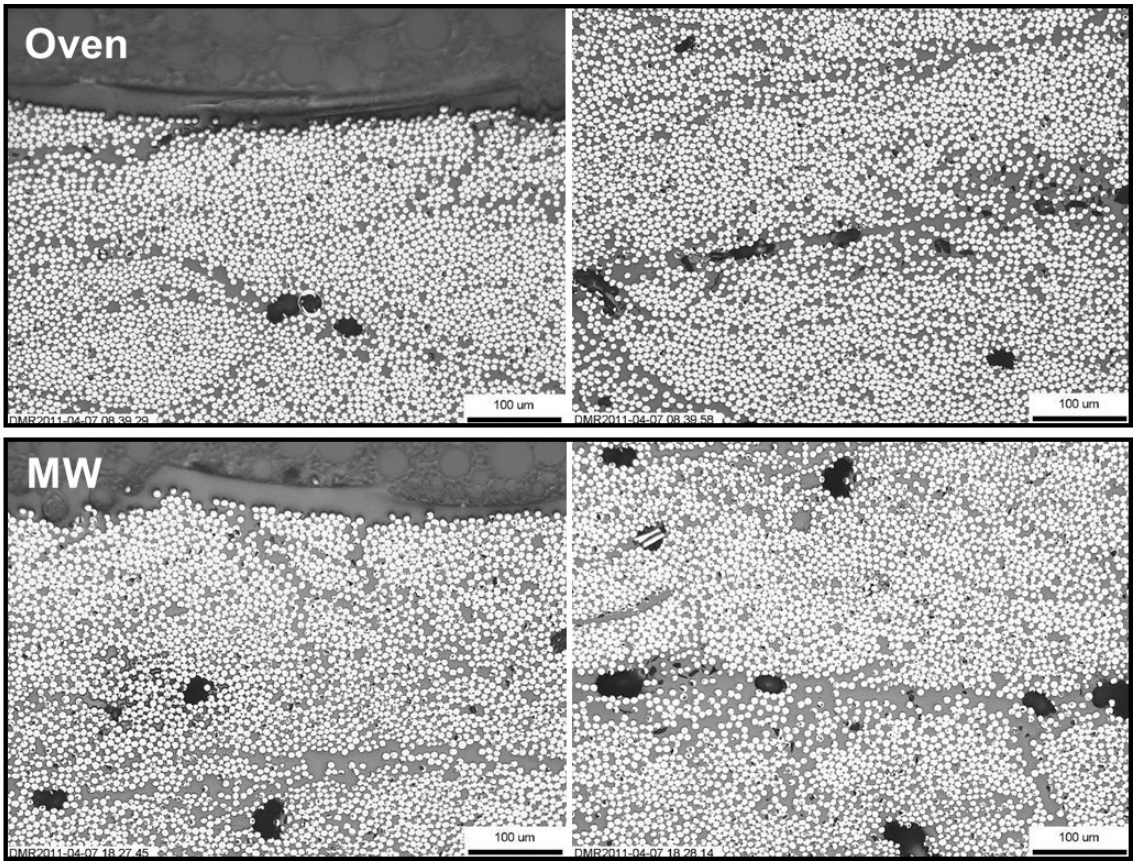


Figure 3.12 Representative micrographs of; top: oven-cured (S26-2_O90), and, bottom: MW-cured (S25-2_MW90) which were used for V_f and V_v measurements.

3.6 Microwave Penetration Depth (D_p)

One of the key parameters for heating materials effectively and efficiently using MWs is the MW penetration depth into the material (D_p). The MW penetration depth of a material at a specific MW frequency is of much importance, as this will determine whether the material under investigation will heat evenly through the thickness of the material. A method to determine the penetration depth of an anisotropic, partially dielectric and electrically conductive material such as carbon-epoxy composites was suggested using an experimental approach. This method could be applied to other isotropic materials as well, but its usefulness may be limited in this case since the theoretical approximations for such materials are already relatively accurate. Testing isotropic and dielectric materials using this method allows however to validate the MW penetration depth results of the carbon-epoxy composites. Additionally, the test method could also be used in the future for validating numerical simulations.

As mentioned in Section 2.2.4, the MW penetration depth of a material is defined as the depth at which the MW magnitude decreases to e^{-1} (i.e. ~0.37) of its original magnitude. The theoretical method of calculation of an electrically conducting material is based on eq. 2.5 [73]:

$$D_p = \sqrt{\frac{1}{\pi \cdot f \cdot \mu\prime \cdot \sigma_{ec}}} \qquad \text{(Eq. 2.5)}$$

where f is the frequency [Hz], μ' is the magnetic permeability [H/m] and σ_{ec} is the electrical conductivity [S/m]. The author has only identified two publications by Cuccurullo *et al*. [114,115] who attempted to measure this parameter experimentally. The methodology relied on using a thin-walled (0.5 mm thick) aluminium cylinder filled with water. A thermal imaging camera was used to measure the temperature gradient along the side of the enclosure as the water in the container was heated using MWs. As the enclosure wall was very thin and made of a material with a high thermal conductivity, the temperature gradient caused by MW heating was rapidly and easily picked up by the thermal imaging camera. This approach is useful for assessing the MW penetration depth of conventional materials, however some modifications are required to be useful for CFRP.

The author has proposed an alternative (Figure 3.13), which was comprised of an aluminium vessel (300 mm × 300 mm × 150 mm), two PTFE sheets (300 mm × 300 mm × 2 mm), a thermally and electrically insulating thermoplastic support (100 mm × 100 mm × 50 mm), a glass bowl containing 1 L of water, aluminium tape and an aluminium sheet with and without a hole (300 mm × 300 mm × 2 mm, hole diameter 150 mm). This was then introduced into the VHM cavity for the heating tests.

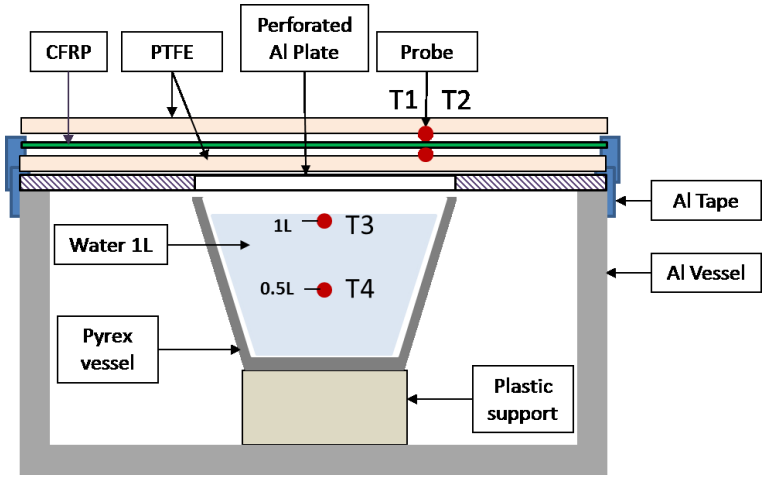


Figure 3.13 Schematic for testing the MW penetration depth of CFRPs.

The main aim in this experiment was to heat the water by MWs passing through the perforated hole only. The MW power and heating time of 1 kW for 10 min was set to provide a significant increase in water temperature, whilst not encouraging heating of the water due to conduction and convection from the laminate. The CFRP laminates were placed between two PTFE sheets, which were used to support and maintain the shape of the laminates. PTFE was used due to its very low dielectric properties (Table 2.2) and, therefore, it was deemed safe to assume little MW absorption and subsequent heating by the PTFE sheets. Temperature probes were located at two different locations on the laminate (T1 and T2) and at two different locations within the water vessel (T3 and T4). The change in water temperature was recorded during a 10 min heating cycle. Various tests were performed with a range of ply thicknesses until the change in water temperature became minimal. Two reference tests (i.e. one with a solid aluminium plate and one with the perforated plate with no CFRP) representing the minimum and maximum MW penetration cases were also carried out in order to test the methodology.

3.7 Mechanical Testing

3.7.1 Tensile Testing

The longitudinal (0°) and transverse (90°) tensile strength and elastic modulus of the manufactured composites (i.e. S4_MW35 to S7_MW40, S11_MW30, S12_MW30, S15_MW45, S16_MW45, S21_O45 and S22_O45) were determined based on ASTM D3039M [104]. The test specimens had dimensions of 230 mm × 25 mm × 2.4 mm. The tensile tests were performed at a cross-head speed of 2 mm/min. The tensile strength was calculated using eq. 3.2 [104]:

$$\sigma_{t,max} = \frac{P_{t,max}}{A} \qquad \text{(Eq. 3.2)}$$

where $\sigma_{t,max}$ is the maximum tensile strength, $P_{t,max}$ is the maximum tensile load at failure and A is the cross-sectional area of the tested specimen. Tensile elastic modulus (i.e. Young's Modulus) was calculated using eq. 3.3 [104]:

$$E_t = \frac{\Delta\sigma_t}{\Delta\varepsilon_t} \qquad \text{(Eq. 3.3)}$$

where E_t is the tensile elastic modulus, $\Delta\sigma_t$ is the change in tensile stress and $\Delta\varepsilon_t$ is the change in tensile strain. The modulus was determined from the slope of the stress-strain curve in the range from 1000 με to 3000 με. The strain was measured using one UF series bi-axial (axial and lateral readings) strain gauge from Tokyo Sokki Kenkyujo Co. Ltd. (Tokyo, Japan) bonded to one face of the test coupon using an aerobic cyanoacrylate (CN) type adhesive (also from Tokyo Sokki Kenkyujo),, which was bonded after degreasing using IsoPropyl Alcohol (IPA). Glass fibre reinforced polymer (GFRP) composite end-tabs were bonded to the end of both 0° and 90° tensile test coupons using Araldite 2014, two-part room temperature cure epoxy adhesive. The adhesive layer had a chamfer in the gauge section to reduce stress concentrations caused by the end-tabs. An Instron 8500 with a 500 kN load cell, and an Instron 5567 with a 30 kN load cell, were used for the 0° and 90° tensile tests respectively. All load cells used in the present study underwent calibration procedures as required by TWI and UKAS (United Kingdom Accreditation Service) standards. The results of a minimum of six coupons (out of ten coupons) with acceptable failure modes were considered and analysed.

3.7.2 Compression Testing

The compression strength and modulus of the manufactured SPARPREG composites (i.e. S1_MW30, S8_MW40, S13_MW35, S18_MW45 and S20_O45) were determined based on ASTM D6641 [105]. The test specimens had dimensions of 140 mm × 12 mm × 2 mm. The tests were performed using a cross-head speed of 1.3 mm/min. The compression strength was calculated using eq. 3.4 [105] and the compression modulus using eq. 3.5 [105]:

$$\sigma_{c,max} = \frac{P_{c,max}}{A} \qquad \text{(Eq. 3.4)}$$

where $\sigma_{c,max}$ is the maximum compressive strength, $P_{c,max}$ the maximum compressive load at failure and A the cross-sectional area,

$$E_c = \frac{\Delta\sigma_c}{\Delta\varepsilon_c} \qquad \text{(Eq. 3.5)}$$

where E_c is the compressive elastic modulus, $\Delta\sigma_c$ the change in compressive stress and $\Delta\varepsilon_c$ the change in compressive strain. The strain range used for the calculation of E_c was 1000 με to 3000 με. Strain values were obtained through one UF series bi-axial strain gauge from Tokyo Sokki Kenkyujo Co. Ltd. on each face of the test coupon to monitor buckling and bending effects. Glass fibre reinforced polymer (GFRP) composite end-tabs were bonded to the compression test coupons using Araldite 2014. The short gauge length of 15 mm meant that there was not sufficient space to produce a chamfered edge with the adhesive. An Instron 5567 with a 50 kN load cell was used for the compression tests. The results of a minimum of six coupons with acceptable failure modes were considered and analysed.

3.7.3 In-Plane Shear (IPS) Testing

The IPS strength and modulus of the manufactured laminates (i.e. S27_O45 to S29_MW45) were determined based on ASTM D3518 [106]. The test specimens had a balanced and symmetric $(\pm 45°)_{2S}$ layup sequence with dimensions identical to those used for the tensile tests (230 mm × 25 mm × 2.4 mm). The tests were performed using a cross-head speed of 2 mm/min. The IPS strength was calculated using eq. 3.6 [106]:

$$\tau_{12} = \frac{P_{max}}{2A} \qquad \text{(Eq. 3.6)}$$

where τ_{12} is the maximum IPS strength, P_{max} is the maximum load at failure and A is the cross-sectional area. IPS chord shear modulus of elasticity was calculated using eq. 3.7 [106]:

$$G_{12}^{chord} = \frac{\Delta\tau_{12}}{\Delta\gamma_{12}} \qquad \text{(Eq. 3.7)}$$

where G_{12}^{chord} is the IPS modulus (GPa), $\Delta\tau_{12}$ is the difference in applied shear stress between two shear strain points and $\Delta\gamma_{12}$ the difference in shear strain between the two shear strain points. The 'Δ' range was between 1500 με to 5500 με. Strain values were measured using one UF series bi-axial strain gauge from Tokyo Sokki Kenkyujo Co. Ltd. attached to one face of the test coupon. Glass fibre reinforced polymer (GFRP) composite end-tabs were bonded using Araldite 2014. The adhesive layer had a chamfer on the gauge section to reduce sudden stress changes due to the end-tabs.

An Instron 8500 with a 30 kN load cell was used for the IPS tests. The results of a minimum of six coupons with acceptable failure modes were considered and analysed.

3.7.4 Mode I Interlaminar Fracture Toughness (G_{1C}) Testing

The mode I interlaminar fracture toughness properties were obtained following ASTM D5528-01 [116], which is carried out using the DCB method. An Instron 5567 B723 testing machine equipped with a 30 kN load cell was used. The test coupons had dimensions of 130 mm × 20 mm × 4 mm. A non-perforated, ETFE non-adhesive insert (i.e. A6000BNP1515 – A6000) was placed half way into the thickness of 2.4 mm. A schematic of the coupon is shown in Figure 3.14.

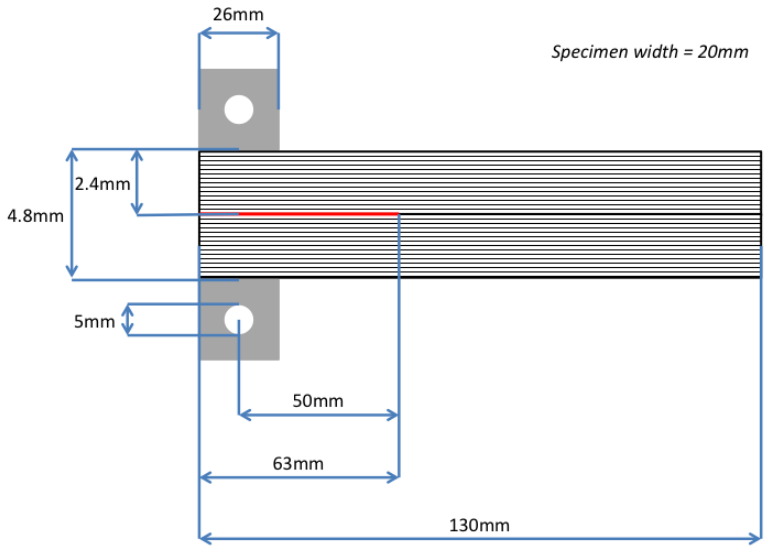


Figure 3.14 Schematic of a mode I DCB interlaminar fracture toughness test coupon.

The cross-head opening displacement rate used for the test was 1 mm/min. The sample was loaded until the crack propagated 3 mm beyond the initial pre-crack. The loading was then stopped and the coupon visually inspected on the front and the back of the coupon to ensure the crack front was approximately in the same location on both sides and that no other cracks were visible. The sample was then unloaded and re-loaded. The crack length was measured every millimetre for the first 5 mm, and then every 5 mm subsequently (where possible).

The crack propagation was recorded on paper and an electronic switch used to mark the time, load and displacement when the crack reached the desired propagation. The modified beam theory (MBT) was used to determine G_{1C} (eq. 3.8):

$$G_{IC} = \frac{3P\delta}{2b(a+|\Delta|)} \qquad \text{(Eq. 3.8)}$$

where P is the load (N), δ the displacement (mm), b the coupon width (mm) and a the crack length (mm). |Δ| was determined experimentally by generating a least squares plot of the cube root of compliance ($C^{1/3}$) as a function of delamination crack length (Figure 3.15).

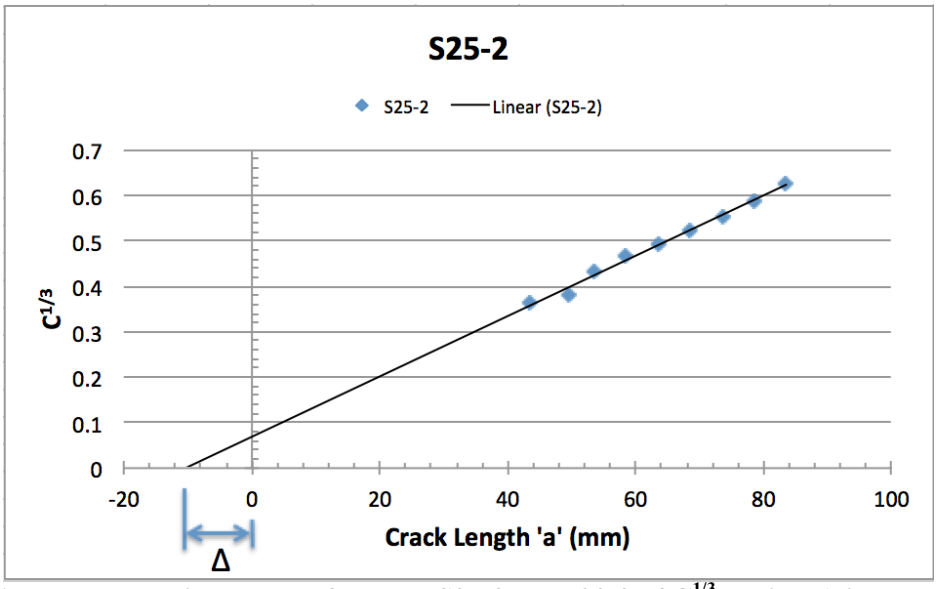


Figure 3.15 Representative graph of sample S25-2_MW90-2 of $C^{1/3}$ against 'a' as described by the modified beam theory (MBT).

The results of a minimum of six coupons with acceptable failure modes were considered and analysed.

3.7.5 Fibre Push-Out Testing

3.7.5.1 Sample preparation

Samples from laminates S23_MW40 (MW-cured) and S24_O45 (oven-cured) were prepared using the methodology described by Godara *et al*. [117]. Briefly, the samples were embedded in a standard epoxy system for the preparation of micrographs (curing time 24 h at room temperature) in a poly-methyl-methacrylate (PMMA) tube to prepare disc-shaped specimens for push-out tests. The composite sample was first cut to achieve a length of approximately 1 mm using a Leica inboard saw with a diamond saw blade. Following the cut, one side of the sample was polished using SiC abrasive paper with 2400 and 4000 grain size. This was then followed by an additional cut to achieve a sample length of approximately 200 µm to 300 µm using the inboard saw. The sample was further polished until a sample length between 25 µm to 30 µm was achieved. The sample preparation was carried out in collaboration with the Bundesanstalt für Materialforschung und -prüfung (BAM) [Federal Institute for Materials Research and Testing] (Berlin, Germany).

3.7.5.2 Testing Methodology

The push-out test is a non-standard test method, which can be used to obtain the fibre-matrix IFSS in actual composite specimens and the methodology used in the present study resembled the one presented by Godara *et al*. [117]. The test rig used for the measurements was a self-made test rig of the BAM Federal Institute of Materials Research and Testing (Figure 3.16). The 25 µm to 30 µm thick sample was placed on an aluminium plate with holes in order to allow the fibres to move once the load is applied. To push a fibre out of a thin composite slice a force was applied at a rate of 0.2 µm/s using a cone-shaped indenter with a flat sapphire tip (diameter of ~5 µm). These tests require selecting a fibre, which is aligned perpendicular to the plane of the slice to accurately determine the contact area. An advantage of the push-out test method is that the sample preparation allows characterisation of a large number of fibres to obtain statistically viable results. The IFSS (τ_{IFSS}) was calculated using maximum fibre push-out force (F_{max}) for each fibre and the average diameter (d_f) of the carbon fibres as well as the thickness of the composite slice (embedded length l_{emb}) using eq. 3.9)

$$\tau_{IFSS} = \frac{F_{max}}{d_f \cdot \pi \cdot l_{emb}} [MPa]. \qquad \text{(Eq. 3.9)}$$

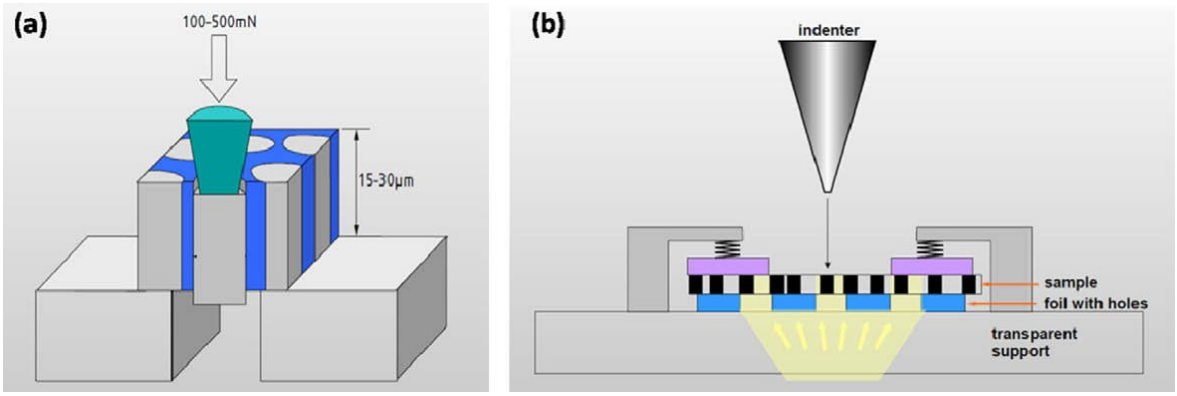


Figure 3.16 Schematic of; (a) basic principle of fibre push-out testing, (b) test setup/methodology [117].

The fibre push-out testing was carried out in collaboration with the Bundesanstalt für Materialforschung und -prüfung (BAM) [Federal Institute for Materials Research and Testing] (Berlin, Germany).

3.7.6 Failure Mode Assessment of Tested Samples

A Zeiss 1455EP SEM with an EDAX Genesis EDX system SEM was used to assess the differences (if any) in failure mode between oven-cured composites and MW-cured composites. Aspects such as degree of matrix remaining on the fibre surfaces, fibre pull-out, fibre disbonding and matrix fracture surface were assessed. The samples were first sputter coated with gold using an Edwards S150B and then introduced into the SEM. Images were taken from the fracture surfaces of 90° tensile test samples S6_MW40 (MW-cured), S16_MW45 (MW-cured) and S22_O45 (oven-cured), and mode I interlaminar fracture toughness test samples S23_MW40 (MW-cured) and S24_O45 (oven-cured).

3.7.7 Matrix Indentation Testing

Indentation testing is a proven technique used to assess a material's hardness, as demonstrated by the standardisation of this technique in international test standards such as ASTM D2583 [118], ASTM E2546 [119] and International Organization for Standardization (ISO) 14577-4 [120]. The difference between standard indentation methods and the more recent instrumented methods is mainly the size of the indenter, which in the case of the recent instrumented methods this is typically a few micrometres wide, and with a Berkovich tip for example, the tip diameter could be in the range of tens of nanometres. Additionally, with the use of highly sophisticated and sensitive equipment, the indentations can be carried out in a controlled manner, thus increasing the reliability compared to standard tests, such as the Barcol hardness method as described in ASTM D2583 [121]. The biggest advantage of small-scale indentation is that very small and local changes in material properties, such as the matrix in between the fibres of CFRPs, can be accurately measured. The objective for the use of small-scale indentation testing in the present study was to identify potential changes in matrix modulus between the conventional oven-cured and MW-cured composite laminates.

During nano-indentation testing the load is measured as function of tip displacement. It is then possible to calculate the reduced modulus (also called indentation modulus) E_r (GPa) using the

unloading portion of the curve and since E_r is a combination of the modulus of the specimen and the indenter material, the elastic modulus E of the specimen can be obtained using eq. 3.10 [122]:

$$\frac{1}{E_r} = \frac{1-\nu^2}{E} + \frac{1-\nu_{in}^2}{E_{in}} \qquad \text{(Eq. 3.10)}$$

where E and ν are the specimen's elastic modulus and Poisson's ratio, respectively, E_{in} and ν_{in} are the same properties of the indenter material. For a diamond indenter tip, E_{in} is 1141 GPa and ν_{in} is 0.07 [123]. The Poisson's ratio of the epoxy was assumed to be 0.35 [124]. A total of 360 indentation tests were performed on laminates S25_MW90 and S26_O90 (i.e. 36 indentations at each of the five oven and five MW cured sub-laminates). The tests were carried out using load control, with a load limit of 5 mN.

Chapter 4

Results

This chapter presents the results of the investigation of the curing process, MW distribution and MW penetration depth, the physical and mechanical tests and the fracture surface inspection performed on oven-cured and MW-cured composites described in chapter 3. Tests included DSC, image analysis (to measure fibre volume and void volume content), standard mechanical tests (i.e. tension, compression, IPS and mode I interlaminar fracture), and less traditional, non-standardised mechanical tests such as matrix indentation and fibre push-out.

4.1 Microwave Field Distribution

The results of the test described in Section 3.3 can be seen in Figure 4.1. The arrangement of the beakers from ‘a’ to ‘f’ were consistent with those described in Figure 3.9.

As it can be seen in Figure 4.1, the most noticeable aspect was the small temperature difference (≤5°C) observed in most cases when comparing T1 and T2 versus T3 and T4 , except test scenario ‘a’, which showed a difference of ~7°C. The time taken to reach 90°C was between 40 minutes (case ‘e’) and 52 minutes (case ‘f’). The shortest time of 40 minutes taken to reach 90°C in case ‘e’ is not surprising since this was the setup without the metallic bench, thus being closer to the idealised case shown in Figure 3.3. Excluding case ‘e’, the time taken was between 44 minutes (case ‘b’) and 52 minutes (case ‘f’). Some variation was observed depending on the setup, thus showing that MW distribution, and therefore heating, depend on what is introduced in the MW cavity and where. This is observed when comparing the temperature profiles of position ‘top centre’ in case ‘c’ and case ‘f’, where the former reaches 90°C in ~46 min, whereas the latter reaches the same temperature in ~51 min. Additionally,

when comparing 'lower centre' in cases 'e' and 'f', it can be observed that the time taken to reach 90°C was ~40 min and ~51 min respectively.

Taking into account these configurations represent the worst case scenarios (i.e. beakers close to the applicator walls and waveguides, and separated from each other by ~1 m, which is close to the maximum allowable in the VHM 100/100 applicator), the differences are small, thus suggesting a high degree of MW field homogeneity within the cavity irrespective of the location. Therefore, the temperature difference across a 300 mm × 300 mm composite laminate is not expected to be much greater, although this is difficult to ascertain at this stage purely based on these results. The temperature difference across a 300 mm × 300 mm composite laminate is described in Section 4.2.

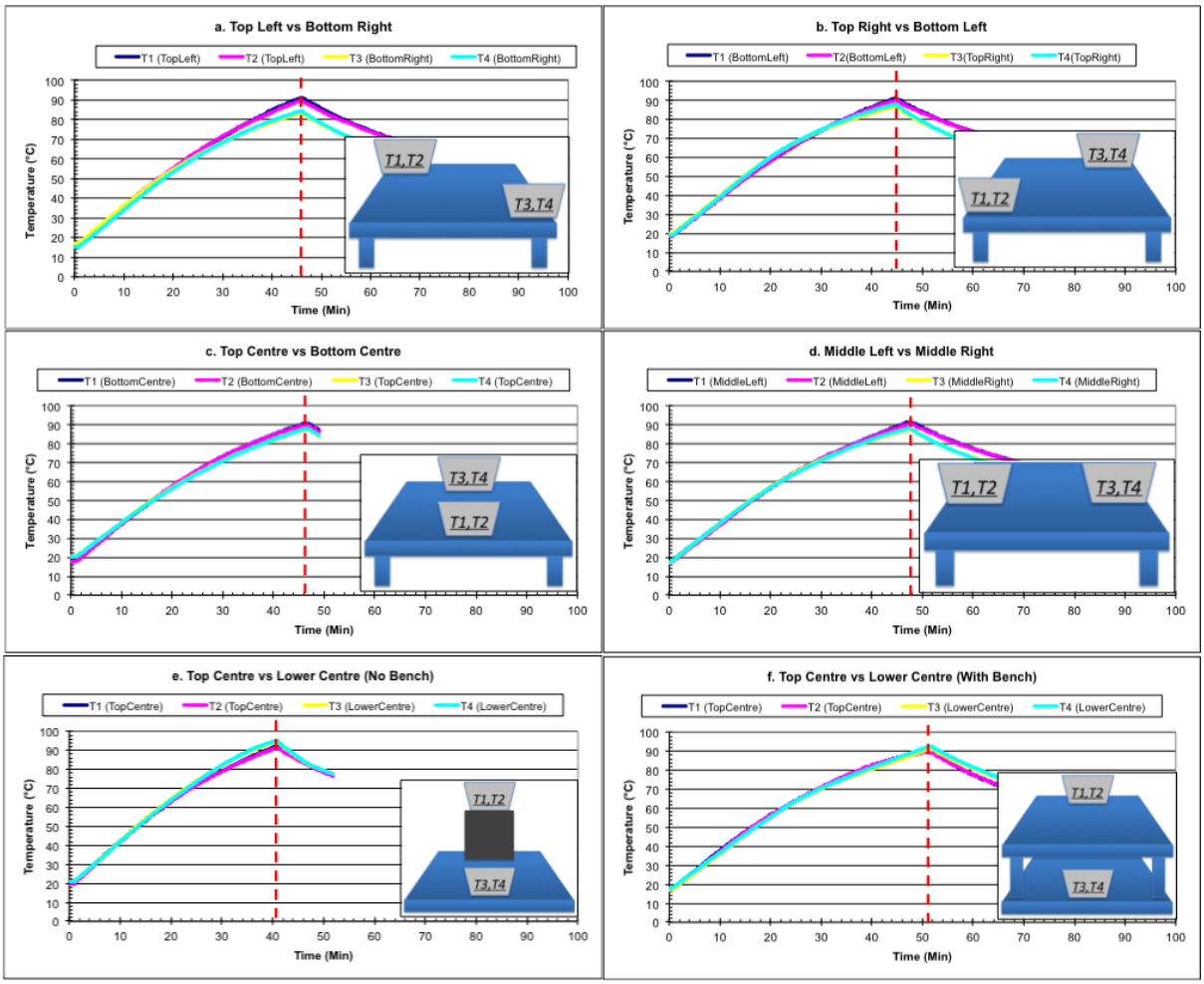


Figure 4.1 MW heating of water – Temperature vs Time as a function of location. a. Top left and bottom right, b. top right and bottom left, c. top centre and bottom centre, d. middle left and middle right, e. top centre and lower centre (no bench), f. top centre and lower centre (with bench).

4.2 Microwave and Oven Heating Profiles

4.2.1 Microwave Heating Profiles of 2.4 mm and 4.8 mm Thick Laminates

The different cure cycles employed to cure the SPARPREG laminates were described in Table 3.1 in Section 3.3.1. The temperatures and MW power recorded during these cure cycles are shown in Figures 4.2 to 4.10.

The temperature profiles of MW-cured laminates were recorded using five fibre-optic probes (T1 to T4, and T_{MW}, where T_{MW} was used to control the cure cycle) where possible (Note: Due to the fragile nature of these probes, in some cases the fibre optic probes were damaged during the process, typically during the application of vacuum, and therefore in these cases it was not possible to record all the temperatures).

Figures 4.2 to 4.5 show the cure cycle data recorded during MW curing of the 2.4 mm thick UD laminates with, respectively, a 30, 35, 40, 45-minute dwell at 120°C. Figure 4.6 shows the cure cycle data for MW curing with a 40-minute dwell for the $(\pm 45°)_{2S}$ IPS laminate. In all of these plots, very steep rises and falls of power can be seen throughout the cycle, however three relatively distinct regions can be observed in all cases. The first is the ramp-up phase, the second is approximately three to five minutes before the dwell temperature is achieved, and three to five minutes subsequent to that, and the third is the dwell phase.

The ramp-up phase showed a power trend increasing with time, until the dwell temperature was achieved (which is approximately when the maximum power was observed). Past this point, the power curve followed a short declining trend, before entering the third phase, which also had large fluctuations, but the minimum and maximum power values were relatively constant. The difference in dwell temperature recorded by the different probes was up to ~30°C from each other, and the average MW power (which was calculated by dividing the power by time) was approximately between 10% and 40% (i.e. ~1 kW and ~5 kW respectively).

The general time-temperature-MW power trend observed between all the cure cycles for the UD laminates shown in Figures 4.2 to 4.5 were very similar from one another. However, for the $(\pm 45°)_{2S}$ IPS laminate the heat-up phase of the cure cycle (Figure 4.6) was noticeably different to those of the UD laminates (Figures 4.2 to 4.5), whereby full MW power was required in order to reach the 120 °C dwell temperature at a 10 °C/min heating rate in the case of the former. Additionally, the MW power was between 75% to 100% from approximately the third minute until the tenth minute, where the UD cure cycles showed typically a maximum MW power of ~80% (i.e. ~8 kW) for a short period of time (<1 minute). No obvious differences in MW power were observed during the dwelling phase (Figure 4.7).

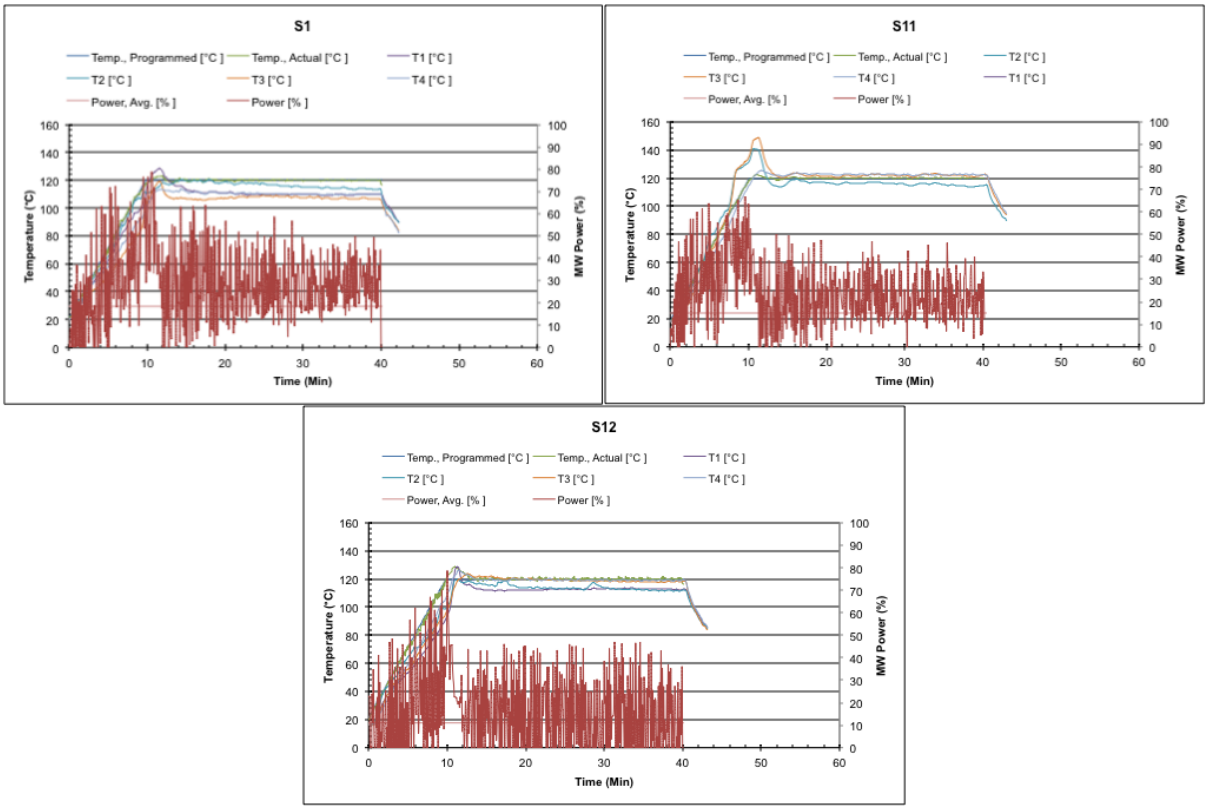


Figure 4.2 Cure cycle of 2.4 mm thick, MW-cured UD laminates with 30-minute dwell at 120°C.

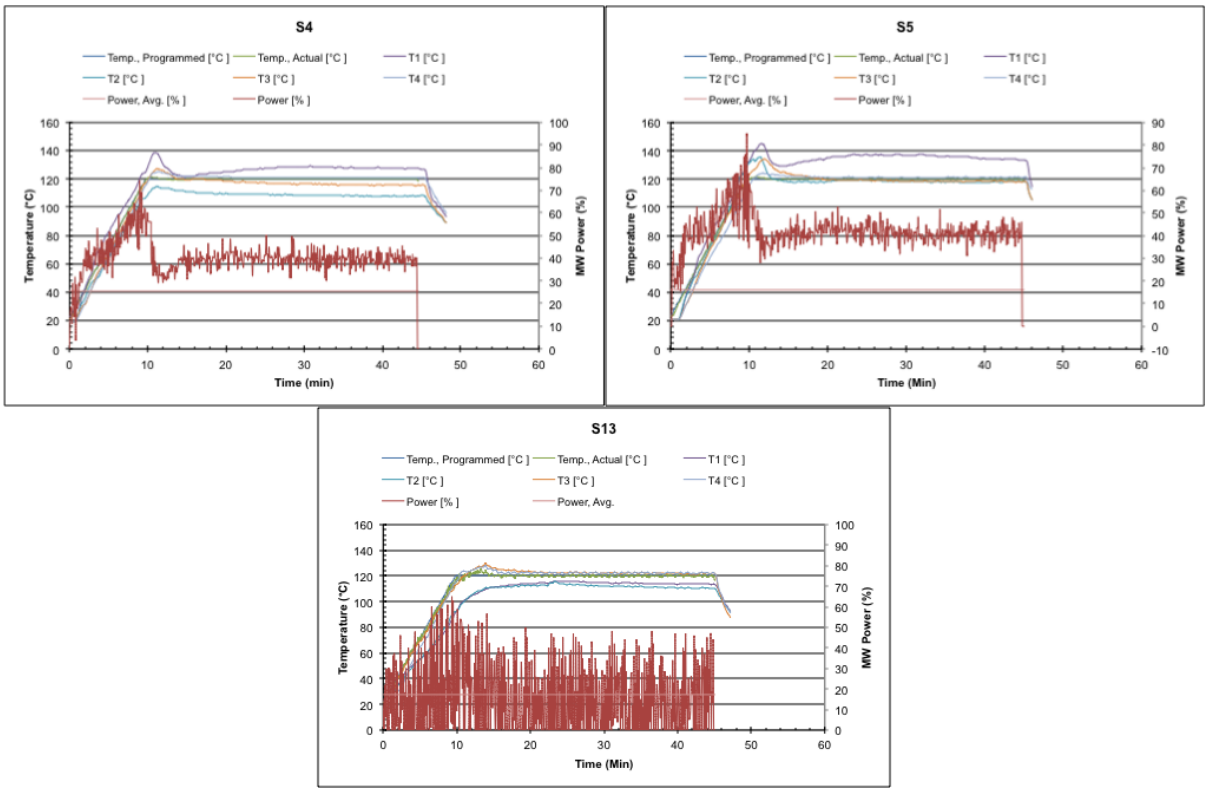


Figure 4.3 Cure cycle of 2.4 mm thick, MW-cured UD laminates with 35-minute dwell at 120°C.

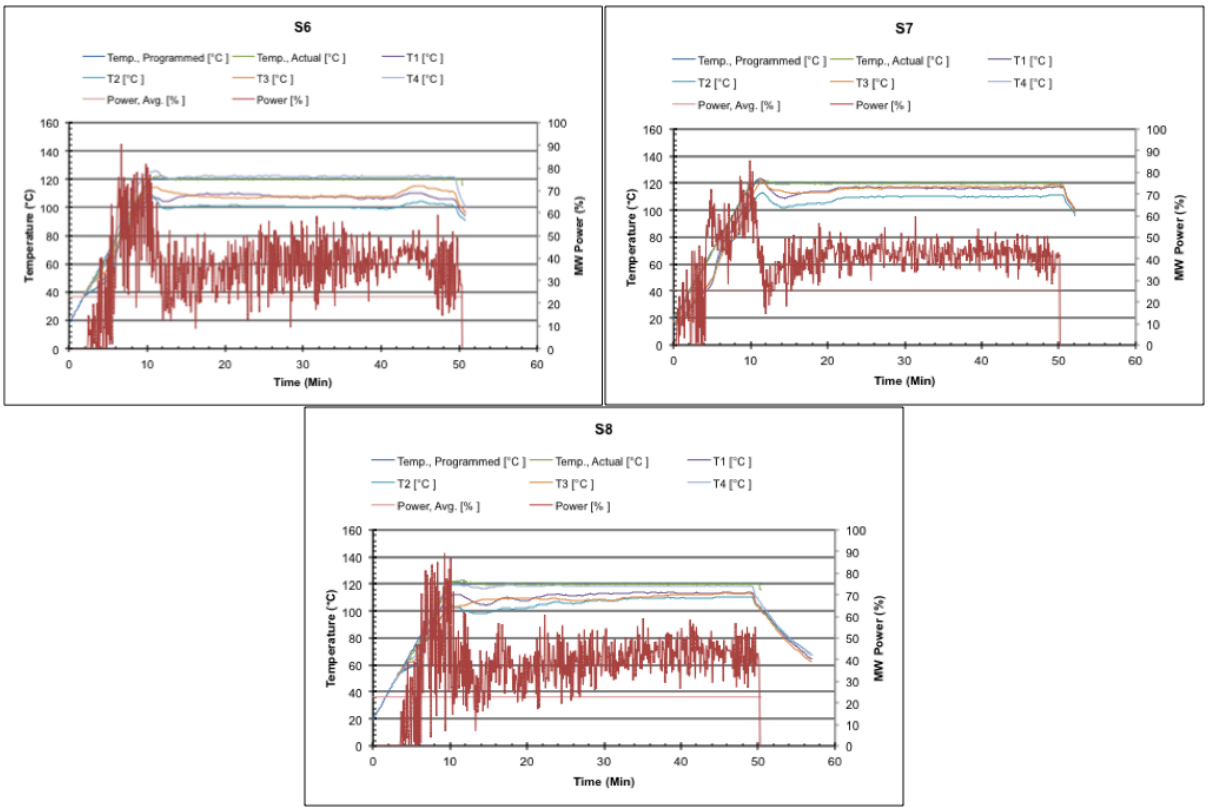


Figure 4.4 Cure cycle of 2.4 mm thick, MW-cured UD laminates with 40-minute dwell at 120°C. Note: Due to software issue the MW power for S6_MW40 and S8_MW40 were not recorded for the first two and three minutes respectively.

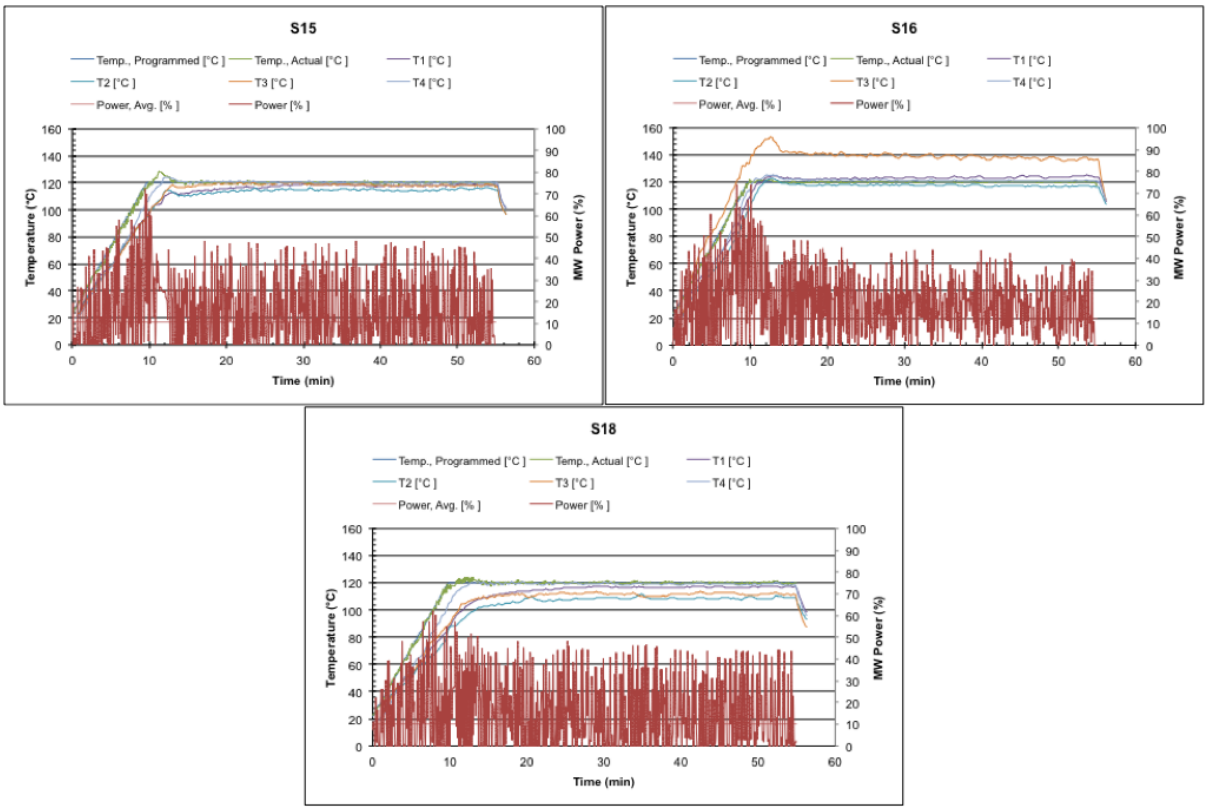


Figure 4.5 Cure cycle of 2.4 mm thick, MW-cured UD laminates with 45-minute dwell at 120°C.

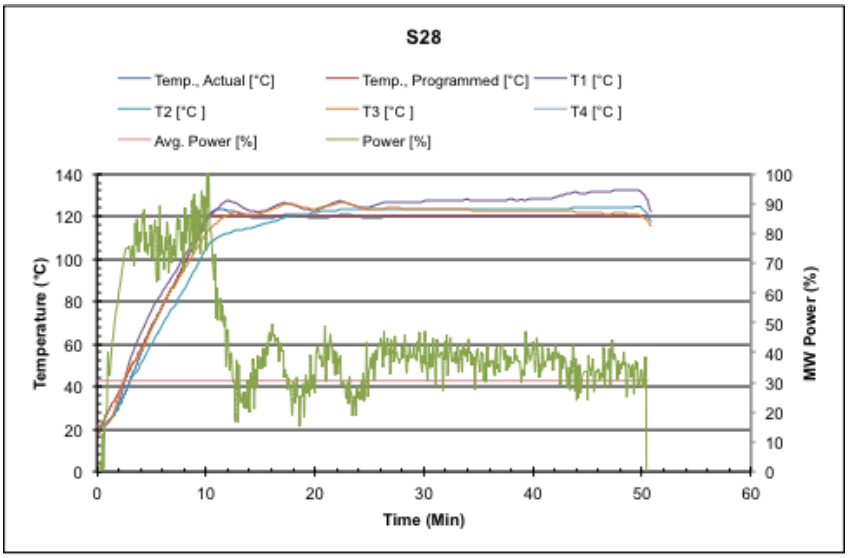


Figure 4.6 Cure cycle of 2.4 mm thick MW-cured $(\pm 45°)_{2S}$ laminates with 40-min dwell at 120°C.

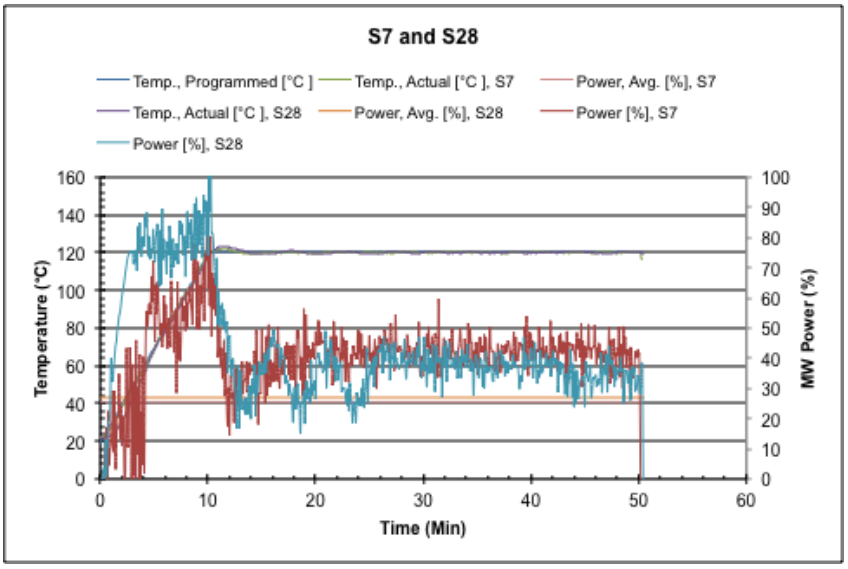


Figure 4.7 Differences in MW power used to cure laminates S7_MW40 and S28_MW40.

In the MW cure of the 4.8 mm thick UD laminate (Figure 4.8), the initial ramp-up from ~20°C to 120°C was achieved in ten minutes (i.e. heating rate of 10°C/min), which was the same as the MW heating rate for the 2.4 mm thick laminates. T2 reached a maximum temperature of ~130°C but cooled down significantly to ~110°C by the end of the dwell period. On the other hand it took an additional ten minutes for T1 to reach 120°C, but stayed at this temperature for the remaining of the dwell period. The MW power did not go beyond 50%, and the average MW power was ~10% (i.e. ~1kW).

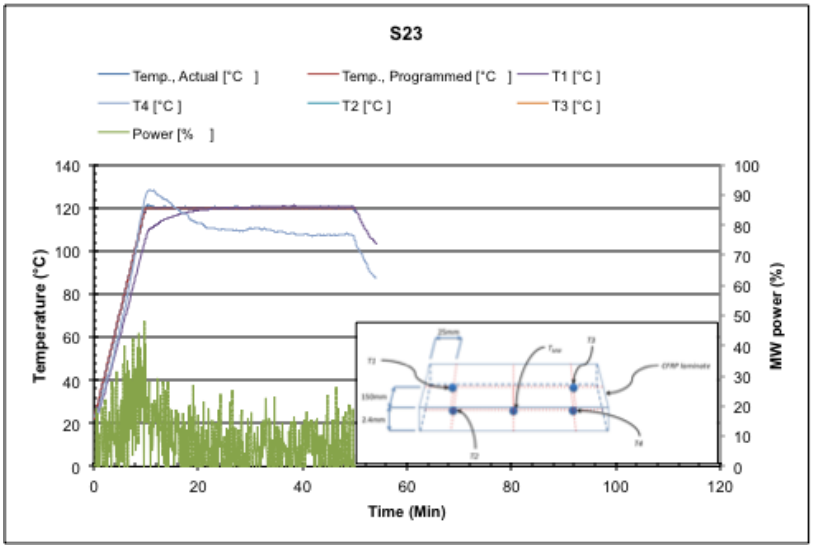


Figure 4.8 Cure cycle of MW-cured 4.8 mm thick laminate with 40-minute dwell at 120°C dwell.

4.2.2 Oven Heating Profiles of 2.4 mm and 4.8 mm Thick Laminates

The oven cure cycle of the 2.4 mm thick laminates (Figure 4.9) was set to an initial heating rate from 20 °C to 100 °C at 4 °C/min and then reduced to 1 °C/min from 100 °C to 120 °C (i.e. average heating rate of 2.5 °C/min) in order to avoid excessive thermal runaway. The temperature was maintained at 120 °C for 45 minutes and then left to cool naturally. All four laminates (i.e. S20_O45-S22_O45 and S27_O45) were produced simultaneously in the same oven. The temperature readings showed little deviation (≤5°C) during ramp-up and dwell. The temperature profiles of the oven-cured composites were recorded using four standard type-N thermocouples for the 2.4 mm and 4.8 mm thick laminates.

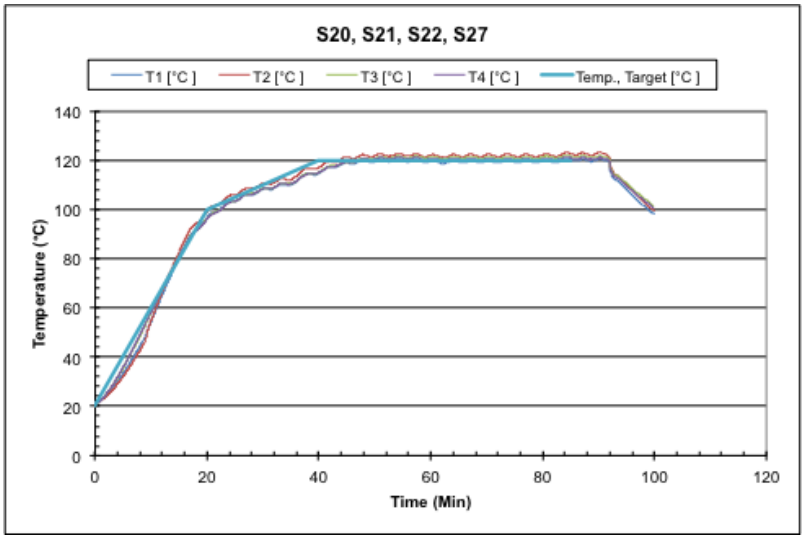


Figure 4.9 2.4 mm thick, oven-cured laminates (UD and $(\pm 45°)_{2S}$) with 45-minute dwell at 120°C.

The temperature readings of the 4.8 mm thick oven-cured laminate S24_O45 (Figure 4.10) showed noticeable variations in temperature from ambient (~20 °C) to the curing temperature of 120 °C at 2 °C/min. The variation in temperature observed by the thermocouples at a heating rate of 2 °C/min suggested that a higher heating rate (e.g. 4 °C/min from 20 °C to 100 °C, and 1 °C/min from 100 °C to 120 °C as used to cure the 2.4 mm thick laminates) would result in an even greater temperature variation across and through the laminate, and was therefore avoided.

Once the laminate achieved the dwell temperature of 120 °C, the temperature was maintained for 45 minutes, then followed by natural cooling to ambient temperature. The temperature difference between the thermocouples was more significant than for the 2.4 mm oven-cured laminates, where the maximum temperature difference between the thermocouples for the 2.4 mm laminates was ~5 °C throughout the cure cycle, but for the 4.8 mm thick laminate a difference of around 30 °C existed when comparing the maximum temperature with the target temperature, and a difference of ~20 °C existed when comparing the maximum and minimum temperatures during the ramp-up phase. It can be easily noticed that the thermocouples on the top surface (T3 and T4) of the laminate suffered the greatest temperature fluctuation compared to the thermocouples between the laminate and the mould (T1 and T2), which was as a result of the typical low transverse thermal conductivity of PMCs.

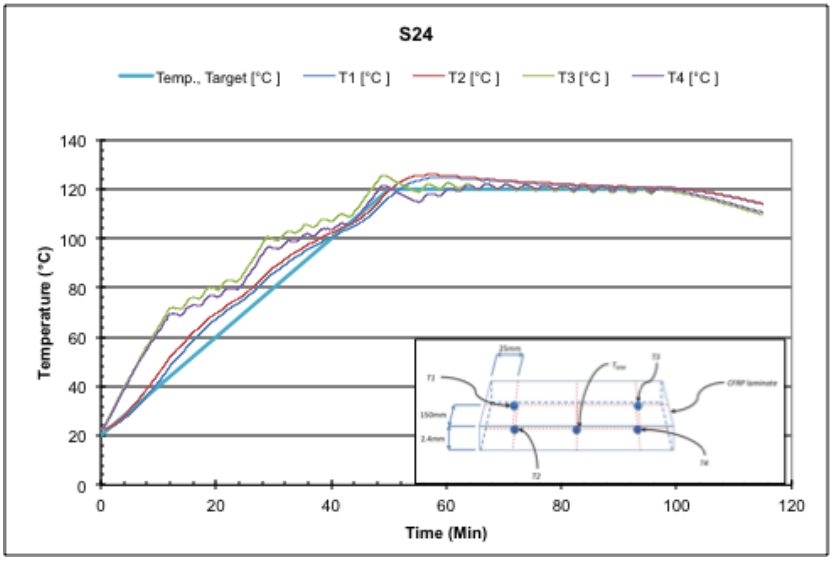


Figure 4.10 Cure cycle of 4.8 mm thick laminates at 120°C dwell; left: MW-cured with 40-minute dwell, right: oven-cured with 45-minute dwell.

4.2.3 Microwave Heating Profile of 60 mm Thick Laminate

Figure 4.11 shows the temperature and power data recorded during the MW cure of the 60 mm thick laminate. As with the 2.4 mm and 4.8 mm thick laminates, T_{MW} was used to control the cure cycle.

Fibre optic probes T1 (closest to the mould) and T4 (farthest to the mould) experienced the highest degree of temperature fluctuation (due to the changes in MW power) during the ramp-up phase,

although the fluctuation exhibited by T4 was significantly greater than that of T1. T1 and T4 reached a maximum temperature of ~110 °C and 143 °C respectively.

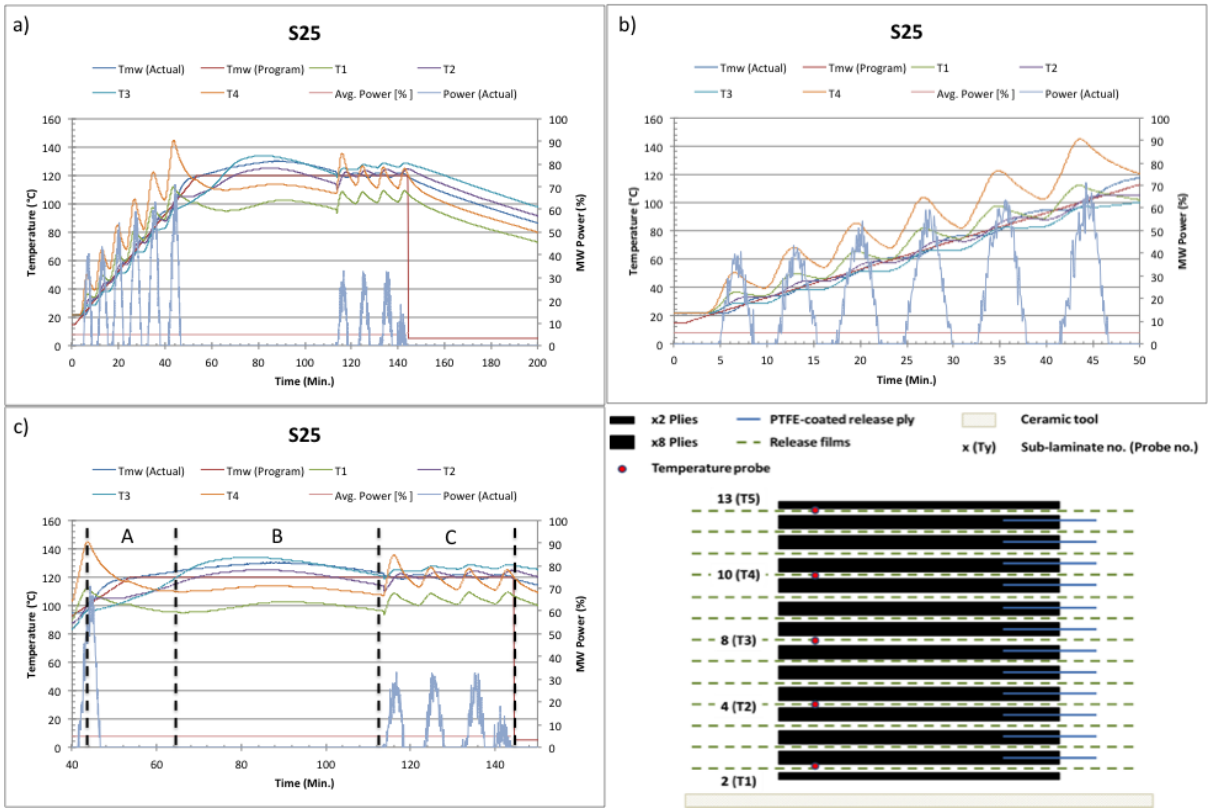


Figure 4.11 MW cure cycle of 60 mm thick laminate.
a) Full cycle, b) ramp-up phase, c) dwell phase.

It is interesting to see that the instantaneous temperature fluctuation was also observed at positions T2, T3 and T_{mw}, i.e. at positions within the laminate thickness that are believed to be beyond the MW penetration depth at this MW frequency for this material.

T2, T3 and T_{mw} (actual) achieved maximum temperatures of ~125 °C, 135 °C and 130 °C respectively. These maximum temperatures were observed during the dwell time, i.e. when the MW power was off, meaning this temperature increase was caused by thermal runaway. T2 exceeded 120 °C for ~50 minutes during the initial ramp-up phase and towards the end of the dwell phase.

T_{mw}, linked to the VHM computer, followed closest to the programmed temperature. During dwell, it reached the second highest temperature of ~130 °C.

The dwell phase for the MW-cured laminate can be split into three regions (A, B and C) as seen in Figure 4.11(c). In region A, the MW power decreased rapidly to 0%, since the T_{mw} temperature had reached the programmed temperature of 120 °C. Therefore, T1 and T4 (i.e. sub-laminates which temperatures are mostly dominated by the MW energy) saw a subsequent instantaneous and rapid decrease in temperature. The remaining sub-laminates (i.e. T2, T3 and T_{mw}) saw an increase in temperature due to thermal runaway. In region B – where MW power was still zero – the temperature of T1 and T4 saw an increase, while T2, T3 and T_{mw} experienced a decrease, attributed to conduction.

In region C, the MW power increased as the T_{mw} temperature decreased to below the level set in the program (i.e. 120 °C). A similar profile to that experienced during the ramp-up phase was observed, where T1 and T4 increased rapidly, however the magnitude was lower due to the lower MW power.

T4 achieved the highest peak temperature during the ramp-up phase (at ~140 °C), but had the second lowest temperature during Part B of the dwell phase when the MW power was zero, and was again the highest and the second highest temperature during Part C of the dwell phase when the MW power was re-activated.

4.2.4 Oven Heating Profile of 60 mm Thick Laminate

Five type N thermocouples were used to measure the temperatures through the thickness of the 60 mm thick laminate The locations of the thermocouples were identical to those described in the 60 mm thick MW-cured case.

The temperature profile of the 60 mm thick laminate through the thickness cured using a conventional oven can be seen in Figure 4.12. Figure 4.12(a) shows the complete cure cycle, Figure 4.12(b) shows the initial ramp-up, and Figure 4.12(c) shows the dwell phase.

As seen in Figure 4.12(a), T2 to T5 experienced a similar heating profile, while T1 was the most reactive, possibly attributed to changes due to the oven power and therefore underwent a slightly different profile. T1 saw the lowest thermal runaway, and reached a maximum temperature of

~121 °C and stayed around this temperature for approximately 80 minutes (i.e. between the 300th and the 380th minute), while T3 and T4 reached 120 °C approximately on the 290th minute and reached ~140 °C approximately 20 minutes later, and went below 120 °C approximately on the 400th minute (i.e. 110 minutes above 120 °C). T3 and T4 experienced the highest level of thermal runaway due to their central location in the laminate, and reached a maximum temperature of ~140 °C. T2 and T5 achieved similar maximum temperatures of 127 °C and 124 °C, respectively, where T2 reached ~120 °C in the 290th minute and reached the maximum temperature in the 310th minute. T5 reached ~120 °C in the 300th minute and reached maximum ten minutes later. The temperature then went below 120 °C after the 390th minute.

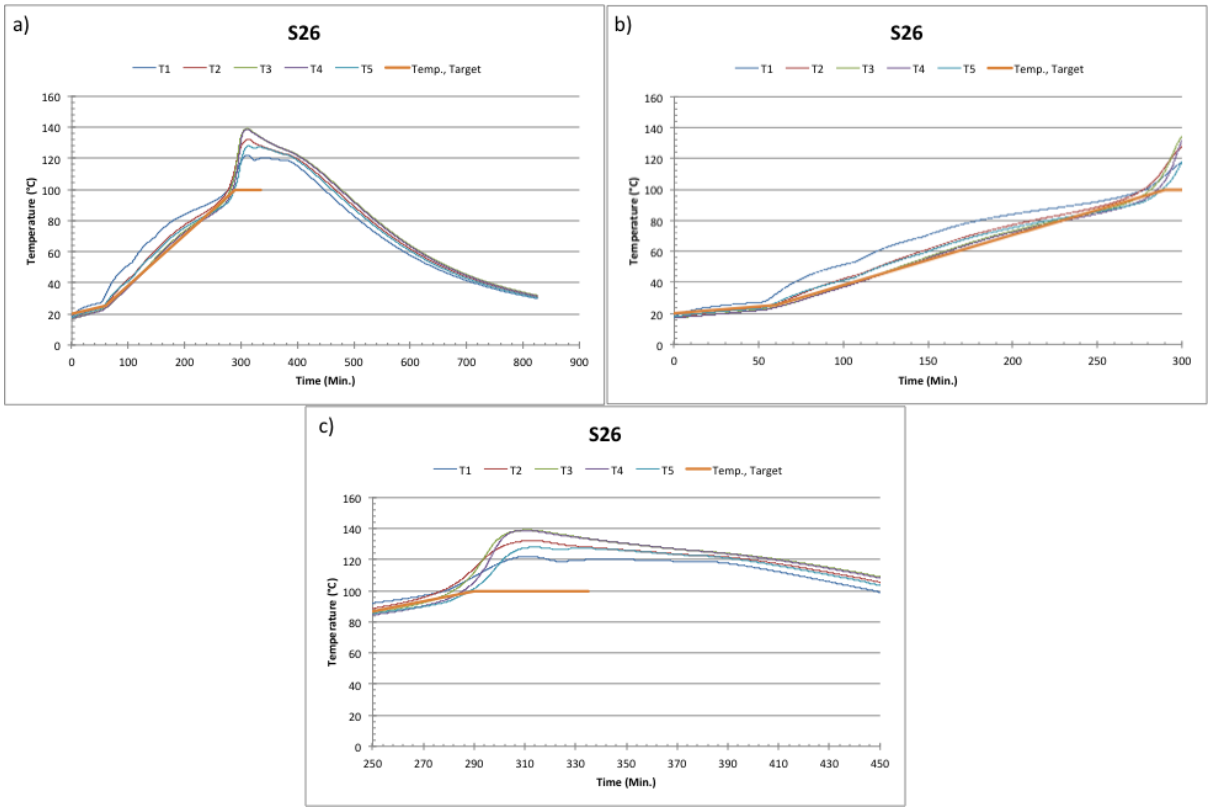


Figure 4.12 Conventional oven cure cycle of 60 mm thick laminate.
a) Full cycle, b) ramp-up phase, c) dwell phase.

Figure 4.12(b) shows how temperature T5 reacted first as the oven was activated. Overall, the maximum temperature difference between the highest (i.e. T3 and T4) and lowest (i.e. T1) was ~20 °C. The maximum temperature difference between the measured temperatures and the programmed temperature was ~40 °C, which was experienced by T3 and T4.

Although the oven was set to 45 minutes at 120 °C as recommended by the material manufacturer's technical datasheet [107], the entire laminate remained at above 120°C in excess of 100 minutes due to thermal runaway and the time taken for the oven to cool naturally. All sub-laminates underwent thermal runaway approximately between 90 °C and 100 °C (observed by the sudden change in temperature gradient).

4.2.5 Heating Profile MW vs Oven – 2.4 mm and 4.8 mm Thick Laminates

The average oven heating rate was 2.0 °C/min and 2.5 °C/min for the 4.8 mm (Figure 4.10) and 2.4 mm (Figure 4.9) thick laminates respectively. The MW heating rate was 10 °C/min for both the 2.4 mm (Figures 4.2 to 4.7) and 4.8 mm (Figure 4.8) thick laminates.

During the dwell phase, the temperatures of the oven-cured 2.4 mm thick laminates were in most cases more consistent and closer to the desired 120 °C cure temperature than the MW-cured laminates. The maximum difference between the probes, and the maximum difference between the probes and the target temperature was ≤5°C during dwell and ramp-up.

The 2.4 mm thick MW-cured laminates on the other hand showed a noticeable temperature difference between each probe (i.e. T1 to T4 and T_{MW}), and from the target temperature of up to 40 °C during the ramp-up phase and up to 30 °C during dwell. These differences in maximum temperature were obtained when the MW power was at its highest, i.e. very close to the 120 °C dwell temperature. In most cases, this large temperature difference was observed only for a brief period of time, and the difference decreased rapidly as soon as the MW power reduced. The high temperature observed initially by T2 caused the lower temperature during dwell, since the molecular movement of the matrix would be more limited, thus causing less heat under MW irradiation due to the self-limiting properties of MW heating. In addition, the cooling and ventilation system in the VHM may have also contributed. The continuously circulating cold outside air in the cavity, and the location of probe T2,

which was close to one of the ventilation holes in the MW cavity are also potential causes of the significant temperature difference.

In the case of the 4.8 mm thick oven-cured laminates, the laminates experienced a maximum temperature difference of ~20 °C between probes, and ~30 °C between probes and the target temperature during ramp-up. During dwell, a maximum temperature difference between probes, and between probes and target temperature was ≤10 °C. On the other hand, the 4.8 mm thick MW-cured laminates experienced a maximum temperature difference between the probes of ~20 °C, and ~10 °C difference from the target temperature, during ramp-up and dwell.

4.2.6 Heating Profile MW vs Oven – 60mm Thick Laminates

As in Section 4.2.1, one of the most evident differences between MW curing and oven curing was in the heating rates that were achieved. The oven-cured laminate (S26_O90) was heated at 0.3 °C/min but the MW-cured laminate (S25_MW90) was heated at a higher rate of 2 °C/min. Due to the fast heating nature of MWs, S25_MW90 experienced an instantaneous reaction with respect to MW power, particularly the top and bottom sub-laminates. In the case of the oven-cured laminate S26_O90, only one surface saw a noticeable change in heating profile due to the changes in oven power. The difference in temperature through the thickness was more noticeable in the MW-cured S25_MW90 than in oven-cured S26_O90 partly because 60 mm is greater than the material's MW penetration depth (D_p), but also due to the very slow heating rate used in the oven cure process to produce laminate S26_O90. The temperature difference through the thickness increased during thermal runaway for both laminates S25_MW90 and S26_O90, although the increase was more pronounced in the latter, i.e. the oven-cured laminate.

In the MW-cured laminate S25_MW90, thermal runaway was only observed in locations where probes T2, T3 and T_{mw} were located (see Figure 4.9). Compared to the same locations in the oven-cured laminate S26_O90, the temperature at which thermal runaway occurred was different. In

laminate S26_O90, thermal runaway initiated at ~90°C, whereas in the laminate S25_MW90 thermal runaway was observed beyond 100°C. Additionally, the magnitude of this thermal runaway was lower in the MW-cured laminate S25_MW90 – despite the higher heating rate. In laminate S25_MW90 the temperatures recorded by the T2, T3 and T_{mw} thermocouples underwent a ~20 °C, ~33 °C and ~34 °C increases respectively. In the oven-cured laminate S26_O90, the temperatures at the same locations (i.e. T2, T3 and T4) experienced ~40 °C, ~50 °C and ~50 °C increases respectively due to the thermal runaway.

In the case of the oven-cured laminate S26_O90, the total time beyond 120 °C was in excess of 100 minutes due to the slow cooling rate in the conventional oven. In the case of the MW-cured laminate S25_MW90, the time beyond, 120 °C was less than 100 minutes. The low temperature in the MW chamber led to, inevitably, a faster cooling.

The total cycle time (excluding cooling) was ~400 and 140 minutes for the oven-cured laminate S26_O90 and MW-cured laminate S25_MW90 respectively. This equates to a reduction in cycle time of ~65% with MW curing).

4.3 Degree of Cure

Table 4.1 shows the degree of cure for each of the cure cycles used in the investigation. The 2.4 mm thick oven-cured laminate S14 showed a degree of cure of 95.3%, which is very close to the value of 95.0% specified by the material manufacturer [107]. The degree of cure of the MW-cured laminates differed according to the dwell duration, ranging from 82% (S2, 30-minute dwell), to ~97% for both S9 and S10 which had a dwell time of 40 and 45 minutes respectively. The biggest increase in degree of cure, from 82% to ~92%, was observed when the dwell time was increased from 30 minutes (laminate S2) to 35 minutes (laminate S3).

For the 4.8 mm thick laminates, there was a ~4% difference between the degree of cure of the MW-cured S23_MW40 and oven-cured S24_O45 laminates. This is possibly attributed to the difference in

dwell time (45 minutes and 40 minutes in the oven and MW, respectively), and the slightly lower temperature achieved on the top surface of the laminate S23_MW40.

With regards to the 60 mm thick laminates S25_MW90 and S26_O90, the long dwell times led to an average degree of cure close to 100% and a very low deviation of 1.1% for both cases.

Table 4.1 Degree of cure of laminates. Results from laminates S25_MW90 and S26_O90 are shown as a function of sub-laminate through-thickness (TT) location.

Laminate S#	Cure Method	Laminate Thickness (mm)	Heating rate, Avg. °C/min	Mins. at dwell temp.	TT location	Degree of cure, %	Degree of cure, Avg., (Deviation) %
S2	MW	2.4	10	30	N/A	–	82.0 (4.5)
S3	MW	2.4		35	N/A	–	91.7 (3.3)
S9	MW	2.4		40	N/A	–	96.7 (1.1)
S10	MW	2.4		45	N/A	–	97.4 (4.6)
S14	Oven	2.4	2.5	45	N/A	–	95.3 (1.0)
S23_MW40	MW	4.8	10	40	N/A	–	91.0 (2.1)
S24_O45	Oven	4.8	2	45	N/A	–	95.0 (2.3)
S25_MW90	MW	60	2	90	13	100.0	99.5 (1.1)
					10	100.0	
					8	100.0	
					4	100.0	
					2	97.5	
S26_O90	Oven	60	0.3	100	13	97.6	99.2 (1.1)
					10	100.0	
					8	100.0	
					4	100.0	
					2	98.6	

4.4 Fibre Volume (V_f) and Void Volume (V_v) Content

Table 4.2 shows the results of the V_f and V_v values obtained for the 4.8 mm thick laminates (MW-cured S23_MW40 and oven-cured S24_O45) and the 60 mm thick laminates (MW-cured S25_MW90 and oven-cured S26_O90), with laminates S25_MW90 and S26_O90 divided by its individual sub-laminates.

Table 4.2 V_f and V_v for all laminates.

Laminate S#	Laminate Thickness (mm)	Heating rate, Avg. °C/min	Minutes at dwell temp.	Cure Method	V_f Average (Deviation), %	V_v Average (Deviation), %
S23_MW40	4.8	10	40	MW	40.8 (4.5) L	2 (1.3)
S24_O45	4.8	2	45	Oven	46.2 (4.5)	0.8 (0.8) L
S25-2_MW90	60	2	90	MW	47.5 (3.9) L	2.7 (1.5) L
S26-2_O90	60	0.3	100	Oven	54.3 (5.0)	3.2 (1.2)
S25-4_MW90	60	2	90	MW	52.7 (5.7)	4.3 (2.9)
S26-4_O90	60	0.3	100	Oven	48.1 (4.3) L	2.7 (1.1) L
S25-8_MW90	60	2	90	MW	49.7 (6.3) L	4.2 (1.6)
S26-8_O90	60	0.3	100	Oven	53.7 (5.3)	1.7 (0.6) L
S25-10_MW90	60	2	90	MW	48.1 (6.1) L	4.3 (2.3)
S26-10_O90	60	0.3	100	Oven	50.4 (4.2)	1.9 (0.7) L
S25-13_MW90	60	2	90	MW	48.5 (5.3)	4.3 (3.0)
S26-13_O90	60	0.3	100	Oven	47.3 (10.1) L	2.6 (1.6) L
S25_MW90 (Avg.)	60	2	90	MW	49.3 (5.5)	4.0 (2.3)
S26_O90 (Avg.)	60	0.3	100	Oven	50.7 (5.8)	2.4 (1.0)

Note: Sub-laminate '-2' was closest to the mould, and '-13' was farthest. L = low for each pair.

Oven-cured laminate S24_O45's V_f value of 46.2% is lower than oven-cured laminate S26_O90's value of 50.7%, which is believed to be attributed to the larger amount of resin bleed observed in the S26_O90 laminate caused by the low heating rate. S24_O45's V_v value of 0.8% is lower than S26_O90's value of 2.4%, which is believed to be related to the thickness of the laminate, caused by the additional difficulties in the removal of air and volatiles in thick laminates. A similar pattern was observed with respect to V_f and V_v values when comparing MW-cured laminates S23_MW40 and S25_MW90.

When comparing the 4.8 mm thick MW-cured laminate S23_MW40 and oven-cured laminate S24_O45's V_f and V_v values, S23_MW40's values were lower by ~5% and higher by ~1%, respectively. Similar results were observed with the 60 mm thick laminates. It can be observed that overall, the 60 mm thick oven-cured laminate S26_O90 had a higher V_f content than the 60 mm thick

MW-cured laminate S25_MW90, however the difference is relatively small, and again, the MW-cured laminate S25_MW90 had a greater V_v value than the oven-cured laminate S26_O90.

When comparing the V_v of the 60 mm thick laminate S25_MW90 (MW-cured) and laminate S26_O90 (oven-cured), with 4.8 mm thick S23_MW40 (MW-cured) and S24_O45 (oven-cured), the values obtained were relatively high for the former – which was possibly attributed to the thickness of the laminate – where the maximum value (i.e. 4.3%) was obtained by the laminate S25_MW90 in three locations out of five. Additionally, the variation observed in the laminate S25_MW90 was also greater. Looking at the V_v of laminates S25_MW90 and S26_O90, the former obtained a value significantly greater than the latter at 4.0% and 2.4% respectively.

4.5 Microwave Penetration Depth

As described in Section 3.6, an aluminium vessel containing a 1 L bowl of water was used to assess the MW penetration depth of the composite laminates. The top of the vessel had a hole, thus allowing MWs to pass through and heat the water. The hole was of a suitable size to allow MWs heat the water, but with sufficient space to support the PTFE sheet that supported the composite laminates. The water temperature was measured as a function of MW power and time, with varying number of composite plies.

The results of the change in water temperature as a function of laminate thickness used to assess the material's MW penetration depth can be seen in Table 4.3 and Figure 4.13. The reference tests showed a high (~19 °C and ~11 °C) and a low (<0.3 °C) temperature change for the R1 (perforated aluminium plate only, i.e. full MW penetration) and R2 (solid aluminium plate only, i.e. no MW penetration) tests respectively. The average and standard deviations are from three tests.

Table 4.3 Change in temperature as a function of laminate thickness.

Number of plies (Laminate Thickness)	ΔT3, Average (°C)	ΔT3, Standard Deviation (°C)	ΔT4, Average (°C)	ΔT4, Standard Deviation (°C)
0 Plies, R1 (0mm)	18.9	2.6	10.8	1.2
0 Plies, R2 (0mm)	0.3	0.0	0.1	0.0
1 Ply (~0.6mm)	5.0	0.8	1.9	0.1
2 Plies (~1.2mm)	2.8	1.2	0.9	0.2
3 Plies (~1.8mm)	2.0	1.6	0.7	0.6
4 Plies (~2.4mm)	2.5	0.9	0.7	0.1

Note: T3 and T4 were positioned on the 1 L and 0.5 L mark in the bowl, respectively.

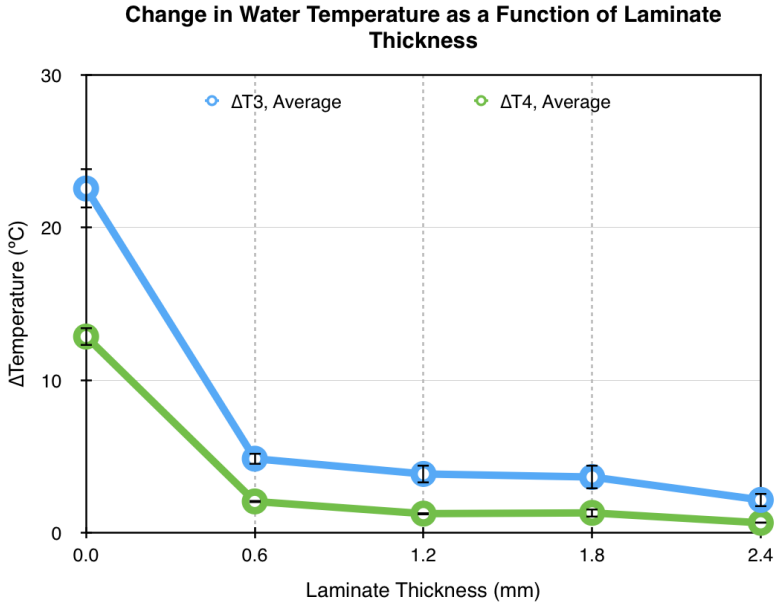


Figure 4.13 Change in water temperature as a function of carbon-epoxy laminate thickness after 10 mins, 1kW MW heating.

The change in temperature as a function of laminate thickness showed a steep decay between no laminate (i.e. reference test R1), and 0.6 mm laminate thickness (i.e. one ply), with small changes from there onwards. The theoretical MW penetration depth based on eq. 2.5 is 1 mm or less than 0.1 mm assuming $\mu=1.26\text{x}10^{-6}$H/m, and $s=2\text{x}10^{4}$S/m or 100S/m at a frequency of 2.45GHz depending on whether the waves are parallel or orthogonal to the carbon fibres [73]. However, since the practical method to measure the MW penetration depth presented here is a maximum, whereas the theoretical value is e^{-1} (i.e. ~0.37), it is necessary to divide the theoretical value by 0.37 (to obtain the maximum theoretical D_p value), which in this case was 2.7 mm, or multiply the experimental value by 0.63 (to obtain the e^{-1} experimental D_p value), which in this case was 1.5 mm. When taking this into account, the difference between the theoretical and experimental D_p values is;

- 2.4 mm (experimental D_p) × 0.63 = 1.51 mm (vs. 1.0 mm (theoretical D_p)), or
- 1.0 mm (theoretical D_p) ÷ 0.37 = 2.7 mm (vs. 2.4 mm (practical D_p)),

where both cases resulted in a difference of less than one ply thickness of 0.6 mm.

4.6 Mechanical Testing

4.6.1 Tensile Testing

The tensile test results are summarised in Figures 4.14 and 4.15, which also include plots of the degree of cure achieved. Figure 4.16 shows the results of the transverse tensile strength with respect to coupon location. The main findings were as follows:

- The maximum longitudinal UTS of MW-cured composites is similar to that of the oven-cured composites.
- The transverse UTS of oven-cured composites was slightly greater (~11%) than the highest of the MW-cured composites.
- MW-cured composites with a 30-minute dwell time produced a transverse UTS ~38% lower than the oven-cured composites.
- Little change in longitudinal and transverse elastic moduli was observed across all the samples regardless of the curing method and curing cycle.
- The standard deviations in both strength and modulus were relatively consistent irrespective of heating method, thus demonstrating the high consistency and reliability of MW heating.
- The oven-cured sample's degree of cure was ~95.3%, which is very similar to the value suggested by the material manufacturer for a 45 minute dwell time at 120°C. The MW-cured samples' degree of cure ranged between 82% (30 min at 120°C) and ~97% (45 min at 120°C).

The largest increase (~9%) was observed when increasing the MW 120°C dwell time from 30 to 35 minutes. 40 minutes at 120°C in the MW achieved the oven sample's degree of cure.

- A 40 minute MW dwell at 120°C provided a longitudinal tensile strength of ~1975 MPa and a transverse tensile strength of ~37 MPa, in comparison to ~1921 MPa and ~41 MPa respectively for the oven-cured laminates. The 45 minute MW dwell at 120°C also produced very similar results within the experimental error margin.

- There was no apparent bias of transverse tensile strength and modulus due to the location of the coupon in the laminate.

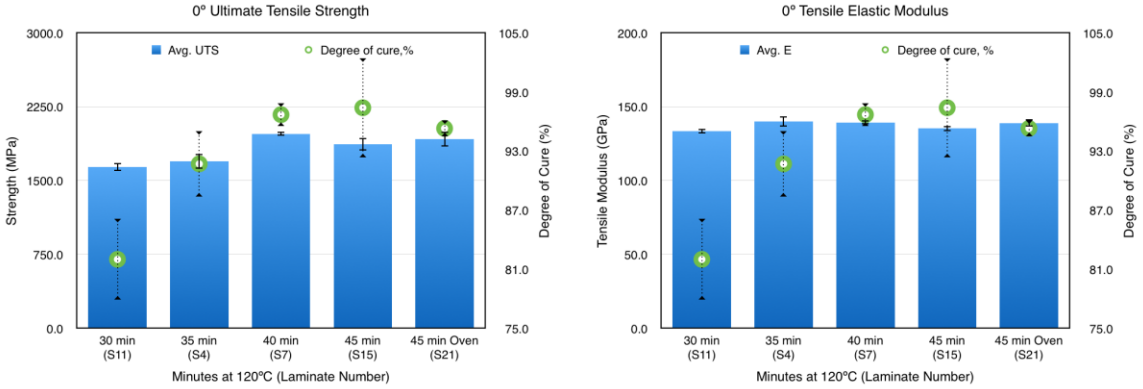


Figure 4.14 Longitudinal tensile strength and modulus, and degree of cure.

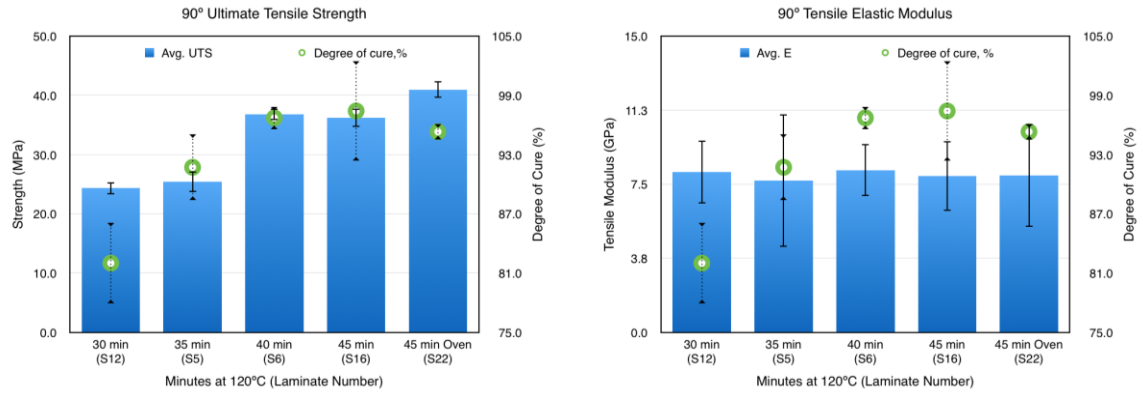


Figure 4.15 Transverse tensile strength and modulus, and degree of cure.

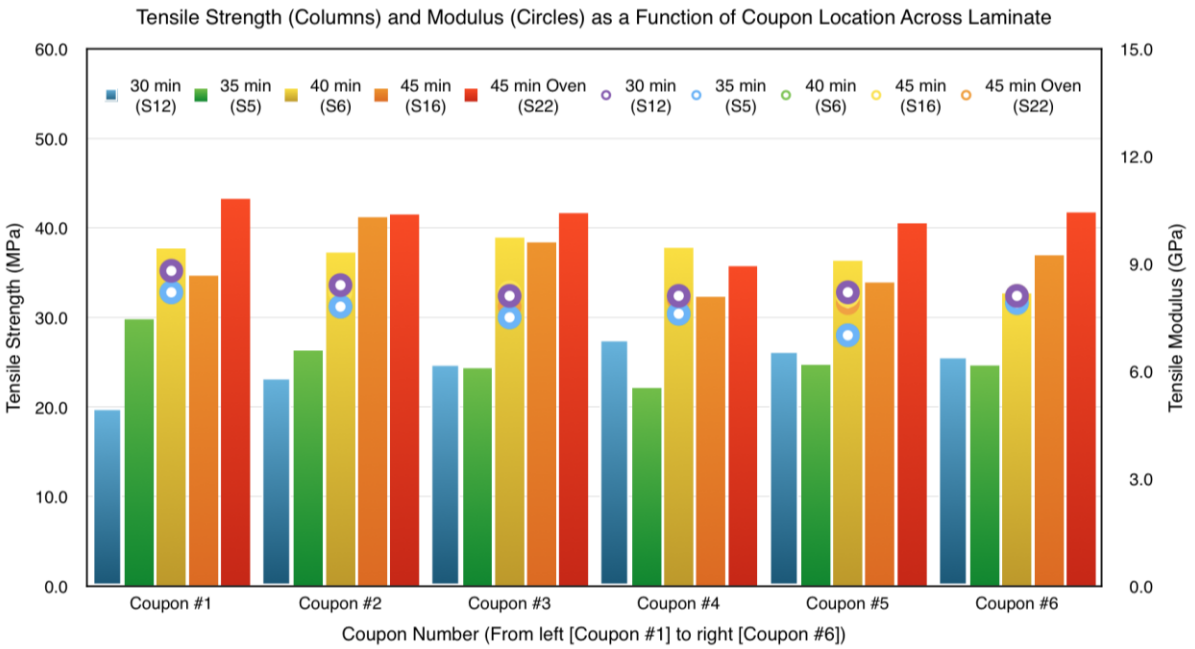


Figure 4.16 Transverse tensile strength (columns) and modulus (circles) as a function of coupon location across laminate.

4.6.2 Compression Testing

The compression test results (Figure 4.17) showed;

- All four sets of MW-cured samples produced greater ultimate compressive strengths (UCS) compared with the oven-cured samples. Coupons from laminate S7_MW40 (40 min at 120°C MW-cured) obtained an UCS of 1159.6MPa compared with coupons from laminate S21_O45 (45 min at 120°C oven-cured), which obtained an UCS of 857.6MPa, i.e. an increase of ~35%.
- No significant changes in elastic modulus were observed, regardless of curing method.
- As with the tensile test results, the standard deviation in both strength and modulus were consistent irrespective of heating method, thus demonstrating the high consistency and reliability of MW heating.

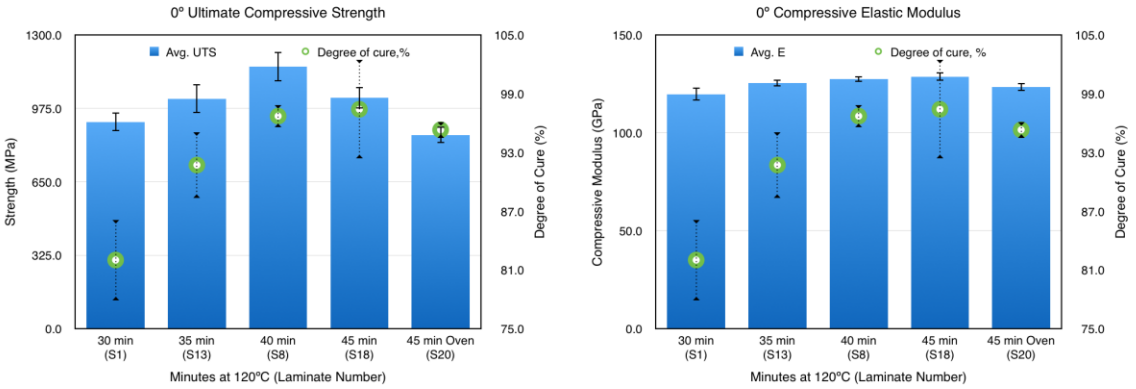


Figure 4.17 Longitudinal compressive strength and modulus, and degree of cure.

4.6.3 In-Plane Shear (IPS) Testing

The IPS test results (Figure 4.18) showed little variation in in-plane shear strength (IPSS) (~9%) and IPS modulus (~2%) regardless of the heating method, once again suggesting a high degree of consistency and reliability with MW heating (using the VHM system).

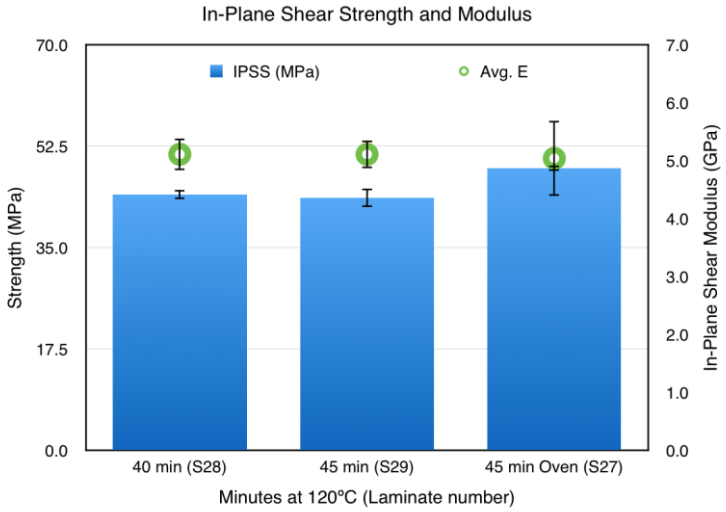


Figure 4.18 In-plane shear strength and shear chord modulus of elasticity.

4.6.4 Mode I Interlaminar Fracture Toughness (G_{1C}) Testing

Figures 4.19 and 4.20 show the R-curves for the 4.8 mm thick S24_O45 (oven-cured) and S23_MW40 (MW-cured) laminates respectively. Generally, it can be observed that coupons from laminate S24_O45's interlaminar fracture toughness values varied between ~105J/m^2 and ~250J/m^2, with an average of ~180J/m^2 (and a standard deviation of ~15.3%). S23_MW40 on the other hand showed an increasing trend as a function of crack propagation, and ranged from ~135J/m^2 to ~430J/m^2 (with an average of ~233J/m^2) with a deviation of ~22.8%, thus equating to an increase of ~29%. S23_MW40 and S24_O45 coupons suffered from crack jumping during testing, albeit to a much lesser extent by the MW-cured coupons from laminate S23_MW40.

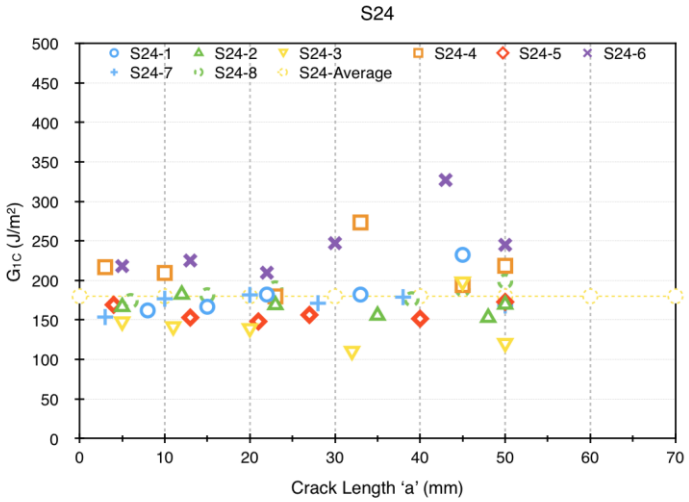


Figure 4.19 R-curves – Oven-cured laminate S24_O45 (Average G_{1C} = 179.9J/m^2).

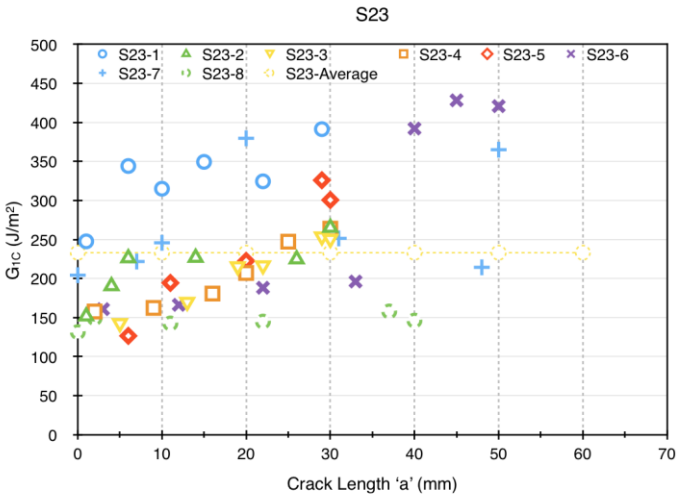


Figure 4.20 R-curves – MW-cured laminate S23_MW40 (Average G_{1C} = 233.1J/m^2).

Figure 4.21 shows the R-curves for the sub-laminates of the oven-cured laminate S26_O90. It can be observed that the curves do not change significantly with crack length. There is a noticeable increase in toughness as a function of the sub-laminate's distance from the mould, where S26-13_O90 (i.e. farthest from the mould) had a higher toughness compared to S26-2_O90 (i.e. closest to the mould). S26-10_O90 produced the highest toughness values, which may be the best compromise between temperature achieved, thermal residual stress due to the mould, and thermal residual stress due to cooling – this pattern was also observed in the MW-cured sub-laminate S25-10_MW90 (Figure 4.22).

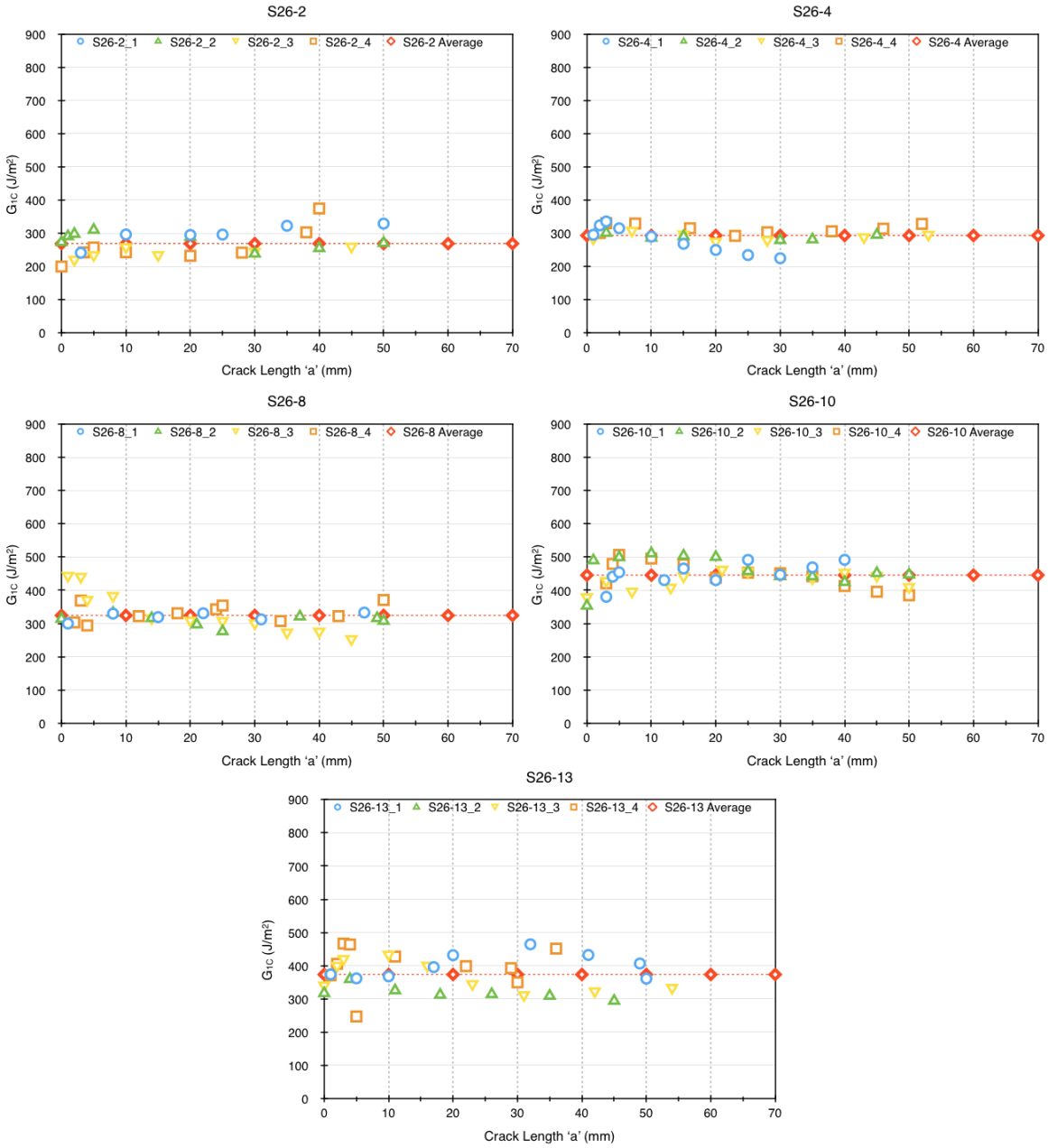


Figure 4.21 R-curves – Sub-laminates of oven-cured laminate S26_O90.

The R-curves for the sub-laminates of the MW-cured laminate S25_MW90 (Figure 4.22) showed some differences compared to the oven-cured laminate S26_O90. The main differences were;

- Greater G_{1C} and standard deviation values were achieved (on average) by the sub-laminates from laminate S25_MW90.
- S25-10_MW90, but more noticeably S25-13_MW90 (i.e. the top sub-laminate directly exposed to MWs) saw an increasing trend in G_{1C} value with crack length.

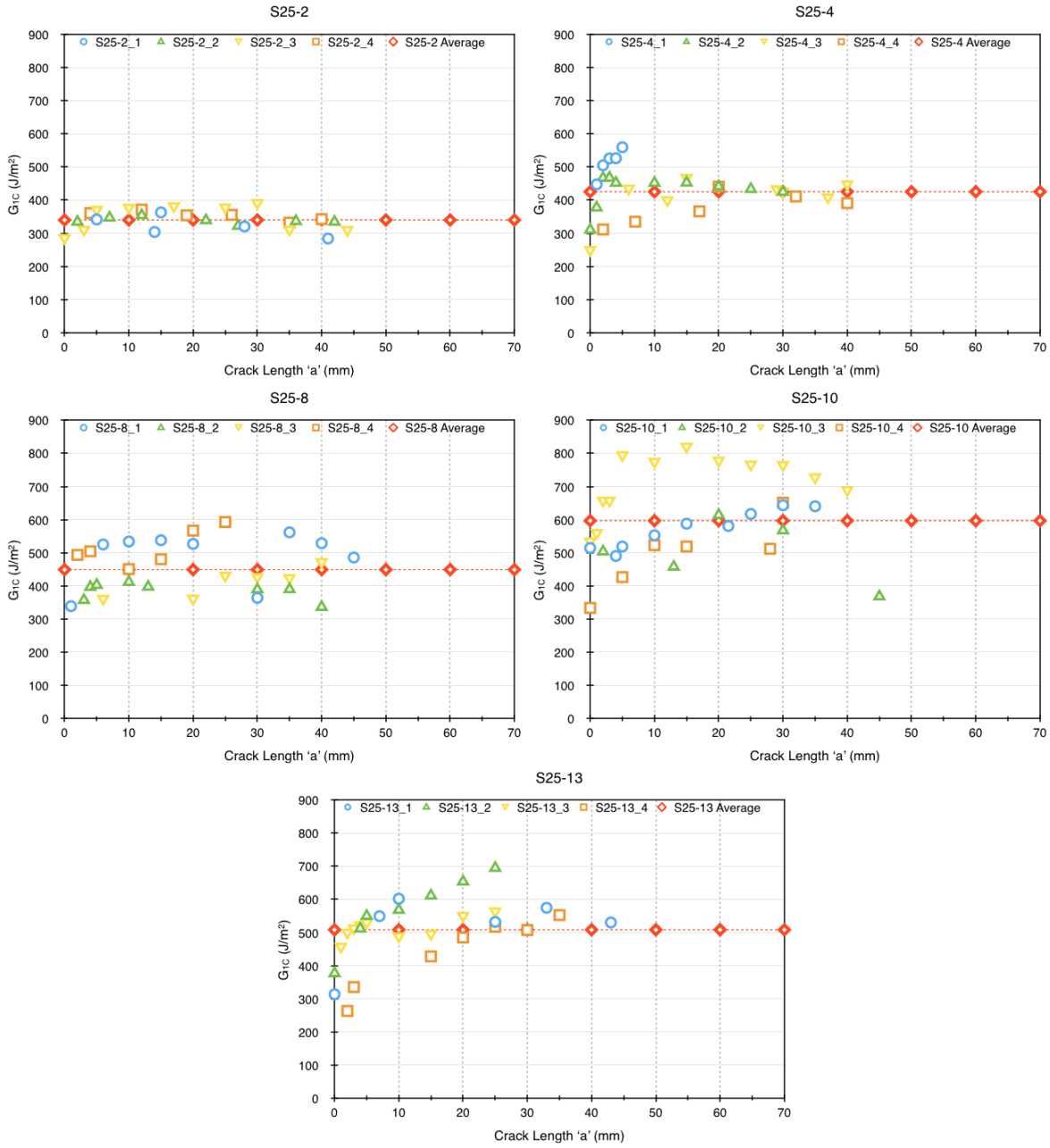


Figure 4.22 R-curves – Sub-laminates of MW-cured laminate S25_MW90.

Similar to the sub-laminates of the oven-cured laminate S24_O45, the sub-laminates of the oven-cured laminate S26_O90 were more prone to crack jumps during testing compared to the MW-cured S25_MW90 sub-laminates, i.e. S25_MW90 sub-laminates were showing a more stable crack growth. Additionally, another remark is that some of the S25_MW90 sub-laminates experienced fibre bridging and crack splitting (Note: test results of samples where crack splitting was observed during testing have not been included in the present calculations), whereas there was no indication any of the S26_O90 sub-laminates experienced the same effect. Although fibre bridging may be as a result of

improved fibre-matrix adhesion, it is believed that the higher V_v content (in addition to the increased fibre-matrix adhesion – described in Section 4.6.5) may have contributed to crack meandering.

The average interlaminar fracture toughness (G_{1C}) values obtained through mode I DCB testing of laminates S25_MW90 and S26_O90 (Figure 4.23) showed similar trends, where the minimum toughness values were obtained by sub-laminate 2, i.e. closest to the mould, and the highest toughness was obtained by sub-laminate 10, and sub-laminate 13 obtained the second highest toughness value. The average G_{1C} values from sub-laminates of laminate S26_O90 ranged from ~275J/m^2 to ~375J/m^2, and S25_MW90's values ranged from ~325J/m^2 to ~590J/m^2. The greater deviations observed by the coupons from laminate S25_MW90 were clearly noticeable.

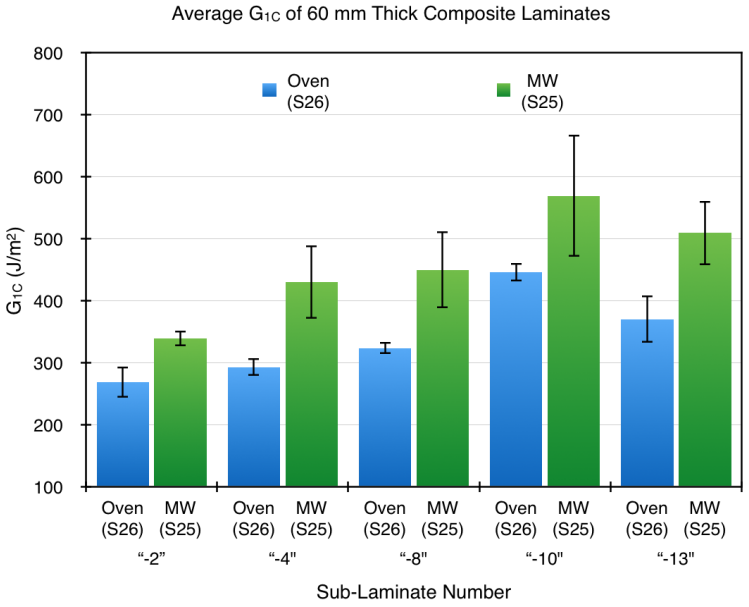


Figure 4.23 Average interlaminar fracture toughness values obtained for laminates S25_MW90 and S26_O90, where '-2' is the sub-laminate closest to the mould, and '-13' is farthest.

The initiation G_{1C} values between the MW-cured (laminates S23_MW40 and S25_MW90) and the oven-cured (laminates S24_O45 and 26) did not seem to differ greatly, as shown by the results shown from Figure 4.19 to 4.22. S24_O45's initiation value (or the first G_{1C} value obtained) was ~160J/m^2, whereas S23_MW40's initiation value was ~150J/m^2. The 60 mm thick laminate results are more scattered (see Figure 4.24), especially the MW-cured (laminate S25_MW90), and therefore the trend is less obvious. S26_O90's fracture initiation value was ~230J/m^2 for '-2', ~290J/m^2 for '-4',

~340J/m^2 for '-8', ~380J/m^2 for '-10', and ~350J/m^2 for '-13', whereas S25_MW90's values were ~330J/m^2, ~330J/m^2, ~390J/m^2, ~470J/m^2 and ~350J/m^2 for '-2', '-4', '-8', '-10' and '-13' respectively.

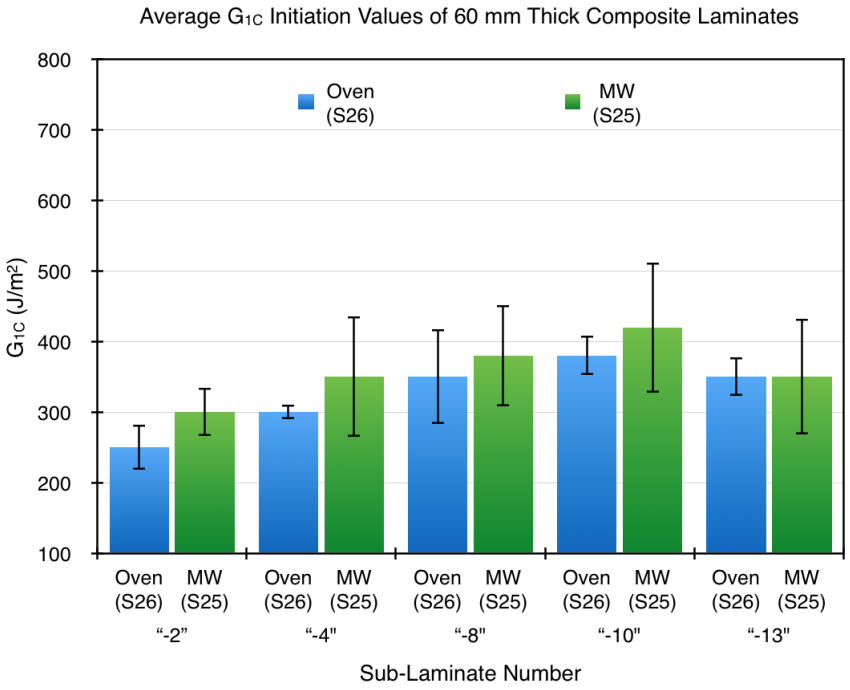


Figure 4.24 Average mode I interlaminar fracture initiation values of 60 mm thick oven-cured (S26_O90) and MW-cured (S25_MW90) laminates.

4.6.5 Fibre Push-Out Testing

The results of 42 fibre push-out test results (21 for the MW-cured laminate S23_MW40 and 21 for the oven-cured laminate S24_O45) can be seen in Figure 4.25. Average IFSS values of 74.4 MPa and 53.1 MPa were obtained for laminates S23_MW40 and S24_O45 respectively. The standard deviation was greater with the S23_MW40 samples (16.7%) compared to the S24_O45 samples (11.1%).

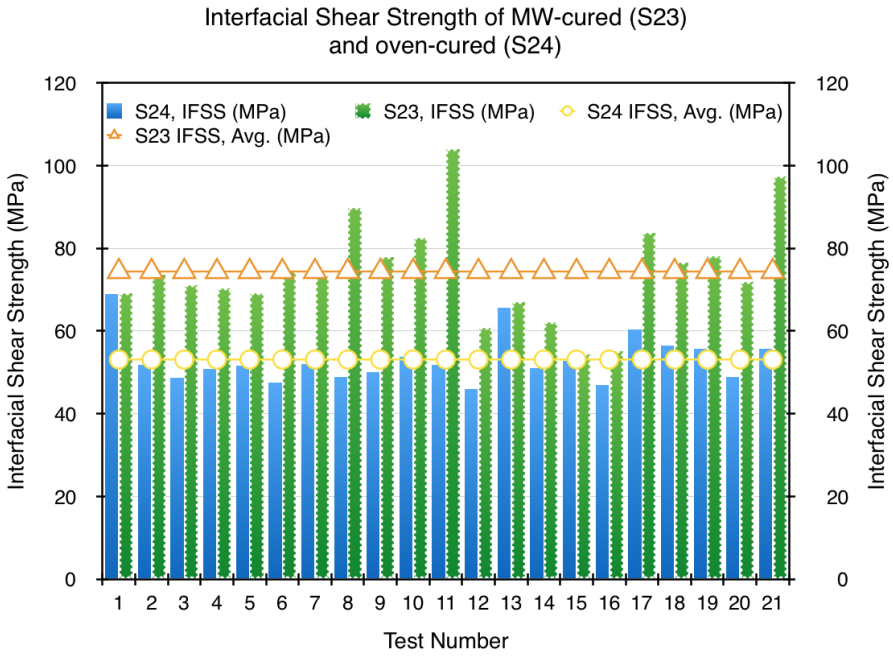


Figure 4.25 IFSS values obtained using fibre push-out testing from MW-cured (S23_MW40) and oven-cured (S24_O45) laminates.

When comparing the change in IFSS against the change in G_{1C} as seen in Figure 4.26, a change in IFSS of ~28% led to a change in G_{1C} of ~23%.

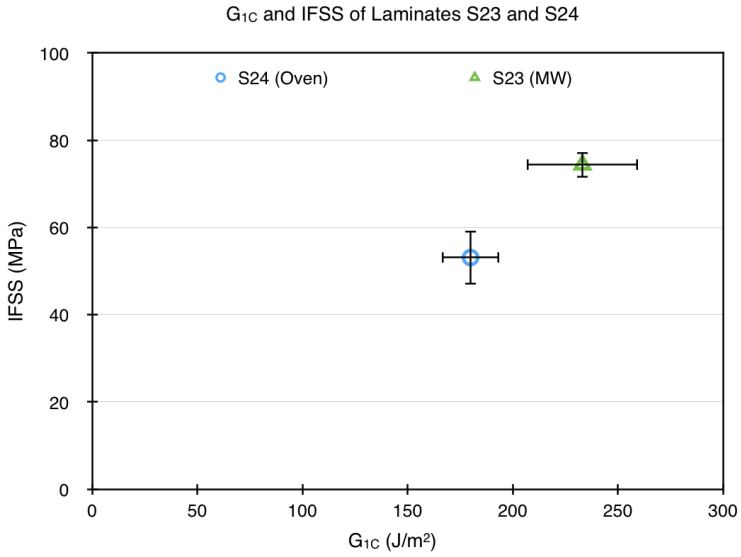


Figure 4.26 Fracture toughness (G_{1C}) and IFSS of samples S23_MW40 and S24 ($\Delta G_{1C} \approx 23\%$, $\Delta IFSS \approx 28\%$).

4.6.6 Failure Mode Assessment of Tested Samples

Some similarities and differences were observed between the conventional oven-cured (S22-5_O45) and MW-cured (S16-5_MW45 and S6-5_MW40) samples when the failure mode was assessed using the SEM. Representative SEM images of the 90° tensile tests can be seen from Figure 4.27 to 4.29. Some of the areas of interest have been highlighted in the figures with labels (i), (ii) and (iii), representing fibre disbonding, matrix remaining on fibre surface, and matrix roughness, respectively. Only some of these features have been highlighted in the figures for clarity purposes.

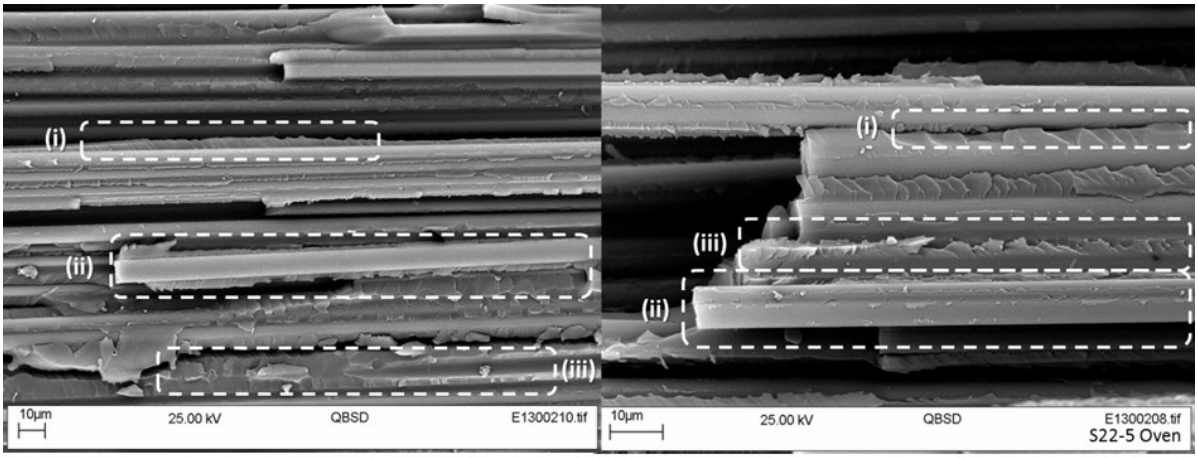


Figure 4.27 Fracture surface SEM of 90° tensile test. Sample S22-5_O45, 45min at 120°C (Oven-cured).
(i) fibre disbonding, (ii) matrix remaining on fibre surface, and (iii) matrix roughness.

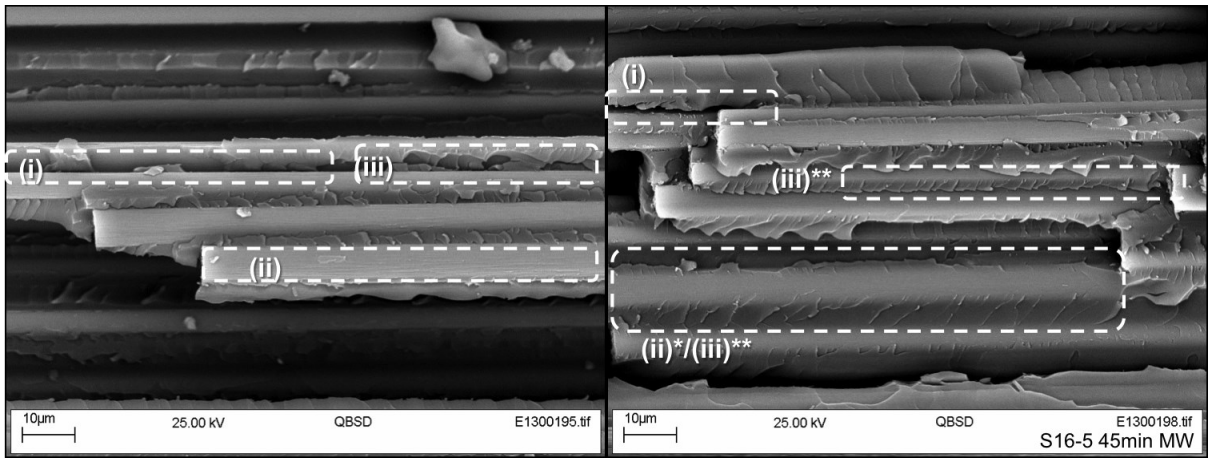


Figure 4.28 Fracture surface SEM of 90° tensile test. Sample S16-5_MW45, 45min at 120°C (MW-cured).
(i) fibre disbonding, (ii) matrix remaining on fibre surface, and (iii) matrix roughness.
***Fully, or almost fully, matrix coated fibres, **ductile and brittle failure.**

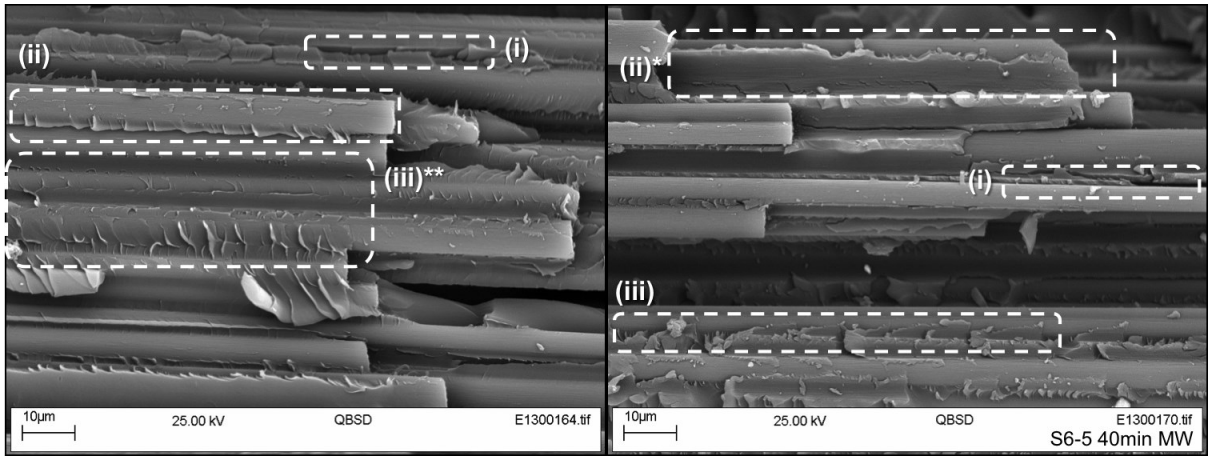


Figure 4.29 Fracture surface SEM of 90° tensile test. Sample S6-5_MW40, 40min at 120°C (MW-cured).
(i) fibre disbonding, (ii) matrix remaining on fibre surface, and (iii) matrix roughness.
***Fully, or almost fully, matrix coated fibres, **ductile and brittle failure.**

The following can be reported based on the fracture surface images;

- Although both oven and MW-cured samples suffered from fibre disbonding, this was clearer in the oven-cured samples (labelled (i) in Figures 4.27 to 4.29).

- Fibre-matrix interfacial failure mode in the oven-cured samples was predominant as observed by the limited matrix remaining on the fibres (labelled (ii) in Figure 4.27). This is an indication of the tougher matrix or weaker interface of the oven-cured sample, since there is a tendency for fracture to occur preferentially at the fibre-matrix interface as the toughness of the material increases [125-127].

  MW-cured samples S16_MW45 (45 min at 120°C) (Figure 4.28) and S6 (40 min at 120°C) (Figure 4.29) showed a more cohesive-dominated failure, as observed by the fibres that were almost fully coated (labelled (ii)* in Figures 4.28 and 4.29). However some clean fibres with little (or no) matrix was also observed (labelled (ii) in Figures 4.28 and 4.29), suggesting the existence of a multi-phase failure in the MW-cured sample's fracture surface.

- Overall, the degree of matrix roughness (labelled (iii) in Figures 4.27 to 4.29) between the samples was similar, however MW-cured samples showed both a rough matrix fracture

surface (i.e. ductile failure) and a smooth matrix fracture surface (i.e. brittle failure) even in the same sample (labelled (iii)** in Figures 4.28 and 4.29).

Fracture surfaces of samples tested for G_{1C} can be seen in Figures 4.30 and 4.31. The white dotted lines in Figure 4.30a and 4.31a represent the end of the release film that was used to create the initial crack, and the black arrow represents the direction of crack propagation. The oven-cured sample S24_O45 showed a relatively smooth fracture surface, indicating little energy absorption during fracture (see region (i) in Figure 4.30a). On the other hand, the MW-cured sample showed crack meandering through various planes through the thickness of the material during crack propagation (see region (i) Figure 4.31a), which is a clear indication of higher energy absorption. It is interesting to see that, like with the 90° tensile fracture surfaces, oven-cured samples showed limited matrix adhesion on the fibres (see region (ii) in Figure 4.30b and 4.30c), whereas the MW-cured samples show some fibres almost entirely coated with matrix material (see region (ii) in Figure 4.31b and 4.31c). Additionally, the MW-cured samples showed a multi-phase failure mode (see region (iii) in Figure 4.31b and 4.31c), as mentioned with the 90° tensile fracture surfaces, where areas with smooth matrix fracture surface and ductile matrix deformation (i.e. rough matrix surface) are clearly visible too. On the other hand, the oven-cured sample showed large regions with a smooth fracture surface as exemplified in region (iii) in Figure 4.30d. The MW-cured G_{1C} fracture surface showed that there were regions which lacked matrix material, as observed in region (iv) in Figure 4.31d, where the fibre surfaces were entirely free from matrix material.

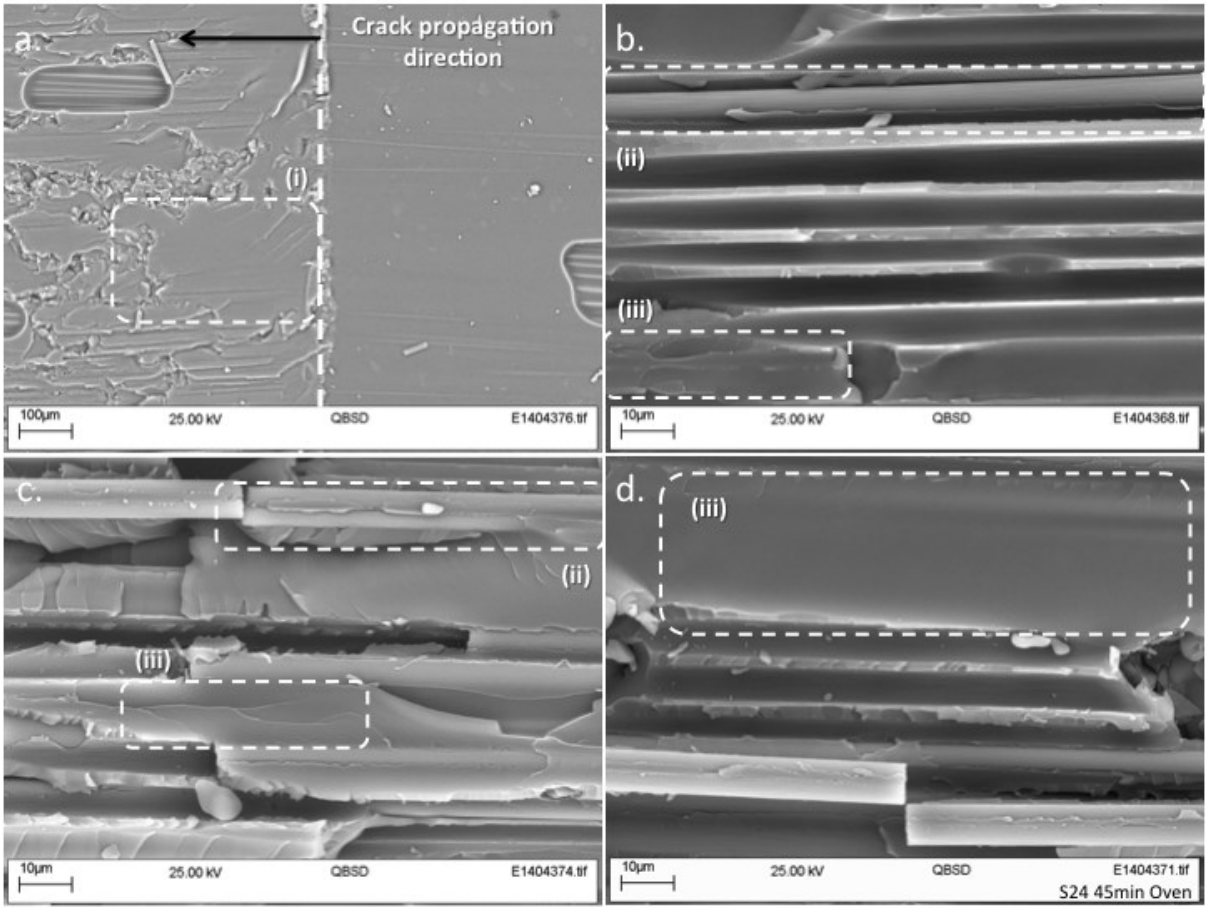


Figure 4.30 Oven-cured sample S24_O45 fracture surface after G_{1C} testing.
(i) Smooth crack surface with crack propagation predominantly on a single plane, (ii) Matrix remaining on fibres, and, (iii) matrix fracture surface roughness.

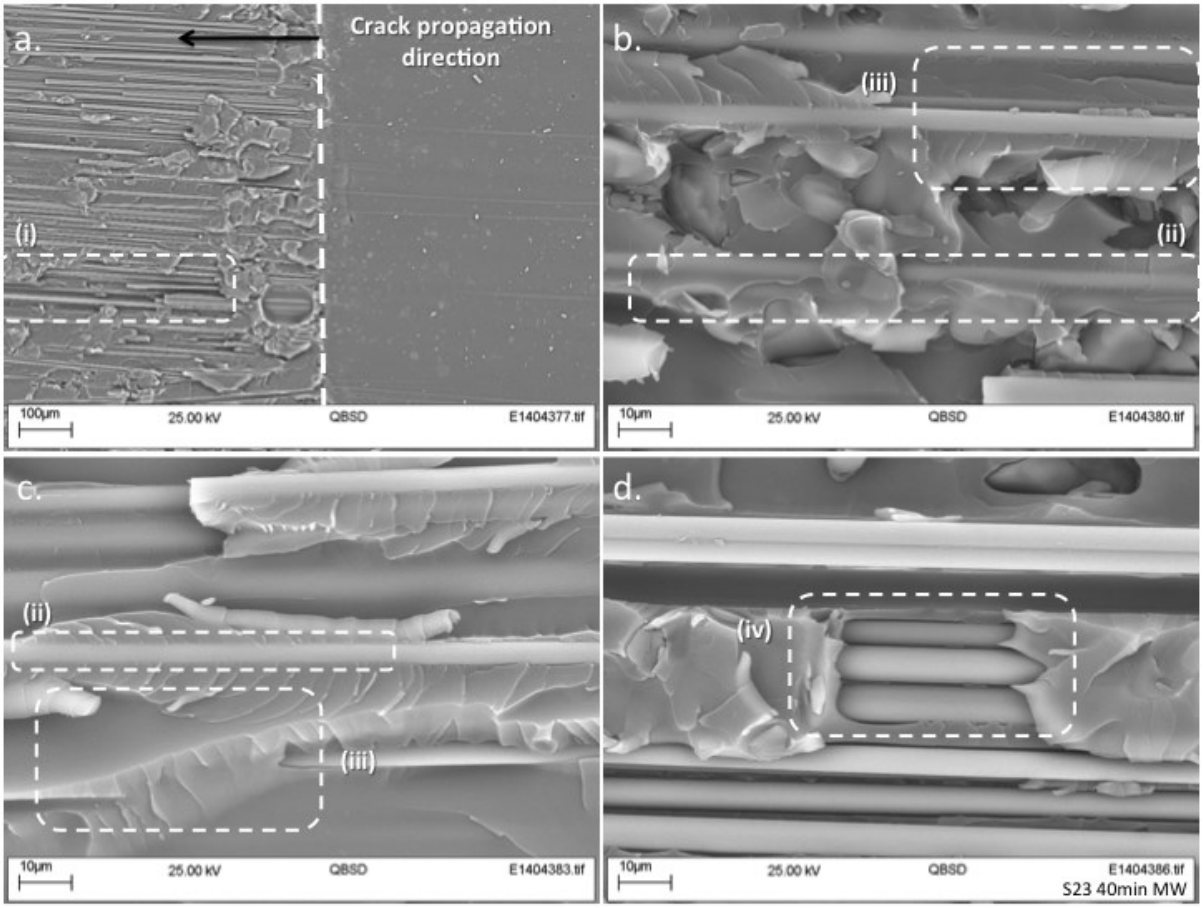


Figure 4.31 MW-cured sample S23_MW40 fracture surface after G_{1C} testing. (i) Crack surface with crack propagation travelling through multiple planes, (ii) Matrix remaining on fibres, (iii) matrix fracture surface roughness, and, (iv) region with apparent lack of matrix or very poor adhesion to fibres.

4.6.7 Matrix Indentation Testing

The elastic modulus of the sub-laminates of laminates S25_MW90 and S26_O90 were calculated from the reduced modulus (also called indentation modulus) using eq. 3.11. As can be seen in Figure 4.32, there was little variation in results irrespective of the heating method and location of the sub-laminate – S25_MW90 and S26_O90's average G_{1C} was ~4.8 GPa and ~4.7 GPa respectively. The difference in elastic modulus between the minimum (S26-2_O90) and the maximum (S25-8_MW90) sub-laminate was ~13%.

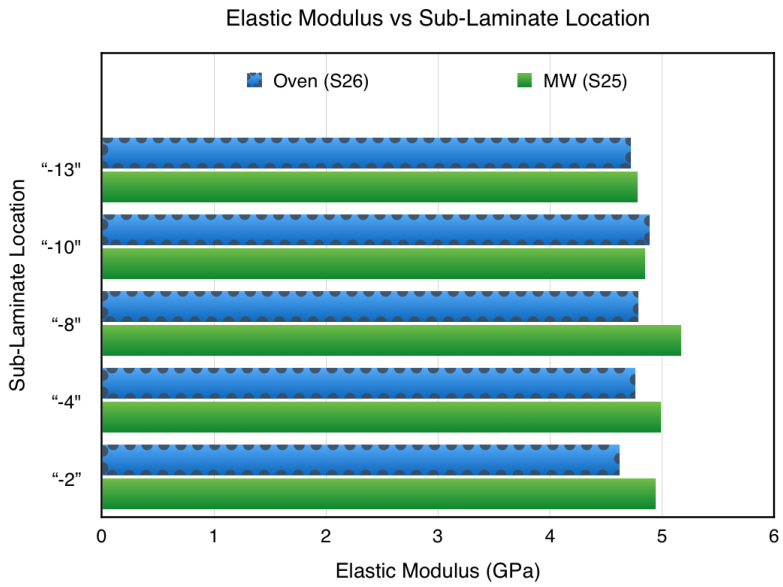


Figure 4.32 Calculated elastic modulus based on indentation modulus as a function of sub-laminate location.

The rule of mixtures equation for the transverse modulus of the composite, E

$$\frac{1}{E} = \frac{V_f}{E_f} + \frac{V_m}{E_m} \qquad \text{(Eq. 4.1)}$$

where V_f is the fibre volume fraction, E_f is the fibre modulus, V_m is the matrix volume fraction and E_m is the matrix modulus.

Applying eq. 4.1 to the elastic modulus values obtained in Section 4.6.1 for the 90° tensile tests, with a fibre volume fraction of ~50% [107], the elastic modulus of the matrix was determined to be ~4.0 GPa, which is ~15% lower than the values obtained using the nano-indentation method.

4.7 Results – Summary

- Heating rate: The heating rates of the 2.4 mm and 4.8 mm thick oven-cured laminates were 2.5°C/min and 2°C/min. respectively, and 0.3°C/min was used to cure the 60 mm thick laminate. The heating rates used with MWs were 10°C/min for the 2.4 mm and 4.8 mm thick laminates, and 2°C/min for the 60 mm thick laminate. The MW heating rate achieved was

significantly greater (up to six times) than conventional heating using the material and configuration presented here.

- Dwell time and temperature: The dwell time for the 2.4 mm and 4.8 mm thick oven-cured laminates was 45 minutes at 120°C as recommended by the material manufacturer. The 60 mm thick oven-cured laminate had a dwell time of ~100 minutes. The 2.4 mm thick MW-cured laminates were manufactured with dwell times of 30, 35, 40 and 45 minutes at 120°C. The 4.8 mm thick MW-cured laminate had a dwell time of 40 minutes at 120°C. The 60 mm thick MW-cured laminate had a dwell time of 90 minutes. The 2.4 mm thick oven cure cycle saw a temperature difference of ≤5°C between the probes, and with the target temperature during ramp-up and dwell, whereas the maximum temperature difference observed in the MW cure cycle for the same laminate thickness was 40°C during ramp-up and 30°C during dwell. The 4.8 mm thick oven cure cycle showed a maximum temperature difference of 30°C between the probes and the target temperature during ramp-up. The 4.8 mm thick MW cure cycle showed a maximum temperature difference between the probes of 20°C during dwell, although this was based on only three probes as two of them broke during the application of vacuum bagging. The oven-cured 60 mm thick laminate had a maximum temperature difference of 20°C during ramp-up, and 40°C during dwell, which were caused by the low thermal conductivity of the laminate, and the exothermic reaction, respectively. The 60 mm thick MW-cured laminate had a temperature difference between the probes and the target temperature of ~40°C during ramp-up and dwell.

  The difference in temperature observed by the MW cycles typically occurred when the magnetrons were activated to match the target temperature. Once the desired temperature was met and the power was reduced, the temperature difference also reduced accordingly, so in most cases the high temperature difference in the MW case between the probes and the target temperature was only for a brief period of time.

- Cure cycle time: When considering the best performing MW-cured samples, the MW cure cycle time achieved a reduction in comparison to the oven cure of up to 65% (excluding

cooling time), although this reduction was mainly due to an increase in heating rate, and not due to a substantial decrease in dwell time.

- Degree of cure: The 2.4 mm thick MW-cured laminates at 40 and 45-minute dwell times (laminates S9 and S10 respectively) achieved a degree of cure of ~97% which was similar to that of the oven-cured sample (~95%) of the same thickness (S14). The degree of cure of MW-cured 4.8 mm thick laminates (S23_MW40) was slightly lower at 91% compared with 95% achieved in the oven-cured samples with the same thickness. The 60 mm thick oven (S26_O90) and MW (S25_MW90) cured laminates achieved ~100% degree of cure.
- Fibre and void volume fractions, V_f and V_v: The V_f of the 4.8 mm thick laminates showed that the MW-cured samples (S23_MW40) had ~41% of fibres, whereas the oven-cured (S24_O45) had ~46%. The 60 mm thick MW-cured laminate (S25_MW90) had ~49% of fibres, and the oven-cured (S26_O90) had ~51%. In terms of V_v, S23_MW40 had ~2% and S24_O45 had ~1% void content. The V_v of the 60 mm thick laminates was ~4% and ~2% for the MW-cured (S25_MW90) and oven-cured (S26_O90) laminates respectively. For the 4.8 mm laminate case (S23_MW40 and S24_O45), V_f and V_v values were similar to those reported by the material manufacturer [67].
- MW penetration depth: Maximum D_p ~2.4 mm for 600g/m^2 UD carbon SPARPREG, using the experimental method presented here. The difference between the theoretical and practical results is less than one ply thickness, i.e. 0.6 mm).
- Mechanical testing:
    - Tension: The best performing MW-cured sample obtained similar values of longitudinal tension (S7_MW40: 1975MPa and S21_O45: 1921MPa), however the oven-cured samples showed a greater transverse tension by ~11% (S6_MW40: 37MPa and S22_O45: 41MPa). The elastic modulus did not show significant changes irrespective of heating method or cure cycle.
    - Compression: All MW-cured samples irrespective of cure cycle showed greater compressive strength than the oven-cured samples. The maximum compressive

strength of MW-cured sample (S7_MW40, 1159MPa) was ~35% greater than oven-cured sample (S21_O45, 857MPa).

- IPS: Some variation between MW-cured (S28_MW40, ~44MPa) and oven-cured (S27_O45, ~48MPa) samples. Chord shear modulus of elasticity also similar at ~5GPa.
- G_{1C}: 4.8 mm thick oven-cured sample (S24_O45) obtained a mode I interlaminar fracture toughness value of ~180J/m^2, whereas the 4.8 mm thick MW-cured (S23_MW40) obtained ~233J/m^2. With regards to the 60 mm thick laminates, the oven-cured (S26_O90) sample obtained fracture toughness values ranging between 275 J/m^2 to 375 J/m^2, whereas the MW-cured (S25_MW90) sample reported figures between 325 J/m^2 to 590J/m^2. Both MW-cured samples (S23_MW40 and S25_MW90) showed an increasing G_{1C} trend with crack propagation.
- IFSS: The IFSS of MW (S23_MW40) and oven (S24_O45) cured samples showed a fibre-matrix IFSS of ~74MPa and ~53MPa respectively. The deviation in the results was more pronounced in the former (16.7% compared to 11.1%). An increase of 28% in IFSS resulted in an increase of 23% in G_{1C} (coupons from laminates S23_MW40 and S24_O45).
- Matrix indentation: The reduced modulus obtained through matrix indentation testing was used to calculate the elastic modulus of the matrix. Using the reduced modulus from the indentation tests, the MW-cured (S25_MW90) and oven-cured (S26_O90) samples' elastic modulus was ~4.8GPa and ~4.7GPa respectively, which were both ~15% greater than the values calculated based on the transverse tensile modulus using the rule of mixtures.
- Failure mode assessment: Oven-cured samples showed fibres with little matrix still attached to the fibres. The matrix is predominantly remaining on the areas that were originally in the resin-rich areas in between the fibres. MW-cured samples showed fibres almost fully coated with matrix material, but also fibres with little matrix attached on the fibre surface. The matrix fracture surfaces of oven-cured composites

were more dominated by smooth surfaces, whereas the matrix fracture surface of MW-cured composites was predominantly more undulated. However, there were regions in the fracture surface of the MW-cured samples where both ductile and brittle regions were observed.

Chapter 5

Discussions

This chapter discusses the results obtained from the tests described from chapter 3 and chapter 4. These results are then, whenever possible, put into context of the work that was published previously, explaining the progress made beyond the state-of-the-art in the present work, and also highlights some of the key advantages of the MW curing process. Information regarding potential process and methodology improvements is also described here.

5.1 The MW Penetration Depth of SPARPREG Composites

In order to understand some of the heating patterns and profiles seen during MW curing, the MW penetration depth (D_p) values were obtained through calculations and experimentally as described in Section 4.5. Both theoretical and experimental results were similar, where the difference was less than one CPT of UD CF SPARPREG. In order to further improve the accuracy of both theoretical and practical results, aspects such as V_f, V_f distribution (i.e. local changes/differences), fibre orientation and lay-up sequence may need to be taken into account in order to estimate the D_p for composites, particularly CFRPs, accurately. In the case of the VHM, the maximum D_p can be multiplied by two when using a mould with a low MW absorption (i.e. low dielectric and magnetic properties) and reflection (i.e. low electrical conductivity) – such as the cordierite plate that was used to manufacture laminates S25_MW90 and S26_O90 – since it has magnetrons all around the cavity. Additionally, it could be argued that for this same reason the thicker the laminate, the greater the MW absorption by the edges of the laminate (and therefore heat), thus there may be a thickness at which D_p becomes less critical as described in Figure 5.1. Assuming that dimensions ‘x’ (i.e. length) and ‘z’ (i.e. width)

remains the same, and 'y' is the only difference, then, a greater value of 'y' may encourage more heating through the sides of the laminate.

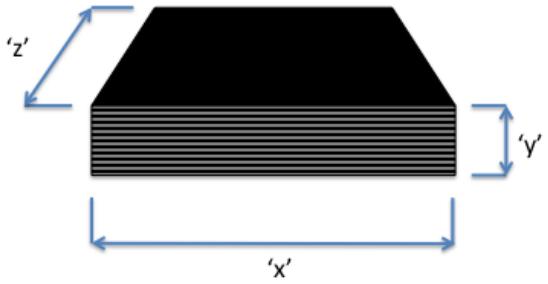


Figure 5.1 Schematic of composite laminate.

Additionally, in the VHM, the direction of the waves (i.e. parallel or orthogonal) to the fibre direction has less relevance due to its high field homogeneity, which assists in the more efficient absorption of MWs by all the faces and edges of the laminate.

MW heating requires careful consideration of the interaction of the part to be heated, with respect to the MW field, for the required temperature range. In the case of thermosetting resins or fibre reinforced thermosetting composites, this temperature will typically be from ambient temperature to the curing or post-curing temperature.

It is assumed that the electrical conductivity and magnetic permeability properties of carbon fibres do not change significantly across this temperature range. This information, together with dielectric, electric and magnetic property-change as a function of the degree of cure of the epoxy resin matrix is not currently available and, therefore, makes theoretical assessments less accurate. Overall, the limited publications available, and the very limited use of MW heating of CFRPs are a good indicator of the difficulties investigators have experienced in the past.

5.2 MW Field and Cure Homogeneity

As it was mentioned in the literature review (Section 2.4), post-cure material quality and consistency will highly depend on the MW field homogeneity in the cavity and is therefore critical to ensure even

heating of the material. The MW field homogeneity in the cavity was something that was not reported in previous publications in the area of MW curing of CFRPs known to date.

MW field homogeneity in the VHM 100/100 was tested in four different ways; firstly, by heating plastic beakers with water distributed in different locations in the cavity and measuring its temperature at fixed MW power for a fixed time. Secondly, by measuring the temperature across the laminate during cure, thirdly by measuring the degree of cure across the laminate after cure, and lastly, by measuring the mechanical properties of the cured laminate. Each of these are discussed in the following sections.

5.2.1 Water Heating

As mentioned above, the first method used to assess the MW field homogeneity was, as described in Sections 3.3 and 4.1, by heating plastic beakers containing 500 mL of water distributed in different locations in the cavity and measuring the water temperature as a function of time at a fixed MW power. The time taken for the water to reach 90 °C, together with the temperature difference within each beaker was compared and reported.

The difference in the time taken for the water to reach 90 °C, i.e. 40 min and 52 min for case ‘e’ and ‘f’ (Figure 4.1) respectively, showed that the MW field changed based on the parts introduced into the cavity and its location, most notably in this case the metallic bench. Therefore, since case ‘e’ was the test without the metallic bench, it is unsurprising that it took significantly less time for the 500 mL of water to reach 90 °C compared with the other tests since this setup was closest to the one shown in Figure 3.3. Additionally, the cooling due to the air flow within the cavity also influenced the heating rate, and thus the time taken to reach the set temperature of 90°C. Excluding case ‘e’, the average time to reach 90°C was 47 ± 2.6 min thus demonstrating the homogeneity of the MW field within the VHM cavity bearing in mind the locations chosen were at opposite locations in the cavity close to the cavity walls and waveguides. The key point however is that the temperature difference between the

different probes in the water beaker, i.e. T1, T2 and T3, T4 (Figure 4.1), in each case was small, and that the gradient of the curves was also similar, representing a reliable and consistent heating during the entire heating cycle for the different configurations.

Attempts were made to reduce the test time by increasing the MW power – with the expectation that this would highlight differences or deviations in temperature between the probes more clearly – but this was not possible because the VHM kept shutting itself down for safety reasons to avoid damaging the magnetrons. This was due to one of the safety features described in Section 3.1.3, which was triggered by the MWs reflected back into the waveguides, as a consequence of the small volume of water compared with the large MW densities generated by the magnetrons.

5.2.2 Temperature Profiles During Curing of 2.4 mm and 4.8 mm Thick Laminates

The second methodology used to test the MW field homogeneity in the VHM 100/100 consisted of taking temperature measurements at different locations across the SPARPREG laminates during curing as described in Section 3.2 and 4.2. The laminates that were cured in the present investigation can be broadly divided into three based on the laminate thickness, i.e. 2.4 mm, 4.8 mm and 60 mm.

With heating in general, the energy required to heat the part is influenced by the ambient temperature, whether it is because the ambient temperature is equal or greater than the desired target temperature as is the case in conventional heating, or whether it is because the low ambient temperature causes a cooling effect as is the case in MW heating. In the latter case, the cooling effect can be significant because of the typically small volume of the part that is required to heat in comparison with the volume of the cavity. When the temperature difference between the part and the ambient temperature in the cavity is high, the convection rate (i.e. heat loss) from the part to the environment will also be high, therefore in an environment where the mould and the chamber are both cold, the heat loss is, inevitably, high. Therefore, when taking into consideration the location of the VHM used throughout

this study (i.e. Middlesbrough, North-East of England), and the fact that the air used to cool the VHM system was directly taken from the outside environment – no heaters were used to warm or to control the air temperature before entering the VHM cavity – the cooling effect can be very significant. A mechanism to control the inlet air temperature may assist in ensuring consistency from one day to another and one facility to another. The same applies to the time of day, and the number of tests performed during the day, i.e. tests carried out later on in the day (e.g. third, fourth test) would typically benefit from a warmer environment within the VHM cavity (as well as the warmer air), and therefore needed a lower MW power to cure the part, which explains the variation in MW power required to heat the same-size laminate. Therefore, some deviation in MW power used to produce the different laminates was to be expected. Because of this, the important aspect regarding MW power was the trend, and not the absolute values. This in turn highlights the criticality of; i) measuring the temperature of the laminate, and, ii) having a temperature-MW power feedback control loop, which were absent in many cases in previous studies as described in Section 2.4, and re-emphasises why it was difficult to assess the quality of the laminates produced previously and do direct comparisons of past work.

In the present investigation, MW power reached its peak towards the end of the ramp-up phase, and then stabilised once the dwell temperature was reached (Figures 4.2 to 4.8). One noticeable difference however was the maximum power required to heat the ±45° IPS laminate, which was the only laminate that required the full MW power of 10.2kW (for approximately 7 min) in order to reach the target dwell temperature of 120°C at a heating rate of 10°C/min (Figures 4.6 and 4.7). This was due to the lay-up sequence of $(\pm 45°)_{2S}$ compared to the UD lay-up sequence in the rest of the laminates due to the greater MW absorption by the fibres compared with the matrix, and thus limited the penetration of the MWs through the thickness of the laminate.

When comparing the MW power of the 2.4 mm and 4.8 mm thick laminates, it was initially expected that given the same ambient conditions, the 4.8 mm laminates would require more MW power for the same cure cycle, since the 4.8 mm laminate has twice the mass of the 2.4 mm thick laminate, however this was not the case. It could even be argued (Figure 4.8) that the MW power required to cure the 4.8

mm thick laminate was lower than the MW power required to cure the 2.4 mm thick laminates. The hypothesis is that this could be due a combination of two reasons:

i. The volume of resin, whereby the 4.8 mm thick laminate had a larger volume of matrix resin, and therefore may have produced a greater exothermic reaction, i.e. the material released more heat when the reaction started, thus requiring less external energy to reach the desired temperature.
ii. More MWs absorbed by the material. In the case of the 2.4 mm thick laminate, it is likely there were more excess MWs than what the material could absorb, thus not absorbing all the available MWs. On the other hand with the 4.8 mm thick laminate, which has double of the volume and mass of the 2.4 mm thick laminate, is likely to have absorbed a greater volume of MWs, thus heating a greater volume of material with similar or less energy.

The average oven heating rate was 2.0°C/min and 2.5°C/min for the 2.4 mm and 4.8 mm thick laminates respectively. The MW heating rate was 10°C/min for both the 2.4 mm and 4.8 mm thick laminates. The temperature variations across the 2.4 mm and 4.8 mm thick laminates during the MW curing process was ~30°C. The oven-cured laminates on the other hand experienced a temperature variation of ~5°C and ~30°C when curing the 2.4 mm and the 4.8 mm thick laminates respectively. Taking into account the MW heating rate was four and five times greater, the difference in temperature across the laminate seen by MW curing was small. Unfortunately, past work do not describe the temperature variation across the laminate during the curing process and therefore it is not possible to compare the results.

The reason why probe temperatures T1 to T4 and T_{mw} differed from one test to another to MW cure the same laminates (Figure 4.2 to 4.8) is uncertain. It is possible that the high peaks could be due to the probe moving during bagging or curing, moving the probes closer to the laminate edge or due to the uneven distribution of epoxy resin that was used to shield the carbon fibres. Machining a slot in

the mould to ensure consistent positioning of the probes, and using an automated method of ensuring shielding consistency may reduce such increasing variations in temperature.

The low temperatures could have been because of cooling effects due to the airflow or the heat loss to the mould. The use of an insulating mould, or placing the part in an insulating box, and designing a better airflow within the cavity is likely to reduce these cooling effects.

Taking into account the recorded differences in temperature, one may expect a significantly greater standard deviation in the mechanical test results of the MW-cured samples, but this was not the case, as seen in Section 4.6. The hypothesis is that, in addition to the aforementioned practical factors, a complex heating pattern occurred when MW curing CFRP laminates. The high temperature on one location of the laminate typically observed during ramp-up led to a lower temperature later in the cure cycle due to the reduced exothermic reaction compared to the other regions of the laminate. The similarity in the degree of cure and mechanical test results, and the standard deviation of these results, suggest that the average time the different regions in the laminate were at the cure temperature of 120°C was similar, and close to the 45-minute dwell suggested by the material manufacturer.

Laminate quality is discussed further in Section 5.3.

5.2.3 Temperature Profiles During Curing of 60 mm Thick Laminates

The large fluctuation in temperature observed during MW curing of the 60 mm thick laminate S25_MW90 (Figure 4.11) especially during the ramp-up phase at 2.0°C/min was to be expected, since the thickness of 60 mm is significantly greater than the material's maximum penetration depth (D_p) of ~2.4 mm (Section 4.5). The maximum temperature difference with the target temperature and the rest of the probes was ~40°C although this was for a short period of time only, typically of a few seconds, which is representative of the rapid heating and control that is possible with MWs. T1 (sub-laminate closest to the mould) and T4 (sub-laminate farthest from the mould) obtained the highest temperatures, with T4 being greater than T1. This is explained by the direct MW exposure seen by T4 where there

was no mould, whereas the ceramic mould under T1 may have absorbed some of the MW energy and therefore dissipated some of the energy. The lower exothermic reaction observed by T1 compared to T5 was also contributed by the lower temperature of T2 compared to T4.

The 60 mm thick oven-cured laminate S26_O90 showed that T1 was the most reactive, and the remaining were quite similar. During the dwell phase, the variation in temperature was ~20°C, despite the very low heating rate of 0.3°C/min. The exothermic reaction from the matrix started at ~90°C, which was ~10°C less than observed in the MW-cured laminate. The cooling in the oven was much slower than in the MW-curing case, since this was dominated by the temperature in the oven chamber. The lower thermal runaway observed by T1 compared to T5 contributed to the lower temperature observed by T2 compared to T4 (Figure 4.12).

During dwell, the temperature difference was still significant, where the lowest temperature was ~100°C (T1, sub-laminate closest to the mould) and the highest temperature was ~130°C (T3, the middle sub-laminate) as seen in Figure 4.11. The second lowest temperature of ~110°C during dwell was recorded by T4.

T1 and T4's low temperatures can be attributed to the selective heating nature of MWs, where the air in the MW cavity was not heated, but the convection of heat from the laminate to the mould and to the cooler ambient air in the cavity acted as a coolant. The reason why the temperature T1 was lower than T4 was due to the temperature of its adjacent sub-laminates T2 and T_{mw} respectively, where T2's temperature was lower than T_{mw}'s.

The heating rate to produce the 60 mm thick laminate S25_MW90 using MWs could have been further reduced in order to maintain a lower temperature difference through the thickness of the laminate, but this would have inevitably led to making the purpose of MW heating redundant, as the main benefit of MWs is heating and processing speed. The cure cycles adopted here are considered to be realistic MW cure cycles.

The sub-laminates located adjacent to the top probe T4 and bottom probe T1 heated first when the MW power was switched on, and also cooled first when the MW power was switched off. The sub-

laminates located in the middle next to the probe T3 underwent the highest exothermic reaction. Inevitably a compromise between these three factors is required to achieve a successful and efficient cure. However, it needs to be born in mind that in addition to the aforementioned factors, the MW power and temperature profile will also change depending on the location of the control probe T_{mw} (Figure 3.6).

Similar to the MW-cured laminate, oven-cured sub-laminates adjacent to T3 and T4 experienced the highest exothermic reaction. Due to the high level of exothermic reaction, all the temperatures reached ≥120°C, and it took ~100 minutes for all temperatures to go below 120°C.

In the MW curing case, insulating the laminate using materials with low MW absorption properties such as PTFE or PEEK, so that; i) the airflow in the cavity does not actively cool the laminate, and, ii) the convection of hot air from the laminate can be used to maintain a high temperature around the laminate, potentially reducing the temperature gradient of the laminate. Additionally, if the VHM system could be modified to have multiple 'T_{mw}' probes, i.e. probes connected directly to the VHM controller, and the software were re-designed to use the average temperature, or to activate magnetrons based on specific need (e.g. top only, bottom only), then this could potentially lead to not only a reduction of temperature gradient through or across the laminate, but further improve the process efficiency.

When the laminate thickness was similar to the laminate's D_p, fluctuations and differences in MW power and temperature were small, as evidenced by the heating of the 2.4 mm and, surprisingly also by the 4.8 mm thick laminates. When the part thickness was much greater than the maximum D_p of 2.4 mm in the case of the 60 mm thick laminate, fluctuations and differences in temperature though the thickness were inevitable. This however assumes that MWs reaching the part on the edges of the laminate were negligible (Section 5.1, Figure 5.1). This may or may not be the case, but if the MW heating of the laminate through the four edges did have a substantial effect, then there may be a thickness where the D_p value becomes less critical, and a full volumetric heating may be achieved, even if the laminate thickness is much greater than the laminate's D_p. This may be the effect that was

observed by temperature readings by T2, T3 and T_{mw} described in Section 4.2.3, where these temperature probes also showed an instantaneous response to temperature with MW power, albeit to a much lesser extent than T1 (located on the bottom sub-laminate) and T4 (located on the top sub-laminate).

It is anticipated that a faster heating rate would produce a greater temperature increase and subsequently a greater temperature difference through the laminate for both the MW and oven-cured cases.

5.2.4 Homogeneity in Degree of Cure

The third method used to assess the MW field homogeneity was by investigating the differences in degree of cure across the different laminates (Section 3.4). The degree of cure values presented in Section 4.3 were taken from three locations in the laminate, and four samples per location.

MW heating with both 40 and 45 min dwell times were able to produce degrees of cure similar (~97%) to samples cured by conventional oven heating (~95%). An additional 5 min MW heating only increased the degree of cure by ~1%, which could be because of the non-linear relationship between time (at a specific temperature) and degree of cure. This phenomenon is not uncommon and is also observed for composites cured using conventional heating methods. The greatest increase in degree of cure for the MW-cured composites was between the 30 and 35 min dwell, which achieved values of 82 and 92%, respectively. Therefore the results indicated that a decrease in dwell time resulted in a similar reduction in degree of cure. The results showed that the standard deviations of MW-cured laminates were in all cases similar to those of the oven-cured laminates, where the difference between them was $\leq$3.5%, thus demonstrating good consistency across the laminate.

5.2.5 Laminate Quality and Consistency

The fourth and final method used to assess the MW field homogeneity was by investigating the difference in physical and mechanical properties of the manufactured laminates (Tables 4.1 and 4.2, Figures 4.14 to 4.32). The quality and consistency of the MW-cured laminates in relation to the conventionally-cured laminates were assessed, together with the aforementioned degree of cure by measuring the laminates' V_f and V_v, the modulus of the matrix through indentation, and mechanical testing of the composite material.

The MW-cured samples obtained similar results in degree of cure (as mentioned in Section 5.2.4), axial tension, and indentation modulus, whereas the oven-cured samples produced greater IPSS, transverse tensile strength and V_f. The MW-cured samples obtained greater mode I interlaminar fracture toughness and compression strengths.

No apparent trend showing higher or lower properties from a specific laminate location was observed, indicating that the cure of the laminate was highly homogeneous (Figure 4.16). The 90° tensile test results were chosen as a representative example since this type of test is known to be highly sensitive to small changes in coupon quality.

The little variation in all test results is an indication that larger laminates can be produced with the same curing methodology.

Laminate quality is further discussed in Sections 5.2.5.1 to 5.2.5.4.

5.2.5.1 Differences in V_f and V_v of MW-Cured and Oven-Cured Laminates

The V_f obtained by the MW-cured laminate (S23_MW40) was lower (~41%) than the values obtained by the oven-cured laminate (S24_O45, ~46%). This was believed to be due to the significantly reduced time (MW heating rates for S23_MW40 was 10°C/min, oven heating rate for S24_O45 was 2.5°C/min) the MW-cured resin was at its lowest viscosity due to the higher heating rate, therefore

limiting the resin flow and resin loss to the bleeder leading to a higher matrix volume content (V_m), and higher V_v content.

V_v values reported by the manufacturer suggests void contents of ~1.5% [107]. Taking this into account, the V_v values obtained for the MW-cured composites were not too different (i.e. ~2% and 4% for the 4.8 mm (S23_MW40) and 60 mm (S25_MW90) thick laminates respectively). This is a similar effect to that presented by Nightingale and Day [95], although the magnitude increase in V_v were very different. Nightingale and Day [95] reported a V_v of ~1% in conventionally-cured composites, whereas the MW-cured samples obtained values close to 20%, which was attributed to the lack of vacuum bagging, as the pressure was only applied using PTFE sleeves, which would have softened at the composite's curing temperature.

The greater V_v observed for MW-cured laminates S23_MW40 and S25_MW90 was attributed to:

- Shielding of the edges of the sub-laminates, thus limiting the flow of the entrapped air and resin flow.

- The high heating rate of the MW samples was believed to have reduced the time the matrix resin was at its lowest viscosity, thus limiting the time available to remove the trapped air, and leading to a higher V_v. The higher MW heating rate would have also caused an increase in V_m due to the reduced time for resin bleed, and therefore reducing V_f.

- The fact that the composites were heated predominantly by the adsorption of the MWs by the CFs that then radiated the heat to the matrix, therefore curing the matrix close to the fibres first, potentially trapping air in the matrix-rich region located between fibres.

5.2.5.2 Matrix Indentation Modulus of MW-Cured and Oven-Cured Laminates

The modulus obtained for MW-cured and oven-cured samples using nano-indentation showed little difference, and the values were slightly greater than expected by ~15% (Section 4.6.7) in comparison to the modulus values obtained from the 90° tensile test. This could be due to a fibre stiffening effect,

where the close proximity of the CFs may potentially limit the flow of matrix from deforming as the indenter penetrates the material. The greater the indentation depths the greater the stiffening effects due to the fibres. A lower indentation depth may potentially limit this effect, however at small depths the indentation may suffer from indentation size effects, where the results become very sensitive to the surface roughness caused by the preparation of the sample [125].

Because of these reasons, the indentation of the fibre-matrix interface or interphase regions of a composite material is very difficult, and since confirmation of indentation is done visually, the only way to do this would be using the SEM – nanometre range indentation – and with a large number of indentations this could become very costly and lengthy. Because of these reasons, indentations were limited to the matrix of the composite material only.

5.2.5.3 Tensile Test Performance of MW-Cured and Oven-Cured Laminates

It is unsurprising that the longitudinal tension results between the MW-cured composites and the oven-cured composites were similar since this is a fibre-dominated test, and therefore it is uncertain how Paulauskas [97] reported a 10% decrease from MW-cured samples. However, it was unexpected that the transverse tensile strength of the MW-cured composites was noticeably lower than the oven-cured composites, since MW heating of CFRPs was supposed to improve fibre-matrix bond, which is similar to what was reported by Paulauskas [97]. The only explanation that has been identified regarding this was the greater void content of the MW-cured composites, since voids act as multiple stress concentration and crack initiation points; a greater void content could also mean greater void sizes. Therefore, it is plausible that the increased void content and void size outweighed the benefits of the increased fibre-matrix bond of the MW-cured samples in this particular loading condition. Discussions regarding how the fibre-matrix IFSS was affected by the curing method is discussed in Section 5.2.5.4.

5.2.5.4 Differences in Interfacial Shear Strength Between Microwave-Cured and Oven-cured Composites

Based on the mechanical test results of oven-cured and MW-cured composites in the present investigation, there is sufficient evidence to suggest that the differences in results were due to the effect each heating mechanism has on the fibre-matrix interface.

As already mentioned in Section 2.3, the fibre-matrix interface has a great influence in the mechanical performance of composite materials, such as under axial compression, IPS and mode I interlaminar fracture.

When composite materials are loaded under axial compression, the failure is typically due to local buckling of the fibres and, therefore, delaying the buckling of fibres will increase the load carrying capacity of the composite sample. Therefore, when taking into consideration that all MW-cured samples had lower V_f, and produced compression strengths from ~13% (S1_MW30) to ~35% (S8_MW40) greater than the oven-cured samples when the degree of cure for the MW-cured samples were as low as ~82% for S1_MW30 and as high as ~97% for S8_MW40 and S15_MW45, this is an indication that the fibres in the MW-cured laminates were held in place for longer than the oven-cured samples thus delaying the onset of fibre buckling. This is very interesting because at a low degree of cure of ~82% one would normally be led to believe that the fibres would not be well supported and therefore suffer from buckling at an earlier stage. And hence when taking into account the compression behaviour and the degree of cure of MW-cured composites, these two results in combination suggest that the T_g values obtained (and hence the degree of cure) for the MW-cured samples were an average of a region with a higher T_g and degree of cure at the fibre-matrix interface and interphase, producing a stiff brittle region, and a more ductile region with a lower degree of cure away from the fibre-matrix interface and interphase.

However, this then contradicts with the previous statements that MW heating reduces the curing time significantly. This can be explained by the results obtained by Agrawal and Drzal [10], where the

temperature between the fibre and the matrix interface during MW curing was estimated by extrapolating measured temperatures at various distances away from the fibre in a single-fibre model composite. This investigation suggested that the temperature at the fibre-matrix interface when heated using MWs could be higher than the matrix temperature by as much as 75°C. It is not certain whether such a high temperature difference is realistic, since the distance from the fibre to the surface of the laminate is typically <100 micrometres, therefore the temperature measured by the probes on the surface of the laminate should not be tens of degrees lower than the fibre-matrix interface temperature. In any case, since the carbon fibres absorb the MWs in a CFRP composite, the heat is predominantly conducted from the carbon fibres to the matrix, therefore it seems plausible that the interface temperature is greater but possibly not by as much as 75°C as reported by Agrawal and Drzal [10] – this may potentially be a hot-spot issue due to uneven MW fields, or the over-magnified value due to the low number of fibres (i.e. one) in a model composite, thus causing a concentration of energy (and therefore heat) at the fibre-matrix interface. This can in turn lead to a shorter curing time at the interface and interphase region based on the Arrhenius relationship, and since the matrix away from the fibres is cured mainly due to thermal conduction from the fibre-matrix interface to the matrix, this area still requires the curing time suggested by the material manufacturer.

Similar to the tensile test results, the standard deviation in both compression strength and modulus were similar irrespective of heating method, thus demonstrating the high consistency and reliability of MW heating with the VHM system, using the operational procedure described in the present study.

The significant enhancement in compression strength may indicate that MW-cured composites should perform well in compression after impact tests. These results could have a large impact in industries where CFRPs are normally preferred due to its advantages in compressive properties. The increase in 0° compression strength of MW-cured samples could lead to changes in design allowables, which in turn could lead to thinner sections, thus offering cost and weight reduction.

The effects MW heating had on the composites' IFSS were more evident in mode I interlaminar fracture, where the G_{1C} obtained for the 4.8 mm thick laminates was higher for the MW-cured sample (S23_MW40) by ~29% compared with the oven-cured sample (S24_O45). Additionally, the increasing G_{1C} value as a function of crack propagation was also clearly visible, as was in S25-13_MW90, i.e. both laminates which were directly cured by MWs. The increasing G_{1C} seen by the MW-cured samples was due to crack meandering in the resin rich region as opposed to crack propagation through one single plane at the fibre-matrix interface as was the case for the oven-cured samples.

Regarding the 4.8 mm thick sub-laminates of the 60 mm thick laminates, once again the MW-cured sub-laminates (S25_MW90) produced greater average G_{1C} (average ~450 J/m^2) compared to the conventionally-cured sub-laminates (S26_O90) (average ~345 J/m^2). The larger standard deviation observed in G_{1C} tests was due to crack meandering caused by the increased IFSS, leading to increased G_{1C} values as a function of crack propagation. The lower V_f and higher V_v of MW-cured composites are believed to have also contributed.

When taking a closer look at the G_{1C} initiation values, it can be observed that these were similar for the MW-cured and oven-cured samples, especially for the 4.8 mm thick laminates (S23_MW40 and S24_O45). This is possibly an indication that the matrix (i.e. the part that is believed to be cured mainly due to conduction and not by direct MW heating) for both cases were in a similar condition. For the 60 mm thick laminates (S25_MW90 and S26_O90) the difference is slightly more pronounced, which was due to a complex combination of MW and conduction heating and different levels of chemical exothermic reactions experienced between the MW and the oven-cured samples.

The lower G_{1C} values measured for the sub-laminates closer to the mould for both MW and oven cure can be attributed to the thermal residual stress, which is usually caused by; i) the difference in coefficient of thermal expansion (CTE) between the fibre and the matrix, and, between the composite laminate and the mould, and, ii) a temperature gradient through the thickness of the laminate during the cooling phase of the composite laminate [126-128]. In this regard, since thermal residual stresses

are mostly produced during the cooling phase, it may be beneficial to control the cooling of the MW-cured laminate to minimise such effect, with the aim of obtaining more consistent, and maybe even increased results.

The above statements related to the increase in IFSS of MW-cured composites can be verified and quantified when looking at the results obtained through fibre push-out testing, which is a technique that allows the practical measurement of the fibre-matrix adhesion. Fibre push-out on MW-cured (S23_MW40) and oven-cured (S24_O45) CFRP UD laminates showed IFSS values of 74.4 MPa and 53.1 MPa. The similarity in the IFSS values produced in the present investigation with the results obtained by Agrawal and Drzal [10] on carbon-epoxy single-fibre model composites (IFSS of 97.6 MPa and 57.2 MPa for the MW-cured and the conventionally-cured, respectively) is quite remarkable since the test method was different, the materials used were different, the fibre sizing methods were possibly different, and the two studies are ~15 years apart from one another.

Additionally, Madhukar and Drzal [78] reported that with conventionally-cured composites, an increase of 19% in fibre-matrix IFSS led to an increase in 17% in G_{1C}, which is similar when compared to the results in the present investigation, where a difference in IFSS of MW-cured and oven-cured composites of 28% led to a change in G_{1C} of 23%.

The only test result that did not agree with the increase in IFSS leading to an increase in mechanical properties was the ±45° tensile IPS test, since the MW-cured samples obtained IPSS values ~10% lower than those of the oven-cured samples.

According to Madhukar and Drzal [77], the IPSS of oven-cured CFRPs are very much influenced by the quality of the fibre-matrix interface. IPSS increased by 162% when the IFSS increased by 118% in conventionally-cured composites. However, as it was reported in Section 4.6.3, this was not the case with MW-cured composites, where the MW-cured composites produced IPSS values ~9% lower than those produced by the oven-cured samples.

The fact that the MW-cured laminate's IPSS did not increase was unexpected, and was due to the limit in the MW penetration behaviour of the material as a function of lay-up sequence. It is believed

that the ±45° fibre orientation reduced the MW penetration depth and, therefore, part of the laminate – possibly the bottom half – was cured mainly due to conduction as opposed to directly by MWs. This could explain why the MW power required to reach 120 °C was significantly greater than those observed for curing UD laminates.

5.3 Failure Mode of Microwave-Cured and Oven-cured SPARPREG Composites

No significant differences could be observed in the failure mode of the MW-cured and oven-cured composites from macroscopic visual inspection. However, when the samples were inspected using SEM, some differences became clear, especially in the mode I interlaminar fracture tested samples.

The oven-cured samples showed regions with smooth matrix fracture surfaces, thus indicating a brittle fracture. This is similar to what was reported by Agrawal and Drzal [13], and Wei et al. [94]. This is an indication of the tough matrix of the oven-cured sample, since there is a tendency for fracture to occur preferentially at the fibre-matrix interface as the toughness of the material increases [129-131]. This was evidenced during testing, where sudden crack jumps were observed regularly. The MW-cured samples on the other hand also suffered from sudden crack jumps, albeit to a much lesser extent, and this was reflected in the SEM images through a more undulated matrix fracture surface. Additionally, the MW-cured samples clearly indicated a higher degree of matrix adhesion on the fibre compared with the oven-cured sample, which once again confirmed the improved fibre-matrix interface of the MW-cured samples. However, the MW-cured samples did show, although to a lesser extent than the oven-cured samples, some regions with little matrix remaining on the fibres, and in certain cases fibres with no matrix were also observed. The hypothesis is that the local distribution of fibres impacted on how the neighbouring fibre-matrix interface and interphase regions and the matrix-rich regions were heated. This could be due to the selective heating nature of MWs, where the brittle region was due to the predominant heating of the MWs from the CFs to the matrix, and the ductile

region could be due to the predominant conduction heating. Therefore, using a technique such as DSC to identify the MW-cured composite's T_g and degree of cure may not show the true state of the material, as the sample cut for investigation will possibly contain many interface and interphase regions, and matrix regions away from the interface and interphase, i.e. DSC shows an average degree of cure of the sample. And this may be the reason why the MW-cured samples showed a multi-phase (i.e. brittle and ductile) failure mode.

One would expect that an increase in IFSS would also increase the transverse tensile strength, but this was not the case, as reported previously, where the oven-cured samples showed greater transverse tensile strengths by ~11% compared to the MW-cured samples. However, the G_{1C} test results showed that the MW-cured samples obtained clearly greater toughness values compared to the oven-cured samples, which was due to two reasons; i) void content, and, ii) fibre-matrix IFSS.

In the first case, an increase in V_v as in the MW-cured sample may assist crack deflection and so energy absorption through crack blunting and plastic hole growth, thus resulting in a greater G_{1C} value. However, a greater V_v in transverse tension could act as multiple stress concentration points and equally multiple crack initiation points, thus reducing the material performance.

In the second case, the increased IFSS exhibited by the MW-cured samples meant that the crack was unable to take the weakest path, which is typically along the fibre-matrix interface. Instead, in the MW-cured samples, the crack had to propagate through a resin-rich region, which was cured predominantly due to conduction and, therefore, retain the ductility and toughness. The failure mode thus changed from being predominantly interfacial in the oven-cured samples to matrix dominated in the MW-cured samples. A schematic representing a crack propagating through a MW-cured and oven-cured sample is shown in Figure 5.2.

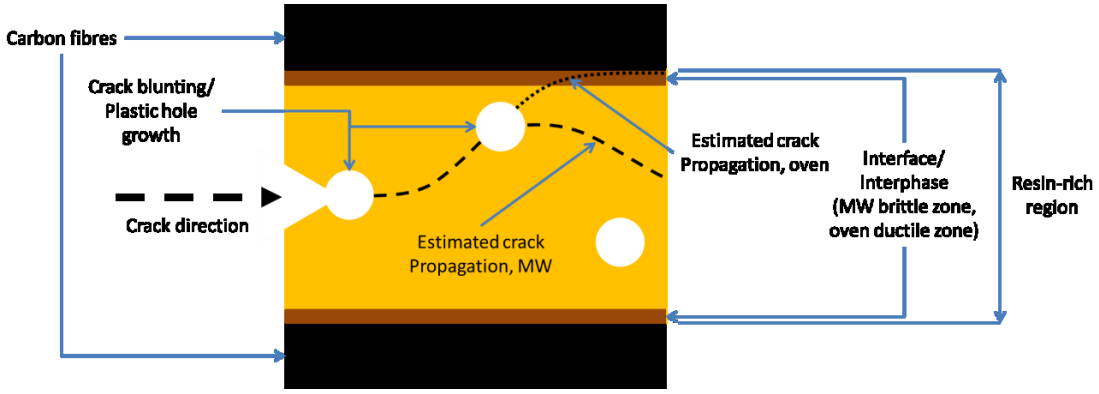


Figure 5.2 Schematic showing the differences in crack propagation in MW-cured and oven-cured CFRP composites, where the former will have a tendency to propagate along the matrix, and the latter propagates along the fibre-matrix interface.

5.4 Discussions – Summary

It is difficult to compare the suitability of the operational procedure employed in the present study with those presented in the past since past work provided little detail regarding the MW field within the cavities used, and no information was provided regarding the temperature difference across the laminate during MW-curing.

In the present study, MW field homogeneity was assessed by heating beakers containing water that were placed in different locations in the cavity, by measuring the temperatures across the laminate during curing, and by assessing the laminate quality after curing and testing.

The temperature difference across the water beakers was minimal, although the time taken to reach the desired temperature varied depending on the setup. The biggest difference was observed when the metallic bench was removed.

During MW curing, the temperature across the laminate was, in some cases, significantly different. However, degree of cure and mechanical tests showed comparable standard deviations to oven-cured samples. The hypothesis is that, in addition to the aforementioned practical factors, a complex heating pattern occurred when MW curing CFRP laminates. The high temperature on one location of the laminate typically observed during ramp-up led to a lower temperature later in the cure cycle due to

the reduced exothermic reaction compared to the other regions of the laminate. The similarity in the degree of cure and mechanical test results, and the standard deviation of these results, suggest that the average time the different regions in the laminate were at the cure temperature of 120°C was similar, and close to the 45 minute dwell suggested by the material manufacturer.

The fibre-dominated mechanical tests showed similar results, regardless of the curing method, and the matrix-dominated 90° tensile test showed lower values for the MW-cured samples, which was believed to be due to the greater V_v in MW-cured samples. The tests that are highly influenced by the fibre-matrix IFSS such as IPSS was unexpected, where the MW-cured laminates showed reduced strength compared to the oven-cured samples. This was believed to be due to the change in penetration depth of MWs through a cross-ply laminate compared to a UD laminate thus changing the through-thickness heating pattern. The other two tests that depend greatly on the fibre-matrix interface, i.e. mode I interlaminar fracture and fibre push-out, both showed that MW-curing produced increased performance. The explanation to this could be seen in the SEM micrographs, where the failure mode changed from interface-dominated in the case of the oven-cured samples, to matrix-dominated in the case of the MW-cured samples. The MW-cured samples also showed increased regions with a rough matrix fracture surface, which is representative of a ductile failure. However there were also regions in the MW-cured samples which showed both brittle and ductile failure mode due to the MW heating near the fibre-matrix interface, and the conduction heating away from this region.

One additional aspect which may have contributed to the changes of the mechanical properties of MW-cured composites are thermal residual stresses caused by the difference in coefficient of thermal expansion (CTE) between the mould and the composite material, and between fibres and matrix as a function of fibre orientation and lay-up sequence. Residual stress has not been taken into consideration in the present study as currently there are no standardised or well-established methods to measure such properties for composite materials [128].

Two of the suggested methods for measuring residual stress in composites include curvature measurement of unsymmetric panels, and through the use of fibre-bragg grating (FBG) sensors [128].

The curvature measurement of unsymmetric panels poses a difficulty that is specific to MW heating of CFRPs. As mentioned previously, CFs are the major contributor to MW heating of CFRPs, and therefore, it is unlikely that unsymmetric laminates will produce even heating across and through the laminate. Uneven heating may then lead to uneven curing, and thus produce laminates which are unsuitable for testing.

The use of FBG sensors is possibly the most ideal method between the aforementioned two methods as a live tool to measure the evolution of thermal residual stresses during MW and conventional curing of composites. However the main drawback with this technique is that the FBG sensors have diameters typically in the millimetre range, whereas carbon fibres have dimensions ranging from 5 μm to 10 μm, thus it is uncertain whether the FBG sensors would accurately reflect the conditions of carbon fibre-matrix interfaces; a better understanding of the measurements and interpretation is required [128]. However since the primary objective of the present investigation was, first and foremost, to produce CFRP laminates of good and consistent quality and, secondly, to understand the potential effects and causes of changes in physical and mechanical properties, the introduction of additional devices that do not contribute directly to the production of the composite laminate using MWs are deemed as additional sources of potential error, most notably related to the possibility of re-distributing the MW field.

Overall, it was evident from the publications in the past that significant effort was put into MW curing of CFRPs, however the success was limited due to issues such as uneven MW heating and the difficulties with identifying a suitable operational procedure as described in Section 2.4 – most notably a lack of information regarding methods to prevent arcing in a MW environment – as demonstrated by the small laminates produced, and the discrepancies in the results obtained.

The operational procedure proposed here – through the use of epoxy tape at the edges of the laminate to avoid arcing, and the use of a MW transparent tool to heat both faces of the laminate to assist through-thickness volumetric heating – are methods that could be adopted in other non-VHM systems.

It is important to note however that without ensuring a high MW field homogeneity in the MW cavity, the results may differ significantly to the ones presented here.

The mechanical test results showed that MW-cured samples were at least as good as oven-cured samples in axial tension, compression and mode I interlaminar fracture, or slightly lower than the oven-cured samples, as in the case of transverse tension and IPS. The standard deviations of the results of MW-cured samples were, in some cases, slightly greater than those obtained by the oven-cured samples. This was believed to be due to the increase in V_v of the MW-cured samples, rather than due to the inconsistent or uneven heating of MWs. There may be however some factors, specifically the local arrangement and distribution of carbon fibres, which may have affected local MW heating, as observed by some of the SEM images. Although in the present study the impact of local fibre distribution may not have been clearly noticeable, the use of materials in other forms (i.e. non-pre-preg), which may be more difficult to ensure consistency, this effect may become more evident.

Chapter 6

Conclusions

The present work has provided some basic insights and theory of MW heating of materials, specifically on carbon-epoxy composites. A literature review of MW curing of composites was then carried out focusing on the same type of material (i.e. carbon-epoxy) as these provide some challenges other materials such as thermoplastics and GFRPs do not. This was then followed by the experimental work that was carried out, including a novel practical method to measure the MW penetration depth of composite materials, the investigation and the description of a suitable procedure to MW cure CFRP materials, and physical and mechanical tests, and the failure mode assessment. The present work finishes with the results of the aforementioned experimental work and its respective discussions regarding the results that were obtained.

The literature review highlighted the main results obtained by previous researchers in the field of MW curing of CFRPs, but it is difficult to provide specific conclusions due to the differences in hardware and software used, and lack of consistency in the operational procedure in comparison with conventional curing methods, which led to uncertain results. Limited publications in MW heating of carbon-epoxy composites were identified and the discrepancies in the results were due to unsuitable MW hardware and operational methodologies, therefore making it inappropriate to derive clear conclusions.

The importance of MW penetration depth was emphasised and a methodology to practically measure or estimate this parameter on composite materials was proposed and deployed. The practical results

showed a difference of less than one CPT with theoretical results, despite the lack of accurate property values of the material, thus suggesting that MW heating of CFRPs is indeed dominated by the CFs, and that the dielectric, magnetic, and electric properties of carbon fibres do not vary greatly in the temperature range employed in the present investigation at 2.45GHz.

The VHM 100/100 system was used to cure 2.4 mm, 4.8 mm and 60 mm thick 600g/m^2 UD SPARPREG prepreg composite laminates. The operational methodology reported in the present study provides a basic procedure that can be easily and consistently reproduced in the future.

A heating rate of up to four, five and six times greater with MWs for the thin (2.4 mm and 4.8 mm thick) and thick (60 mm thick) laminates respectively did not produce excessive thermal runaway as it would occur in a conventional oven for a laminate of these thicknesses at these heating rates. MW heating of thin and thick composites provided significant benefits in terms of cycle time reduction (~50 and ~60% respectively). The cycle time reduction was mainly due to the increase in heating rate. A reduction in dwell time led to an approximately proportional reduction in degree of cure (i.e. a thermosetting resin's dwell time is defined by the resin chemistry and MW does not promote shorter dwell times to achieve full cure). However, the concentration of MW energy on the CF leads to greater temperatures at the fibre-matrix interface and therefore leads to a shorter curing time in this region due to the Arrhenius relationship.

The laminates produced using the VHM 100/100 equipment and the methodology presented were compared with conventionally-cured laminates through DSC, image analysis, interlaminar mode I fracture toughness, tension, compression, IPS, matrix indentation and fibre push-out testing. Failure assessment of oven and MW-cured samples tested under transverse tensile and mode I fracture were carried out using SEM.

The axial tensile properties showed little difference between MW and oven-cured samples, whereas the transverse tensile and IPS results were lower for the MW-cured samples. The difference in mechanical properties in compression were significantly higher for the MW-cured samples, and the consistency in test results observed in MW-cured composites was an indication of even heating through and across the laminate.

The V_v of MW-cured composites was significantly greater than those cured conventionally. In order to be able to take full advantage of MW heating technology for curing composite materials, resin systems need to be developed in order to suit this process. This also applies to reduced dwell cycle times as mentioned earlier.

Despite the noticeably higher V_v values obtained by the MW-cured laminates, the G_{1C} values and IFSS values were significantly greater than conventionally-cured composites. The change in IFSS led to a proportional change in G_{1C}. The relationship between IFSS and G_{1C}, and its close resemblance to the values obtained by Madhukar and Drzal [19], is an indication that the increase in such properties is a real increase, and not due to crack splitting, fibre bridging or other undesired effects as one could expect from increased V_v values.

The selective heating nature of MWs (predominantly from the carbon fibres to the matrix in the case of CFRPs) created local variations in material ductility, indicating that the matrix of the MW-cured composites was comprised of a two-phase system with a hard brittle region close to the fibre, and a more ductile and tougher region away from the fibre. It is believed this was the main reason why MW-cured samples produced significantly increased compressive strength values. This is evidenced by the fact that; i) all MW-cured samples performed better under compression than the oven-cured samples, even the sample with 82% degree of cure, ii) indentation tests demonstrated there is very little difference in matrix modulus between the MW-cured and oven-cured samples, and, iii) SEM shows significantly higher degree of matrix remaining after testing of MW cured samples.

The suitability of MW heating of a material (particularly CFRPs) need to be investigated on a case-by-case basis, i.e. pre-work is required prior to attempting to process materials using MWs, since the global and local MW field will vary depending on factors such as the part's geometry, temperature, dielectric and conductivity properties.

The methodology used to cure CFRPs in the current investigation showed positive indications regarding its suitability for heating and curing relatively thin carbon fibre UD laminates, but further improvement is required for thick UD laminates, and possibly for MD laminates, e.g. quasi-isotropic, due to the high MW absorption of the carbon fibres.

Based on the above assessments and results, the following conclusions were drawn:

- Limited publications in the field of MW heating of CFRPs were identified. The discrepancies in the results were due to unsuitable MW hardware and operational methodologies, therefore making it inappropriate to derive clear conclusions.
- The axial tensile properties showed little difference between MW and oven-cured samples. The transverse and IPS properties of MW-cured samples were lower than the oven-cured samples. The difference in mechanical properties in compression and mode I interlaminar fracture toughness was very significant, where the MW-cured samples showed increased performance. The consistency in mechanical test results observed in MW-cured composites was an indication of even heating through and across the laminate. It is anticipated that with a matrix resin purposely designed to cure with a short dwell time, the benefits of MW heating could be more evident.
- The selective heating nature of MWs (predominantly from the carbon fibres to the matrix in the case of CFRPs) created local variations in material ductility, essentially transforming the matrix into a two-phase system with a hard brittle region close to the fibre, and a more ductile and tougher region away from the fibre. It is believed this was the main reason why MW-

cured samples produced significantly increased compressive strength and mode I interlaminar fracture toughness values. This was evidenced by;

  - All MW-cured samples produced greater compression strengths than the oven-cured samples, including the MW cured sample with 82% degree of cure.
  - Indentation tests demonstrated that there is very little difference in matrix modulus irrespective of heating method.
  - SEM showed significantly higher degree of matrix bond remaining after testing of MW-cured samples compared with oven-cured samples.
  - MW-cured samples suffered far less crack jumps during mode I interlaminar fracture testing, indicating a predominantly ductile failure. This was confirmed by the roughness of the matrix fracture surface.

- The success or failure of MW-heating of a material, particularly CFRPs, needs to be investigated on a case-by-case basis, i.e. pre-work is required prior to attempting to process materials using MWs, since the global and local MW field will vary depending on various factors such as the part's geometry, temperature, dielectric and conductivity properties. It is anticipated that the designer of the part needs to take into account the manufacturing process using MW heating early in the design process. The user should not expect that a composite part with a relatively complex geometry can be introduced into the MW cavity and be cured successfully as one would normally expect when introducing the same part into a conventional oven. A global approach, involving the material manufacturers (i.e. chemical engineers and materials scientists), part designers, test engineers (i.e. materials and mechanical engineers), quality engineers, manufacturing engineers and physicists/electrical engineers is required in order to fully develop MW heating.

Chapter 7

Future Work

The area of MW curing of CFRPs could be regarded to be in its early stages of development, despite the fact that MWs have been used since the Second World War, and significant further development work is required. Some of the key areas based on the author's work and experience are proposed:

- Curing parts with complex geometries, e.g. double curvatures, and analysis of how the MW field (and subsequent heating) changes according to the part geometry.
- MW curing of woven and MD laminates, including laminates with a quasi-isotropic lay-up sequence in order to assess the feasibility, practicality, efficiency and performance of MWs for curing laminates similar to those used in real structures. This will in turn allow scaling up the process further, and testing of larger, real structures.
- Modelling and simulation of MWs and MW-material interaction to help improve the understanding of the process, and reduce the number tests which are based on trial and error.
- Multi-scale finite element analysis (FEA) to assess the changes in mechanical performance with a stronger fibre-matrix adhesion, and a stiffer fibre-matrix interface and analyse its effects on a global scale. The aim of this exercise would be to assess whether MW curing can provide benefits in terms of reducing the number of plies required, which in turn would lead to reduced costs and reduced structural weight.
- FEA modelling and simulation to assess the changes in thermal residual stress, in conjunction with identifying and validating a method to measure thermal residual stresses in a MW environment to quantify the level of thermal residual stress in a MW-cured laminate

compared with a conventionally-cured laminate. A MW-thermal-mechanical simulation would be highly desirable.

- VHM hardware and software updates:
    - Add multiple T_{mw} with live communication with one another to assess which magnetrons need to be activated and its duration. This could assist in reducing the temperature variations between the target temperature and the actual temperature, across and through the thickness of the laminate. This should in turn lead to more consistent physical and mechanical performance.
    - Re-direct the airflow in the cavity to minimise cooling of the laminate during curing to enhance process consistency, and therefore physical and mechanical performance consistency to match (or exceed) those produced using conventional curing methods.
    - Investigate an alternative MW curing methodology in order to take advantage of the improved fibre-matrix adhesion that MWs offer without being limited by the MW penetration depth. MWs can be used to heat ply by ply in order to achieve a high degree of cure at the fibre-matrix interface. Once all the plies are laminated, and the fibre-matrix interface has already obtained a high degree of cure, then the entire laminate can be cured.
- Material assessment and development:
    - Effects of very fast heating and cooling in short bursts of the material (i.e. emulate the initial heating phase of the composite material with MWs particularly observed with thick laminates.
    - Development of matrix resins specific to MW-heating at the frequency of interest (in this case 2.45GHz), which at the same time achieve low V_v and full cure in a short dwell time. Similar matrix development exercises have been performed by BMW

[132] and Dow Automotive [133] for conventional heating methods for automotive applications.

- Compression-after-impact tests (or other tests in which the specimen is predominantly loaded under compression, such as open hole compression) should be performed to establish if the significant increase in axial compression strength of the MW-cured composites reported in Section 4.6.2 also translates to these other compressions tests. Compression strength after impact is an important property as this is a measure of the material's damage tolerance by quantifying its ability to retain its structural integrity despite having a defect [134]. A suitably high compression strength after impact is a key requirement for many industries, but particularly aerospace.

- Mechanical tests under other environmental and loading conditions, such as testing environmentally aged samples, or fatigue testing to assess whether the differences observed in quasi-static tests are translated to longer-term performance.

- Measurement of dielectric properties (ε' and ε'') , electrical conductivity, magnetic permeability properties at 2.45GHz (or at other frequencies of interest) from ambient temperature to the required curing temperature of the material under investigation. This data can then be input into the simulation to obtain more accurate results.

References

[1] Heuss R, Müller N, van Sintern W, Starke A and Tschiesner A. Lightweight, heavy impact. McKinsey & Company Technical report. February 2012.

[2] White SR and Kim YK. Staged curing of composite materials. Compos A Appl Sci Manuf 1996; 27(3):219-227.

[3] Ciriscioli PR, Wang Q and Springer GS. Autoclave Curing - Comparisons of Model and Test Results. J Compos Mater 1992; 26(1): 90-102.

[4] Bogetti TA and Gillespie JW. Two-Dimensional Cure Simulation of Thick Thermosetting Composites. J Compos Mater 1991; 25(3):239-273.

[5] Al-Shamasi, Abdullah S., New trend reflects growing demand for small aircraft, www.arabnews.com/new-trend-reflects-growing-demand-small-aircraft, 25 July 2012.

[6] Olivier, P. and Cavarero, M., Comparison between longitudinal tensile characteristics of thin and thick thermoset composite laminates: influence of curing conditions, Computers and Structures, Vol. 76, pp.125-137, 2000.

[7] Guo, Z., Du, S. and Zhang, B., Temperature field of thick thermoset composite laminates during cure process, Composites Science and Technology, Vol. 65, pp.517-523, 2005.

[8] Hsiao, K., Little, R., Restrepo, O. and Minaie, B., A study of direct cure kinetics characterization during liquid composite molding, Composites: Part A, Vol. 37, pp.925-933, 2006.

[9] Metaxas, A.C. and Meredith, R.J., Industrial Microwave Heating (IEEE Power Engineering Series), 1st ed., London: Institution of Engineering and Technology, March 1983.

[10] Jovan Mijovic , Arnon Fishbain , Jony Wijaya. Mechanistic modeling of epoxy-amine kinetics. 2. Comparison of kinetics in thermal and microwave fields. Macromolecules, 1992, 25 (2), pp 986–989.

[11] Wang T and Liu J. A review of microwave curing of polymeric materials. J Electron Manuf 2000; 10(3):181-189.

[12] Mijović J and Wijaya J. Review of cure of polymers and composites by microwave energy. Polym Compos 2004; 11(3):184-191.

[13] Agrawal RK and Drzal LT. Effects of microwave processing on fiber-matrix adhesion in composites. J Adhesion 1989; 29(1-4):63-79.

[14] Hook, K.J., Agrawal, R.K. and Drzal, L.T., Effects of microwave processing on fiber-matrix adhesion. II. Enhanced chemical bonding of epoxy to carbon fibers, Journal of Adhesion, Vol. 32, pp. 157-170.

[15] Wei, J., Chang, Y., Thomas, B.J. and Hawley, M.C., Microwave heating of thick-section graphite fiber/epoxy composites, Proceedings of International Conference on Composite Materials 8 (ICCM-8), Honolulu, USA, 15-19 July, pp. 10-L-1 to 10-L-10, 1991.

[16] Papargyris DA, Day RJ, Nesbitt A and Bakavos D. Comparison of the mechanical and physical properties of a carbon fibre epoxy composite manufactured by resin transfer moulding using conventional and microwave heating. Compos Sci Technol 2008; 68(7-8):1854-1861.

[17] Rao, R., Rao, S. and Sridhara, B., Studies on tensile and interlaminar shear strength properties of thermally cured and microwave cured glass-epoxy composites, Journal of Reinforced Plastics and Composites, Vol. 57, pp. 783-795, 2006.

[18] Fang, X. and Scola, D.A., Investigation of microwave energy to cure carbon fiber reinforced phenylethynyl-terminated polyimide composites, PETI-T/IM7, Journal of Polymer Science, Part A: Polymer Chemistry, Vol. 37, pp. 4616-4628, 1999.

[19] Boey, F.Y.C. and Lee, T.H., Electromagnetic radiation curing of an epoxy/fibre glass reinforced composite, Radiation Physics and Chemistry, Vol. 38, pp.419-423, 1991.

[20] Yue, C.Y. and Boey, F.Y.C, The effect of microwave and thermal curing on the interfacial properties of an epoxy/glass composite, Proceedings of 2nd International Conference on Deformation and Fracture of Composites, Manchester, UK, pp. 12.1-12.8, 1993.

[21] Yue, C.Y. and Looi, H.C., Influence of thermal and microwave processing on the mechanical and interfacial properties of a glass/epoxy composite, Composites, Vol. 26, pp. 767-773.

[22] Boey, F.Y.C., Humidity and autoclave pressure effect on the interfacial shear strength of a microwave cured epoxy-glass fibre composite, Polymer Testing, Vol. 14, pp. 471-477, 1995.

[23] Boey, F.Y.C. and Yue, C., Interfacial strength of a microwave cured epoxy-glass composite, Journal of Materials Science Letters, Vol. 10, pp. 1333-1334, 1991.

[24] Boey, F.Y.C., Effect of moisture content on the high pressure microwave curing of a thermoset fiber reinforced composite, Polymer Materials Science and Engineering, Vol. 66, pp. 422-423, 1992.

[25] Day, R.J. and Samoladas, E., Micromechanics of model carbon epoxy composites cured using microwave heating, Science and Engineering of Composite Materials, Vol. 7, pp. 23-50, 1998.

[26] Palumbo, M and Tempesti, E. On the nodular morphology and mechanical behavior of a syntactic foam cured in thermal and microwave fields. Acta Polymerica 1998; 49(9):482-486.

[27] Composites World, GKN invests in microwave oven for composites curing, www.compositesworld.com/news/gkn-invests-in-microwave-oven-for-composites-curing, Accessed: 5 March 2011.

[28] Sloan, J., Microwave: An alternative to the autoclave? www.compositesworld.com/articles/microwave-an-alternative-to-the-autoclave, Accessed: 10 May 2011.

[29] Quickstep, www.quickstep.com.au

[30] Tian W, Aubriot A, Varley R and Hodgkin J. An initial research work on evaluation of Quickstep product. In: Proc ICCM 13, Beijing, China, 2001.

[31] Khan L, Nesbitt A, Day R. Hygrothermal degradation of 977-2A carbon/epoxy composite laminates cured in autoclave and Quickstep. Composites: Part A 2010 41:942-953.

[32] Unknown author, Quickstep logs first Quickstep Process sale, fast-tracks RST development. Composites World (2013). www.compositesworld.com/news/quickstep-logs-first-quickstep-process-sale-fast-tracks-rst-development.

[33] Mondo J, Wijskamp S and Lenferink R. Overview of Thermoplastic Composite ATL and AFP Technologies. In: Proc ITHEC 2012, Messe Bremen, Germany, 2012.

[34] Unknown author, Laser heating for thermoplastic, thermoset fiber placement. Composites World (2013). www.compositesworld.com/products/laser-heating-for-thermoplastic-thermoset-fiber-placement.

[35] Sloan J, ATL and AFP: Defining the megatrends in composite aerostructures. Composites World (2008). www.compositesworld.com/articles/atl-and-afp-defining-the-megatrends-in-composite-aerostructures.

[36] Sloan J, AFP/ATL evolution. Composites World (2014). www.compositesworld.com/articles/afpatl-evolution.

[37] Funck, R. and Neitzel, M., (1995), Improved thermoplastic tape winding using laser or direct-flame heating, Composites Manufacturing, 6, 189-192

[38] Wolff-Fabris F, Altstädt V, Arnold U and Döring M. Electron Beam Curing of Composites (2011). Hanser, Munich, Germany.

[39] Berejka, A.J. and Eberle, C., (2002), Electron Beam Curing of Composites in North America, Radiation Physics and Chemistry, 551-556

[40] Ghosh, N. N., Palmese. G. R., Electron-beam curing of epoxy resins: effect of alcohols on cationic polymerization. *Bull. Mater. Sci*. (2005) 28(6), p. 603-607.

[41] Kerluke, D. R., Cheng, S., *Proceedings of the 2nd annual automotive composites conference and exposition of the society of plastics engineers* (2002).

[42] Lopata, V.J., Saunders, C.B., Sing A., Janke C.J., Wrenn, G.E. and Havens, S.J. Electron beam curable epoxy resins for the manufacture of high-performance composites, Radiat. Phys. Chem. (1999) 56(4), p. 405

[43] Janke C.J. Properties of electron beam cured vs. autoclave cured composites and adhesives. In: Proc. of the second electron beam curing of composites workshop, Sept. 10-11 1997, Oak Ridge, Tennessee, USA.

[44] C. Saunders, V. Lopata, J. Barnard, T. Stepanik. Electron beam curing – taking good ideas to the manufacturing floor. Radiation Physics and Chemistry 57 (2000) 441±445.

[45] Parrot, P, Electron beam curing of Aerospatiale. In: Proc. 44th International SAMPE Symposium, Long Beach, CA, USA. 23-27 May 1999, pp.1354-1358.

[46] Rudnev V, Loveless D, Cook R, Black M. Handbook of induction heating. Basel: Marcel Dekker AG; 2003.

[47] Roctool: Innovative Moulding Technologies, www.roctool.com, Accessed: 16/11/09.

[48] Advani S and Hsiao KT. Eds. Manufacturing Techniques for Polymer Matrix Composites (PMCs). Woodhead Publishing. 2012.

[49] Marsh G, Autoclave liberation gathers pace, Reinforced Plastics, November/December 2014.

[50] Schut, Jan H., Induction heated molds produce Class A thermoplastic composites, Plastics Technology, November 1, 2006

[51] Unknown author. Electronics maker expands RocTool-based manufacturing system. Composites World (2014). www.compositesworld.com/news/electronics-maker-expands-roctool-based-manufacturing-system.

[52] Airbus, www.airbus.com.

[53] German Aerospace Center, www.dlr.de/dlr/en/desktopdefault.aspx/tabid-10002/ Unknown Author, www.dlr.de/desktopdefault.aspx/tabid-1/86_read-8535/, Deutsche Zentrum fur Luft- und Raumfahrt, (2007), Accessed: 24/11/09.

[54] Carracedo I.F., Final Report Summary – MAC-RTM (Microwave Assisted Curing for Resin Transfer Moulding), European Commission, 2014.

[55] Sutton, W.H., Microwave processing of ceramic materials (1989), American Ceramic Society Bulletin, 68, pp. 376-386.

[55] Manoj, G. and Wong, W.L.E., Microwaves and Metals, 1st ed., Wiley, November 2007.

[56] Benitez, R., Fuentes, A. and Lozano, K., Effects of microwave assisted heating of carbon nanofiber reinforced high density polyethylene (2007), Journal of Materials Processing Technology, Vol. 190, no. 1-3, pp. 324-331.

[57] Vankoughnett, A.L., Fundamentals of microwave heating (1973), Transactions of International Microwave Power Institute, Vol. 1, pp. 17-39.

[58] Understanding Microwaves, Allan W. Scott. John Wiley & Sons, Inc. 1993.

[59] Osepchuk, J.M., Basic principles of microwave ovens: Interaction of microwaves with materials (1975), iMPI Ltd., Canada.

[60] Bada J. Encyclopedia of Astrobiology. 2011. Springer Berlin Heidelberg.

[61] Thuery J, Microwaves: Industrial, Scientific and Medical Applications. Artech House Publishers, Norwood, USA, 1992.

[62] Ishii T. Theoretical analysis of arcing structure in microwave ovens. Journal of Microwave Power, 18, Number 4, 1983, pp.337-344.

[63] Peng Z, Heat transfer in microwave heating, PhD thesis, Michigan Technological University, USA, 2012.

[64] www.kayelaby.npl.co.uk/general_physics/2_6/2_6_5.html, Accessed: 01/10/10.

[65] Von Hippel, A., Dielectric Materials and Applications, Artech House, 1995.

[66] London South Bank University, www1.lsbu.ac.uk/water/microwave.html#equ

[67] Zong L, Zhou S, Sgriccia N and Hawley MC. Dielectric properties of an epoxy-amine system at a high microwave frequency. Polymer Engineering and Science 2005 45(12):1576-1580.

[68] Huang, H.F., Temperature control method in a microwave resonant cavity system for rapid heating of nylon monofilament, Journal of Microwave Power, Vol. 11, pp.305, 1976.

[69] Microwaves in Organic Synthesis, 2nd ed., Ed. Loupy, A., September 2006.

[70] Livi A, Levita G and Rolla PA. Dielectric behavior at microwave frequencies of an epoxy resin during crosslinking. Journal of Applied Polymer Science 1993 Vol.50, 1583-1590.

[71] Ku, H., Trada, M. and Puttgunta, V.C., Mechanical properties of vinyl ester composites cured under microwave conditions, Journal of Engineering Science and Technology, Vol. 16, no. 6, pp. 741-745, 2007.

[72] Ku, H., Chan, W.L., Trada, M. and Baddeley, D., An evaluation of fracture toughness of vinyl ester composites cured under microwave conditions, Journal of Engineering Science and Technology, Vol. 16, pp. 741-745, 2007.

[73] Beaumont, M. and Filsinger, J., Potential of microwave heating for out-of-autoclave composite manufacturing of aerospace structures, Proceedings of SAMPE 2013, Long Beach, USA, 2013.

[74] F.L. Matthews, R.D. Rawlings. Composite materials: Engineering and Science. Great Abington, UK: Woodhead Publishing; 1999.

[75] Madhukar MS and Drzal LT. Fiber-Matrix Adhesion and Its Effect on Composite Mechanical Properties: II. Longitudinal (0°) and Transverse (90°) Tensile and Flexure Behavior of Graphite/Epoxy Composites. J Compos Mater 1991; 25(8):958-991.

[76] Madhukar MS and Drzal LT. Fiber-Matrix Adhesion and Its Effect on Composite Mechanical Properties: III. Longitudinal (0°) Compressive Properties of Graphite/Epoxy Composites. J Compos Mater 1992; 26(3):310-333.

[77] Madhukar MS and Drzal LT. Fiber-Matrix Adhesion and Its Effect on Composite Mechanical Properties: I. Inplane and Interlaminar Shear Behavior of Graphite/Epoxy Composites. J Compos Mater 1991; 25(8):932-957.

[78] Madhukar MS and Drzal LT. Fiber-Matrix Adhesion and Its Effect on Composite Mechanical Properties: IV. Mode I and Mode II Fracture Toughness of Graphite/Epoxy Composites. J Compos Mater 1992; 26(7):936-968.

[79] Scola, DA and Brooks, CS. Surface aspects of new fibers, Boron, Silicon Carbide and Graphite, Journal (1970), J Adhesion, 2:213-237.

[80] Broutman, LJ and Sahu, S. The Effect of Interfacial Bonding on the Toughness of Glass Filled Polymers. In: Proc 26th Annual Technical Conference, Reinforced Plastics/Composites Division, The Society of the Plastics Industry, Inc., Section 14C:1-8. Washington DC, USA, 1971.

[81] Mullin, J V. Analysis of Test Methods for the High Modulus Fibers and Composites. Baltimore, USA: ASTM STP 521; 1973.

[82] Norita, T, Matsui J. and Matsuda HS. Effect of Surface Treatment of Carbon Fiber on Mechanical Properties of CFRP. In: Proc First International Conference on Composite Interfaces. 1986.

[83] White WC. Early History of Industrial Electronics. In: Proc IRE, 1962. pp1129-1135.

[84] Krieger B. Vulcanization of rubber, a resounding success for microwave processing. Polym Mater Sci Eng 1992; 66:339-400.

[85] Marand E, Baker, KR and Graybeal, JD. Comparison of reaction mechanisms of epoxy resins undergoing thermal and microwave cure from in situ measurements of microwave dielectric properties and infrared spectroscopy. Macromolecules 1992; 25(8):2243-2252.

[86] Bai SL, Djafari V, Andréani M and François D. A comparative study of the mechanical behaviour of an epoxy resin cured by microwaves with one cured thermally. Eur Polym J 1995; 31(9):875-884.

[87] Wei J, Hawley MC, Delong JD and Demeuse M. Comparison of microwave and thermal cure of epoxy resins. Polym Eng Sci 1993; 33(17):1132-1140.

[88] Wei J, Hawley MC and Demeuse M. Kinetics modeling and time-temperature-transformation diagram of microwave and thermal cure of epoxy resins. Polym Eng Sci 1995; 35(6):461-470.

[89] Chen M, Siochi EJ, Ward TC and Mcgrath JE. Basic ideas of microwave processing of polymers. Polym Eng Sci 1993; 33(17):1092-1109.

[90] Bai SL and Djafari V. Interfacial properties of microwave cured composites. Composites 1995; 26(9):645-651.

[91] Fang X and Scola DA. A comparison of microwave and thermal cure of penylethynyl-terminated polyimide composites. Polym Mater Sci Eng 1999; 80:322-323.

[92] Outifa L, Delmotte M, Jullien H and More C. A homogeneous microwave curing process for epoxy/glass fibre composites. Polym Mater Sci Eng 1995; 72:341-344.

[93] Lee WI and Springer GS. Microwave curing of composites. J Compos Mater 1984; 18(4):387-409.

[94] Wei J, Hawley M, Jow J and DeLong J. Microwave processing of crossply continuous graphite fiber/epoxy composites. SAMPE J 1991;27(1):33-39.

[95] Nightingale C and Day R. Flexural and interlaminar shear strength properties of carbon fibre/epoxy composites cured thermally and with microwave radiation. Compos Part A-Appl S 2002; 33(7):1021-1030.

[96] Wei J, Chang Y, Thomas BJ and Hawley MC. Microwave heating of thick-section graphite fiber/epoxy composites. SAMPE J 1991; 8:1-10.

[97] Paulauskas FL, Variable frequency microwave (VFM) curing, processing of thermoset prepreg laminates, ORNL/TM-13381. Oak Ridge National Laboratory, Lockheed Martin for the United States Department of Energy 1996.

[98] L. T. Drzal, K. J. Hook and R. K. Agrawal. Enhanced Chemical Bonding at the Fiber-Matrix Interphase in Microwave Processed Composites. MRS Proceeding, Volume 189, 1990. 449-454.

[99] Martin C. Hawley and Jianghua Wei. Processing of Polymers and Polymer Composites In a Microwave Applicator. MRS Proceeding, Volume 18, 1990. 413-420.

[100] Wei J, Hawley MC. Utilization of microwaves in processing of polymer composites – Past, present and future. Conference: 209. American Chemical Society (ACS) national meeting, Anaheim,

CA (United States), 2-6 Apr 1995; Other Information: PBD: 1995; Related Information: Is Part Of 209th ACS national meeting; PB: 2088 p.

[101] Xiao, Y; Scola, D. Microwave cure of graphite fiber/polyimide composites. Conference: 209. American Chemical Society (ACS) national meeting, Anaheim, CA (United States), 2-6 Apr 1995.

[102] X. Fang, D. A. Scola, and C. DiFrancia, "Investigation of microwave energy to fabricate phenylethynyl terminated polyimide/IM7 graphite composites", Proc. C. Polym. Mater. Sci. Eng. ACS Spring Meeting, vol. 76, pp.7-8 1998.

[103] ET Thostenson, TW Chou. Microwave processing: fundamentals and applications. Composites Part A: Applied Science and Manufacturing 30 (9), 1055-1071. 1999.

[104] ASTM, D3039. Standard test method for tensile properties of polymer matrix composite materials (2006).

[105] ASTM, D6641. Standard test method for determining the compressive properties of polymer matrix composite laminates using a combined loading compression (CLC) test fixture (2001).

[106] ASTM, D3518. Standard Test Method for In-Plane Shear Response of Polymer Matrix Composite Materials by Tensile Test of a ±45° Laminate (2013).

[107] Gurit. SPARPREG Datasheet. 2012.

[108] Gurit. SP9435 Datasheet. 2012.

[109] Process Materials, Cytec. www.cytec.com/businesses/industrial-materials/products/process-materials. 2011.

[110] Vötsch Industrietechnik. Microwave Heating and Drying Cabinets VHM Hephaistos. www.voetsch-ovens.com/en/products/microwave_system/schunk01.c.59509.en?_pid=51758, Accessed: 10 June 2010.

[111] West System. Vacuum bagging techniques. Catalogue number 002-150. 2010.

[112] Composite Materials Handbook. MIL-HDBK-17-3F. Volume 3. Polymer Matrix Composites Materials Usage, Design, and Analysis. Department of Defense Handbook. 2002.

[113] ASTM, E2109-01. Test Methods for Determining Area Percentage Porosity in Thermal Sprayed Coatings (2007).

[114] Cuccurullo G, Berardi PG, Carfagna R and Pierro V. IR temperature measurements in microwave heating. Infrared Phys Techn 2002; 43(3-5):145-150.

[115] Cuccurullo G and Pierro V. A procedure to measure electromagnetic skin depth in microwave heating. Infrared Phys Techn 2004; 46(1-2):49-55.

[116] ASTM Standard D5528-01(2007). Standard Test Method for Mode I Interlaminar Fracture Toughness of Unidirectional Fiber-Reinforced Polymer Matrix Composites, 2001.

[117] Godara A, Gorbatikh L, Kalinka G, Warrier A, Rochez O, Mezzo L, Luizi F, van Vuure AW, Lomov SV and Verpoest I. Interfacial shear strength of a glass fiber/epoxy bonding in composites modified with carbon nanotubes, Compos Sci and Technol 2010; 70(9):1346-1352.

[118] ASTM, D2583. Standard Test Method for Indentation Hardness of Rigid Plastics by Means of a Barcol Impressor (2013).

[119] ASTM, E2546. Standard Practice for Instrumented Indentation Testing (2007).

[120] ISO, 14577-4. Metallic materials – Instrumented indentation test for hardness and materials parameters – Part 4: Test method for metallic and non-metallic coatings (2007).

[121] ASTM, D2583. Standard Test Method for Indentation Hardness of Rigid Plastics by Means of a Barcol Impressor (2013).

[122] Qian H, Kalinka G, Chan KL, Kazarian SG, Greenhalgh ES, Bismarck A and Shaffer MSP. Mapping local microstructure and mechanical performance around carbon nanotube grafted silica fibres: Methodologies for hierarchical composites, Nanoscale 2011; 3(11):4759-4767.

[123] Briscoe BJ, Fiori L and Pelillo E. Nano-indentation of polymeric surfaces, J. Phys. D: Appl. Phys. 1998; 31:2395.

[124] Zhang YF, Bai SL, Li XK and Zhang Z, Viscoelastic properties of nanosilica filled epoxy composites investigated by dynamic nanoindentation, J Polym Sci Part B: Polym Phys 2009; 47:1030-1038.

[125] Fischer-Cripps, Anthony C. Nanoindentation, 2nd ed. 2004, Springer-Verlag, New York, USA.

[126] Parlevliet P, Bersee H and Beukers A. Residual Stresses in Thermoplastic Composites – A Study of the Literature – Part I: Formation of Residual Stresses. Compos A Appl Sci Manuf 2006; 37(11):1847-1857.

[127] Choo H, Bourke M and Daymond M. A finite-element analysis of the inelastic relaxation of thermal residual stress in continuous-fiber-reinforced composites. Compos Sci Technol 2001; 61(12):1757-1772.

[128] Maxwell AS, Broughton WR, Lodeiro MJ and Shaw R. Measurement of residual stresses and strains in carbon fibre composites. NPL Report MN7, 2009.

[129] Hunston DL, Moulton RJ, Johnston NJ and Bascom WD. Matrix resin effects in composite delamination: Mode I fracture aspects. United States. 1987.

[130] Hiley MJ. Fractographic study of static and fatigue failures in polymer composites. Plastics, Rubber and Composites 1999; 28:210-227.

[131] E.S. Greenhalgh. Failure Analysis and Fractography of Polymer Composites. Great Abington, UK: Woodhead Publishing; 1999.

[132] Sloan J, Auto composites quest: One-minute cycle time? Composites Technology (2012). www.compositesworld.com/articles/auto-composites-quest-one-minute-cycle-time

[133] Sloan J, Dow epoxy joins the fast-cure race. Composites World (2014). www.compositesworld.com/blog/post/dow-epoxy-joins-the-fast-cure-race

[134] Xiong Y and Poon C. A prediction method for the compressive strength of impact damaged composite laminates. Compos Struct 1995 30:357–367.